TRYPANOSOMA BRUCEI: MITOCHONDRIAL PROTEIN DIVERSITY AND CELLULAR COMMUNICATION

by

ANTHONY JAMES SZEMPRUCH

(Under the Direction of Stephen L. Hajduk)

ABSTRACT

Trypanosomes are protozoan parasites, which are characterized by their large single mitochondrial genome termed the kinetoplast. *Trypanosoma brucei* cycles between an insect vector, the tsetse fly, and a mammalian host where it causes human African sleeping sickness and the cattle wasting disease Nagana. Though *T. brucei* undergoes a complex life cycle, with extensive developmental regulation, these organisms lack intron splicing the most common mechanism for expanding functional diversity at the transcript level. Instead, these parasites may rely on their unique mitochondrial process of RNA editing for the generation of novel open reading frames and the process of moonlighting to expand the functional repertoire of protein products. By developing new methods to investigate mitochondrial RNA function *in vivo* and analyzing mitochondrial protein moonlighting functions this work sets out to expand out understanding of mitochondrial protein diversity in *T. brucei*. Disruption of a critical

mitochondrial moonlighting protein within *T. brucei* revealed that these parasites undergo a process of extracellular vesicle (EVs) mediated cellular communication. Bloodstream form *T. brucei* generate membrane nanotubes originate from the flagellar membrane and disassociate into free EVs. These EVs contain virulence factor proteins including the *T. b. rhodesiense* specific serum resistance-associated protein (SRA) necessary for human infectivity. *T. b. rhodesiense* EVs transfer SRA to non-human infectious trypanosomes allowing evasion of human innate immunity. These EVs are also able to fuse with host erythrocytes resulting in anemia. Studying the complex biological processes employed by these parasites to generate protein diversity allowed for the identified of a novel mechanism of *T. brucei* virulence.

INDEX WORDS: African trypanosomes, RNA editing, mitochondria, moonlighting proteins, extracellular vesicles, cellular communication

TRYPANOSOMA BRUCEI: MITOCHONDRIAL PROTEIN DIVERSITY AND CELLULAR COMMUNICATION

by

ANTHONY JAMES SZEMPRUCH

B.S. North Carolina State University, 2007

A Dissertation Submitted to the Graduate Faculty of The University of Georgia in Partial Fulfillment of the Requirements for the Degree

DOCTOR OF PHILOSOPHY

ATHENS, GEORGIA

2016

TRYPANOSOMA BRUCEI: MITOCHONDRIAL PROTEIN DIVERSITY AND CELLULAR COMMUNICATION

by

ANTHONY JAMES SZEMPRUCH

Major Professor:	Stephen L. Hajduk
Committee:	David Garfinkel
	Robert Sabatini
	Michael Terns

Electronic Version Approved:

Suzanne Barbour
Dean of the Graduate School
The University of Georgia
August 2016

DEDICATION

This dissertation is dedicated to my late grandparents: James Richard Lanspery Sr. and Anna Rose Lanspery; my parents: Jamie Ann Lanspery and Steven Michael Price Sr.; to my siblings: Steven Michael Price Jr. and Anna Rose Wilbanks; and to my significant other Sherrie Ellen Emerine.

ACKNOWLEDGEMENTS

I would like to thank my mentor Steve Hajduk for providing me with an excellent environment to excel. During my time in the Hajduk lab I was given the freedom to explore many different scientific questions and the training that prepared my mind to investigate them. I would also like to thank the current and previous members of the Hajduk and Sabatini labs, especially Steve Sykes, David Seidman and John Harrington who helped create a fun environment that fostered deep discussions about science.

I would especially like to thank my family and friends for their years of love and support.

TABLE OF CONTENTS

Page

CHAPTER 1

INTRODUCTION AND LITERATURE REVIEW

Biology of the Kinetoplastid *Trypanosoma brucei*

The kinetoplastidae is a diverse group of eukaryotic microbes responsible for several important human and animal diseases including African sleeping sickness (*Trypanosoma brucei rhodesiense* and *Trypanosoma brucei gambiense*), Chagas disease (*Trypanosoma cruzi*), Kala azar (*Leishmania donovani*) and Nagana in cattle (*Trypanosoma brucei brucei; Trypanosoma congolense; Trypanosoma vivax*). These unicellular flagellated protozoans are characterized by a larger mitochondrial genome termed the kinetoplast. The human infectious *T. brucei* spp., often referred to as African trypansomes because of their geographic distribution, are endemic to 36 countries in sub-Saharan Africa and cause more than 100,000 infections yearly [1]. Infection is fatal unless treated by a limited repertoire of therapeutic compounds that cause toxic side effects. The infection of cattle by *African trypanosomes* also results in significant economic burden to these regions, resulting in a loss of ~ 4 billion US dollars yearly [1].

T. brucei spp. are transmitted by the tsetse fly (*Glossina* spp.), which becomes infected after ingestion of a blood meal containing bloodstream form (BF) *T. brucei* [2]. The parasite establishes an infection within the midgut of the insect and differentiates into the procyclic form (PF) (**Figure 1.1**) [3]. After establishing the midgut infection the parasite migrates to the salivary gland and differentiates into the mammalian transmissible metacyclic form of the parasite (**Figure 1.1**) [1,2]. The metacyclic form is then transmitted to the mammalian host by the bite of the infected vector (**Figure 1.1**). *T. brucei* undergoes developmental changes during

differentiation into the BF form [2]. This complex development process and changes in both morphology and metabolism are in part due to the carbon sources available for energy production. Consistent with these older observations, recent studies have shown that BF trypanosomes migrate to adipose tissue and up-regulate expression of genes necessary for β-oxidation of fatty acids [4].

Within the bloodstream of the mammalian host, BF *T. brucei* has access to a large supply of glucose and exclusively utilizes glycolysis for energy production (**Figure 1.2**) [5,6]. This requires high rates of glycolysis and has resulted in many of the glycolytic enzymes being localized to a specialized series of organelles called glycosomes. These organelles are evolutionarily related to the peroxisome organelle and retain many of the signals associated with protein import into the peroxisome. This compartmentalization results in efficient conversion of glucose to glyceraldehyde 3-phosphate and allows for the high rates of glycolysis required to meet the ATP demands of BF *T. brucei* [7,8,9]. Due to the essential role of glycolysis in ATP production, the mitochondrion of BF *T. brucei* is reduced to a tubular acristate organelle lacking both respiratory cytochromes and a functional Krebs cycle (**Figure 1.3**) [1]. During this stage of *T. brucei's* development cells are unable to carry out mitochondrial oxidative phosphorylation and are repressed in the expression of other components of the electron transport chain (**Figure 1.2**). Mitochondrial ATP production is driven by the F_oF_1 ATPase, which couples the membrane potential ($\Delta\Psi m$) generated by the electron transport chain [6,10]. Since BF *T. brucei* lack a functional electron transport chain, ATP hydrolysis by the F_oF_1 ATPase drives the movement of protons into the inner membrane space of the mitochondria (**Figure 1.2**). This catalytic reversal of the F_oF_1 ATPase establishes the $\Delta\Psi m$ needed for fatty acid synthesis and import of proteins and RNAs into the mitochondria [5,11].

Within the insect vector, PF *T. brucei* has access to the amino acid substrates proline and glutamate, which are degraded by the Krebs cycle enzymes α-ketoglutarate dehydrogenase (α-KD) and succinyl-CoA synthetase to succinate (**Figure 1.2**) [12]. Use of the Kreb cycle for the breakdown of these amino acids results in the production of NADH and $FADH_2$, which are in turn used by the electron transport chain for mitochondrial oxidative phosphorylation and ATP production (**Figure 1.2**) [12]. The active mitochondria of PF *T. brucei* show a volumetric increase and the formation of cristae within the organelle (**Figure 1.3**) [12]. This shift in metabolism in PF *T. brucei* results in a drastic reduction in the number of glycosomes within the cell when mitochondria becomes the source of ATP.

Mitochondrial Genome and RNA Editing

T. brucei is a member of the class Kinetoplastida, whose defining feature is a unique mitochondrial genome known as the kinetoplast DNA (kDNA) [13,14]. The genome is visible using DNA staining dyes and comprises ~20% of the total cell DNA content (**Figure 1.3**). The kDNA is a catenated network of two types of circular DNA elements, maxicircles and minicircles. Maxicircles encode for the functional genes of the mitochondria, while minicircles encode for a unique class of small RNAs called guides (gRNA) [15,16]. The kDNA contains approximately 50 maxicircles (~23kb in size) and as many as 10,000 minicircles (~1kb in size) divided into over 300 sequence classes (gRNA size ranges from 40-70nts in length) [17]. This large number of minicircles suggests that the sequenced repertoire of gRNAs may be a vast underrepresentation of the true number of gRNAs. It has been hypothesized that the actual number of gRNAs required to edit all known canonically edited mRNAs is ~ 200. However, to date ~ 450 gRNAs have been identified [18]. Many of these gRNAs lack any known target

sequence in canonically edited mRNAs. Current estimates suggest that there are over 1,000 unique gRNAs [18].

The transcripts encoded by the maxicircles are largely incomplete and must first undergo the process of uridine insertion/deletion RNA editing before they produce functional open reading frames. First the pre-mRNA is recognized in a sequence specific manner by the 5' "anchor" sequence of the gRNA. This initial 5' region (8-12nts) is followed by a region of the gRNA that has specific adenosine or uridine mismatches that correspond to insertion or deletion editing of the pre-mRNA substrate (**Figure 1.4**) [19]. Mismatches produce secondary structural elements between the pre-mRNA/gRNA duplex that are a signal to the RNA editing complex, called the editosome, to add or remove uridine residues in the pre-mRNA [19,20,21]. After editing at a site is complete, new gRNAs will continue the editing process. Recognition by additional gRNAs often requires edited sequences before the anchor duplex can form; this process occurs 3' to 5' in relation to the pre-mRNA (**Figure 1.4**) [20,21]. All known components of the editosome are nuclear encoded and transported into the mitochondria of *T. brucei* [19,20,21].

Mitochondria as a Site of Protein Diversity

Sequencing of mitochondrial cDNA libraries suggested that a subset of mature mRNAs utilize alternative uridine insertion and deletion sites [18,22]. Sequencing of cDNAs from small mitochondrial RNAs yielded a subset of gRNAs required for editing at these sites (**Table 1.1**) [18]. Initial research focused on the alternatively edited version of the cytochrome c oxidase III (COXIII) gene. The protein generated by this alternatively edited mRNA has been termed Alternatively Edited Protein 1 (AEP-1) [22,23]. However, alternatively edited mRNAs have also been identified for the trypanosome mitochondrial genes ND7, ND8, ND9, and A6 [18]. In many

of these cases multiple differentially edited mRNAs have been sequenced (**Table 1.1**) [18]. Alternative editing may result in several types of alterations to the encoded protein. First, subtle changes can result in modulation of enzymatic activity of a canonical protein. Second, novel functions may be imparted by addition of new functional domains to currently existing domains, like AEP-1. Third, generation of novel open reading frames could be utilized to create entirely new proteins. Sequence analysis of COXIII in comparison to the alternatively edited AEP-1 isoform has shown conservation of the C-terminal membrane-spanning domains [23]. Alternative editing of COXIII mRNA occurs at the 5' region and results in a polar unstructured N-terminus. This polar N-terminus of AEP-1 associates with kDNA networks [23]. Expression of a nuclear encoded AEP-1, containing a mitochondrial localization sequence and the polar N-terminus, but lacking the transmembrane anchoring domains, results in a disruption of kDNA [23]. Utilizing the extensive array of gRNAs encoded by the mitochondrial genome, trypanosomes are able to generate protein diversity that has the potential to be regulated during different life stages of the organism [18,22,23].

Analyzing the function of mitochondrial transcripts is challenging because of a lack of reverse genetic or molecular approaches amenable to the mitochondria. These organelles lack RNAi and there has been limited success directly transfecting this organelle. Recently, artificial-site specific RNA endonucleases (ASREs) have been developed for use in mammalian mitochondria [24]. These engineered proteins are a fusion of Pumilio/FBF (PUF) domains, Pumilio (from *Drosophila melanogaster*) and FBF (Fem-3 mRNA-binding factor from *Caenorhabditis elegans*) engineered to specifically recognize and bind an 8-nucleotide single-stranded RNA target sequence, with the PIN domain of SMG6 which has nonspecific

endoribonuclease activity (**Figure 1.5**) [24,25]. In Chapter 2 of this thesis I show that ASREs can be used to knockdown mitochondrial mRNA levels in PF *T. brucei* [26].

In addition to alternative RNA editing, *T. brucei* may also rely on moonlighting proteins to expand its repertoire of functional proteins. Moonlighting proteins are defined as having at least two unrelated biological functions within the same organism encoded by the same protein [27]. The dual functions are conveyed by the same protein and do not require alterations to the amino acid sequence. These multi-functioning proteins add an additional layer of protein diversity. Metabolic enzymes comprise a large portion of the identified moonlighting proteins [28,29,30]. A recent study showed that the α-ketoglutarate dehydrogenase E2 protein has a moonlighting role in *T. brucei* [31]. Canonically this protein plays a critical role in the TCA cycle, however, it has been shown to associate with mitochondrial DNA (mtDNA) in yeast and several other eukaryotes [30]. Initial observations in T. *brucei* showed that α-ketoglutarate dehydrogenase E1 and E2 were expressed in the bloodstream form trypanosome [31]. The expression of these genes was an interesting observation, due to the fact that bloodstream form cells lack a functional TCA cycle. Further investigation of E2 resulted in the finding that this protein associates with and is essential for organization of kDNA in T. *brucei* [31]. In Chapter 3, of this thesis I show that α-ketoglutarate dehydrogenase E1 shares dual organelle localization in bloodstream form *T. brucei* [32]. The majority of the E1 protein no longer localizes with its E2 partner and instead localizes to glycosomes in the BF *T. brucei* (**Figure 1.6**) [32].

Infection of the Mammalian host

During mammalian infection BF *T. brucei* are free living in the circulation of the host. This results in parasite exposure to components of the innate and adaptive immune response. *T. brucei* spp. have evolved a mechanism to circumvent the adaptive immune response through the

monoallelic expression of the highly immunogenic variant surface glycoproteins (VSGs) [33,34]. The BF parasite expresses a single VSG at a time and though the process of antigenic variation periodically switches the expressed VSG protein [35,36]. This has resulted in the *T. brucei* genome containing more than 2,000 different VSG genes and specific mechanisms for VSG recombination resulting in mosaic VSGs [37].

Though all *T. brucei* spp. express VSGs not all trypansomes are human infectious. Higher primates including humans are innately immune to many African trypanosomes mediated by the circulating trypanosome lytic factors (TLF) (**Figure 1.7**) [38]. Circulating TLF-1 is a minor subclass of high-density lipoprotein (HDL) particles comprised of two primate-specific proteins, apolipoprotein L1 (ApoL-1) and haptoglobin-related protein (Hpr) [38,39]. The ApoL-1 protein is an ion pore-forming toxin, which inserts in to the parasite endosomal membrane at low pH. ApoL-1 insertion ultimately results in rapid swelling and lysis of non-human infectious *T. brucei* spp [39]. This trypanocidal activity can be reconstituted with purified ApoL-1, though at higher concentrations than relative to the killing activity of the TLF-1 particle [40]. The increase in activity is due to the presence of the Hpr protein within the TLF-1 molecule. Hpr shares a high degree of sequence similarity with the haptoglobin proteins, which are free heme scavengers within mammalian circulation [40]. Hpr is able to bind free heme and enter *T. brucei* through a high affinity haptoglobin-hemoglobin receptor [38,40]. This receptor mediated endocytosis results in rapid internalization of the TLF-1 particle and delivery to the endocytic pathway of the parasite.

However there are two human pathogenic African trypanosomes, *T. b. rhodesiense* and *T. b. gambiense,* which have evolved mechanisms to circumvent these TLF molecules. *T. b. rhodesiense* inactivates TLF activity through expression of a virulence factor termed the serum-

resistance associated protein (SRA) (**Figure 1.7**)[41,42,43,44], which directly binds to the ApoL-1 pore forming toxin within TLF [44]. When TLF is bound, endocytosed and trafficked to early endosomes of *T. b. rhodesiense* it co-localizes with SRA resulting in the neutralization of ApoL-1 activity by blocking its ability to insert in to the parasite endosomal membrane [43]. Ectopic expression of the gene encoding SRA in *T. b. brucei* is sufficient to confer TLF resistance. Co-infection of tsetse flies with *T. b. rhodesiense* and *T. b. brucei* allows for transfer of *SRA* to *T. b. brucei* and also confers resistance to TLF [43,44,45]. In Chapter 4, of this thesis I show that the SRA protein can also be transferred via extracellular vesicles to *T. b. brucei* resulting in non-heritable transfer of TLF resistance [46]. The mechanism of *T. b. gambiense* resistance to TLF is more complex, instead these parasites use a combination of mechanisms to circumvent TLF mediated killing [47,48]. The haptoglobin-hemoglobin receptor contains a point mutation that prevents TLF bind and is also down regulated in *T. b. gambiense* [49]. As an additional layer of protection against TLF killing, these cells express a truncated VSG gene termed TgsGP, which may function through altering the membrane fluidity of *T. b. gambiense* preventing TLF association [50].

T. brucei infection is complex and dynamic, like many extracellular pathogens, African trypanosome infection initially elicits a type 1 immune response that includes expression of inflammatory cytokines and activation of myeloid cells. These host immune responses have been implicated in the pathology of trypanosomiasis-associated anemia [51]. During infection anemia is markedly severe during acute infection and is the major cause of cattle death due to Nagana [52]. Recently, erythrophagocytosis by activated liver and spleen myeloid cells has been identified as a major contributor to erythrocyte clearance. These studies have also shown that the lipid composition of erythrocytes is altered during trypanosome infection, and modified

erythrocytes are preferentially phagocytosed by host myeloid cells [51]. While host responses that contribute to anemia have been characterized, the parasite factors that elicit erythrocyte clearance were unknown until recently. In Chapter 4, of this thesis I investigated the role of trypanosome derived extracellular vesicles (EVs) secreted by *T. brucei* that fuse with host erythrocytes, transferring parasite lipids and proteins. Fusion with erythrocytes also results in physical changes to the cell membrane and ultimately cause anemia *in vivo* [46].

Extracellular Vesicle Mediated Cellular Communication in Protozoan Parasites

EVs are important molecules for cellular communication with in a cell population and with other cell types [53, 54]. This has also been found to be true for other parasitic eukaryotes. In general, pathogenic protozoans cause a wide range of human and animal diseases globally that results in significant socioeconomic burden in many developing nations. These parasites exploit diverse mechanisms for survival and persistence within their hosts. Many of these parasites use extracellular vesicles (EVs) as a vehicle for the delivery of biologically active effector molecules. EVs can be divided into two major classes of secreted vesicles, which are defined by their mechanism of formation. These two classes are 1) exosomes, which are generated within multivesicular bodies (MVBs) and 2) ectosomes, which are produced by budding of the plasma membrane (**Figure 1.8**). It has been shown that distinguishing the difference between exosomes and ectosomes can be difficult with current methods. This is especially true in a mixed population, as these vesicles share similar features including size, density and shared cargo. This has resulted in exosomes and ectosomes being described as EVs, which serves as a general term for all secreted vesicles [53]. Secretion of EVs can have profound biological effects resulting from the transfer of proteins, lipids and nucleic acids to both adjacent and distant cells [54]. EVs interact with target membranes through receptor dependent and receptor independent processes

[55,56,57]. A single organism may exploit multiple mechanisms of EV production and interaction, generating a population of EVs with mixed cargos and functions [53]. In Chapter 5, of this thesis I discuss additional findings on the role of EVs in pathogenic protozoans.

Though the field of EV biology has undergone rapid expansion in other eukaryotes, resulting in several thousand publications since the mid 2000s, parasitology has largely lagged behind in EV research generating only a few dozen papers. This may be due to the difficulty associated with identifying and characterizing EV production within a multi-cellular host, which has also been an issue for EV characterization in mammalian systems. Another challenge has been identifying tissues and cells specifically targeted by EVs *in vivo*. Cancer derived EVs play a role in tissue specific metastatic niche formation within an animal model [58]. A recent study developed a powerful toolset exploiting Cre mRNA secretion in murine EVs, where EV interaction with Cre mRNA resulted in expression of a GFP reporter in target cells [59]. This tool was used to determine organ specific interactions and cell reprogramming mediated by metastatic tumor cells and opens up the potential to investigate EV targets *in vivo* for other organisms, including pathogenic protozoans.

Recent studies in pathogenic protozoans have focused on how EVs modulate the host immune system and elicit a pro-inflammatory response [55,60,61]. Many of these studies have presented compelling evidence that pathogenic protozoans use EVs for cellular communication with their hosts and within the parasite population. For example, treatment with EVs from *T. vaginalis* mimics changes to interleukin (IL) levels observed during infection [62]. Similarly purified EVs from *L. donovani* stimulate the same Th1 response from CD4 T cells as those caused by *L. donovani* infection [63,64]. Purified EV-derived protein has also been shown to mirror alterations to host liver function, reducing circulating cholesterol, as observed during *L.*

donovani infection [65]. EV-mediated effects are not limited to host alterations and can also result in significant changes to the parasite population. EVs have been shown to cause cellular differentiation, critical for continuation of the plasmodium life cycle [66,67]. Studies in *Trypanosoma cruzi* have also shown that EVs may play a role in life cycle progression [68].

In Chapter 4, of this thesis I show that purified EVs generate disease pathology that mimics *T. brucei* effects *in vivo* [46]. Additionally, EVs can transfer functional virulence factors within the *T. brucei* population that allow for resistance to innate host immune factors [46].

Types of EVs

Exosomes

Exosomes are membrane bound structures of homogeneous size derived from MVBs. MVBs are specialized late endosomes, containing exosomes, which are able to traffic to the plasma membrane. Upon trafficking MVBs fuse with the plasma membrane and release their exosome cargo [69,70]. Exosomes form by the invagination of endosomal membranes and result in vesicles with a topology that displays cell outer-membrane lipids and proteins on the exterior face [70,71] (**Figure 1.8**). Exosomes interact with target cells through three major mechanisms: receptor mediated binding, membrane fusion and bulk phase nonspecific entry into the endocytic pathway, and fusion with endosomal membranes [69,70] (**Figure 1.8**). Though exosomes contain cell surface proteins and lipids, they are often enriched in unique molecules and show a differential distribution when compared to the plasma membrane [70]. They are also enriched in luminal cargo molecules including proteins and nucleic acids [54]. Electron microscopy studies showed that erythrocytes produce MVBs and release EVs as a mechanism for membrane maturation and homeostasis [71,72]. It has been shown that *T. vaginalis* produces large MVB-like structures that can be observed by conventional microscopy [62]. Additionally, EM studies

show that the kinetoplastids *T. cruzi* and *Leishmania* spp. produce MVBs as a mechanism for vesicle secretion [73,74]. The mechanisms governing parasite MVB formation and subsequent exosome release are not known.

Ectosomes

Ectosomes form from budding of the plasma membrane and represent a wide range of vesicle types [69,75]. Ectosomes have a lipid bilayer structure and are often of heterogeneous size [69]. They can be derived from the entire cell membrane or specialized portions of the membrane, such as the cilium/flagellum or membrane nanotubes [69,75] (**Figure 1.8**). Much like exosomes, ectosomes interact with target cells through the three major mechanisms of receptor mediated binding, membrane fusion and bulk phase nonspecific entry into the endocytic pathway, and fusion with endosomal membranes [75] (**Figure 1.8**). Ectosome secretions, by budding of plasmodium infected erythrocyte membrane, generate EVs containing parasite proteins [66,67]. Kinetoplastids employ several methods of ectosome generation for EV release. Both *T. cruzi* and *Leishmania* spp. release EVs through budding along the cell body and flagellar membranes [63,73,74,76]. Recent work suggests that *Trypanosoma brucei* flagellum gives rise to membrane nanotube structures, which are able to break down and release free EVs [77]. Thus, a single parasite uses multiple mechanisms for EV generation. Since methods to dissect the function of individual subpopulations of EVs require further development, most EV experiments likely involve a mixture of subpopulations [58].

The Role of Kinetoplastid EVs in parasite cellular communication

Research in related kinetoplastids has focused on the presence of immunogenic proteins and RNAs with in EVs. Early work on the *T. cruzi* secretome showed that immunogenic mucin proteins were released as components of EVs [78,79]. Recently, further characterization of EVs

using mass spectrometry showed enrichment in additional immunogenic proteins and additional fractionation detected the tRNA-derived small RNAs (tsRNAs) [68,73,80]. It has been proposed that tsRNAs have functions similar to siRNAs in other organisms [68,80]. These tsRNAs were found to co-localize with the *T. cruzi* specific argonaute protein TcPIWI-tryp and transferred between cells [68]. Addition of purified EVs also resulted in *T. cruzi* differentiation [68,81] (**Table 1.2**). Similarly, EVs purified from the *L. donovani* and *L. braziliensis* were enriched in tsRNAs, but it remains to be determined if tsRNAs have a function [82] (**Table 1.2**). EV-mediated transfer of small regulatory RNAs may play a role in transcriptional regulation during infection or in response to stress.

In Chapter 4 of this thesis, I show that BF *T. brucei* generate cell membrane extensions termed membrane nanotubes. These membrane nanotubes form through budding and extension of the flagellar membrane [77]. Nanotubes vesicularize, and result in free EVs ~80 nm in size that are enriched in flagellar proteins. Vesicularization appears similar to ciliary release of EVs in the unicellular alga *Chlamytomonas reinhardtii* [75,83]. *Trypanosoma brucei brucei* is non-human infectious and is killed in serum by TLF. However, the closely related subspecies *Trypanosoma brucei rhodesiense* has evolved the SRA protein as a mechanism of resistance to TLF [41,43]. Experimental evidence showed that transwell co-cultivation or direct addition of EVs from *T. b. rhodesiense* or a *T. b. brucei* strain expressing an SRA trans-gene resulted in the transfer of SRA to wild type *T. b. brucei* and subsequent TLF resistance (**Table 1.2**) [77]. This transfer of SRA was shown to be transient and removal of the SRA donor resulted in loss of TLF resistance. These observations may explain reported mixed trypanosome infections in humans [84].

The Role of *T. brucei* EVs in host cellular communication

Research in the related kinetoplast *T. cruzi* has focused on enrichmened proteins implicated in host-parasite interactions, immunomodulation and cell signaling [80]. Several A series of robust studies focused primarily on the immunological response associated with these parasite EVs. It has been shown that injection of purified EVs into naïve mice results in significantly increased parasitemia and reduced survival, of the host, after challenge with *T. cruzi* [85]. Mice treated with EVs prior to infection also had higher cardiac tissue invasion than controls and injection of EVs was shown to result in a 70 fold increase in IL-4 and IL-10 mRNA in cardiac tissue (**Table 1.2**). To determine if increased mortality was linked to secreted IL-4 and IL-10, mice were treated with monoclonal antibody against both cytokines, which eliminated the enhanced killing of EV-pretreated mice. These EVs also caused splenocytes to produce pro-inflammatory cytokines with parasite strain-specific variation [86] (**Table 1.2**). The proteome from *in vitro* derived EVs contain a class of antigens termed *T. cruzi* surface membrane proteins (TcSMP) [87]. Purified TcSMP interact with host cells and results in alterations to calcium signaling. Addition of purified TcSMPs caused inhibition of host cell invasion [87]. This observation may suggest that EVs play a role in local dispersion of TcSMP, which in turn would limit parasite invasion of host cells immediately adjacent to sites of high parasite burden [87]. This would allow for reduction in parasite invasion limiting tissue pathology and recruitment of immune cells to the local area. These findings suggest that parasite EVs may play an important role in tissue tropism.

Characterization of protein secretion by *L. donovani, L. mexicana* and *L. major* showed that EVs were present in culture media. Subsequent proteomic analysis detected a significant enrichment in proteins previously identified in EVs from other eukaryotes and known parasite virulence factors [88,89]. Many of these immunomodulatory proteins are required for survival

during host cell invasion [76]. Functional studies showed that the addition of purified *L. donovani* EVs to host derived macrophages *in vitro* resulted in an initial induction of IL-8 secretion. Subsequent long-term treatment of monocytes with purified EVs inhibited TNF production and decreased secretion of IL-8 [76] (**Table 1.2**). Consistent with *in vitro* immunomodulation, direct injection of *Leishmania* spp. EVs followed by parasite challenge three weeks post injection significantly increased parasite loads for *L. donovani* and *L. major [63]*. A recent study has also shown that EVs may play an important role in *Leishmania* spp. transmission to a mammalian host. These parasites produce EVs with in the sand fly vector and are egested, along with parasites, into the mammalian host and cause an increased inflammatory response [90]. EVs have also been implicated in parasite-mediated alterations to organ function. Infection of *L. donovani* in mice results in liver cell invasion and reduction in serum cholesterol levels due to altered lipid metabolism in the liver [65]. This reduction in serum cholesterol levels is due to alterations in miR-122 mediated gene repression [65]. Treatment of hepatoma cells with purified EVs recapitulated observed changes to host miR-122 and was dependent on the EV cargo protein metalloprotease gp63 [65]. Purified gp63 degraded Dicer1 *in vitro* and decreased miR-122 processing. Over expression of Dicer1 or expression of a miR-122 variant that does not require processing by Dicer1 rescued EV-mediated changes to miR-122 regulation. Subsequent treatment of mice with gp63 decreased Dicer1 levels and miR-122 processing *in vivo* [65] (**Table 1.2**). These studies suggest that *Leishmania* spp EVs may have a wide range of targets within a mammalian host, alter the immune response and change host cell metabolism.

Previous studies showed the secretome of *T. brucei* differs between isolates and that this difference correlates with increased virulence, disease progression and immune responses [91]. In studies reported in Chapter 4, of this thesis I show that EV fusion with murine and human

erythrocyte membranes is mediated by an unidentified EV surface exposed protein [77]. Through membrane fusion with erythrocytes, *T. brucei* EVs transfer lipids and parasite specific antigens, including the immunogenic variant surface glycoprotein (VSG). Fusion of EVs with erythrocytes results in alterations of the membrane physical properties by increasing lipid packing interactions and rigidity. These changes may cause clearance by liver and spleen myeloid cells, as deposition of foreign antigens and membrane revivification are signals for erythrocyte clearance [77]. *T. brucei* infection results in severe anemia in non-primate mammals, often causing death of the host [92,93]. The *ex vivo* treatment of erythrocytes with purified EVs caused rapid erythrocyte removal in naïve mice with ~20% clearance of treated erythrocytes in one hour (**Table 1.2**). The population of EV treated erythrocytes became stable in the circulation, such that at twenty-four hours there was no additional clearance. These observations suggest that there may be an erythrocyte repair mechanism or off rate associated with parasite antigen transfer. This could be explained by the constant clearance of erythrocyte membrane components by their EVs. The direct *in vivo* injection of EVs caused anemia in two different mouse strains showing 6-11% clearance within twenty-four hours [77] (**Table 1.2**). These study suggest that severe anemia during *T. brucei* infection may be caused by biochemical and biophysical remodeling of host erythrocytes mediated by EVs.

References

1. Matthews KR (2005) The developmental cell biology of Trypanosoma brucei. J Cell Sci 118: 283-290.

2. Vickerman K (1985) Developmental cycles and biology of pathogenic trypanosomes. Br Med Bull 41: 105-114.

3. Dyer NA, Rose C, Ejeh NO, Acosta-Serrano A (2013) Flying tryps: survival and maturation of trypanosomes in tsetse flies. Trends Parasitol 29: 188-196.

4. Trindade S, Rijo-Ferreira F, Carvalho T, Pinto-Neves D, Guegan F, et al. (2016) Trypanosoma brucei Parasites Occupy and Functionally Adapt to the Adipose Tissue in Mice. Cell Host Microbe 19: 837-848.

5. Timms MW, van Deursen FJ, Hendriks EF, Matthews KR (2002) Mitochondrial development during life cycle differentiation of African trypanosomes: evidence for a kinetoplast-dependent differentiation control point. Mol Biol Cell 13: 3747-3759.

6. Bringaud F, Riviere L, Coustou V (2006) Energy metabolism of trypanosomatids: adaptation to available carbon sources. Mol Biochem Parasitol 149: 1-9.

7. Parsons M (2004) Glycosomes: parasites and the divergence of peroxisomal purpose. Mol Microbiol 53: 717-724.

8. Michels PA, Bringaud F, Herman M, Hannaert V (2006) Metabolic functions of glycosomes in trypanosomatids. Biochim Biophys Acta 1763: 1463-1477.

9. Haanstra JR, Gonzalez-Marcano EB, Gualdron-Lopez M, Michels PA (2016) Biogenesis, maintenance and dynamics of glycosomes in trypanosomatid parasites. Biochim Biophys Acta 1863: 1038-1048.

10. Coustou V, Besteiro S, Biran M, Diolez P, Bouchaud V, et al. (2003) ATP generation in the Trypanosoma brucei procyclic form: cytosolic substrate level is essential, but not oxidative phosphorylation. J Biol Chem 278: 49625-49635.

11. Brown SV, Hosking P, Li J, Williams N (2006) ATP synthase is responsible for maintaining mitochondrial membrane potential in bloodstream form Trypanosoma brucei. Eukaryot Cell 5: 45-53.

12. van Weelden SW, Fast B, Vogt A, van der Meer P, Saas J, et al. (2003) Procyclic Trypanosoma brucei do not use Krebs cycle activity for energy generation. J Biol Chem 278: 12854-12863.

13. Rohrer SP, Michelotti EF, Torri AF, Hajduk SL (1987) Transcription of kinetoplast DNA minicircles. Cell 49: 625-632.

14. Adler BK, Hajduk SL (1994) Mechanisms and origins of RNA editing. Curr Opin Genet Dev 4: 316-322.

15. Hajduk SL, Harris ME, Pollard VW (1993) RNA editing in kinetoplastid mitochondria. FASEB J 7: 54-63.

16. Pollard VW, Rohrer SP, Michelotti EF, Hancock K, Hajduk SL (1990) Organization of minicircle genes for guide RNAs in Trypanosoma brucei. Cell 63: 783-790.

17. Harris ME, Moore DR, Hajduk SL (1990) Addition of uridines to edited RNAs in trypanosome mitochondria occurs independently of transcription. J Biol Chem 265: 11368-11376.

18. Ochsenreiter T, Cipriano M, Hajduk SL (2008) Alternative mRNA editing in trypanosomes is extensive and may contribute to mitochondrial protein diversity. PLoS One 3: e1566.

19. Hajduk S, Ochsenreiter T (2010) RNA editing in kinetoplastids. RNA Biol 7: 229-236.

20. Aphasizhev R, Aphasizheva I (2011) Uridine insertion/deletion editing in trypanosomes: a playground for RNA-guided information transfer. Wiley Interdiscip Rev RNA 2: 669-685.

21. Aphasizhev R, Aphasizheva I (2011) Mitochondrial RNA processing in trypanosomes. Res Microbiol 162: 655-663.

22. Ochsenreiter T, Hajduk SL (2006) Alternative editing of cytochrome c oxidase III mRNA in trypanosome mitochondria generates protein diversity. EMBO Rep 7: 1128-1133.

23. Ochsenreiter T, Anderson S, Wood ZA, Hajduk SL (2008) Alternative RNA editing produces a novel protein involved in mitochondrial DNA maintenance in trypanosomes. Mol Cell Biol 28: 5595-5604.

24. Choudhury R, Tsai YS, Dominguez D, Wang Y, Wang Z (2012) Engineering RNA endonucleases with customized sequence specificities. Nat Commun 3: 1147.

25. Zhang W, Wang Y, Dong S, Choudhury R, Jin Y, et al. (2014) Treatment of type 1 myotonic dystrophy by engineering site-specific RNA endonucleases that target (CUG)(n) repeats. Mol Ther 22: 312-320.

26. Szempruch AJ, Choudhury R, Wang Z, Hajduk SL (2015) In vivo analysis of trypanosome mitochondrial RNA function by artificial site-specific RNA endonuclease-mediated knockdown. RNA 21: 1781-1789.

27. Jeffery CJ (1999) Moonlighting proteins. Trends Biochem Sci 24: 8-11.

28. Gancedo C, Flores CL, Gancedo JM (2014) Evolution of moonlighting proteins: insight from yeasts. Biochem Soc Trans 42: 1715-1719.

29. Gancedo C, Flores CL (2008) Moonlighting proteins in yeasts. Microbiol Mol Biol Rev 72: 197-210, table of contents.

30. Perham RN (1991) Domains, motifs, and linkers in 2-oxo acid dehydrogenase multienzyme complexes: a paradigm in the design of a multifunctional protein. Biochemistry 30: 8501-8512.

31. Sykes SE, Hajduk SL (2013) Dual functions of alpha-ketoglutarate dehydrogenase E2 in the Krebs cycle and mitochondrial DNA inheritance in Trypanosoma brucei. Eukaryot Cell 12: 78-90.

32. Sykes S, Szempruch A, Hajduk S (2015) The krebs cycle enzyme alpha-ketoglutarate decarboxylase is an essential glycosomal protein in bloodstream African trypanosomes. Eukaryot Cell 14: 206-215.

33. Hutchinson OC, Picozzi K, Jones NG, Mott H, Sharma R, et al. (2007) Variant Surface Glycoprotein gene repertoires in Trypanosoma brucei have diverged to become strain-specific. BMC Genomics 8: 234.

34. Rudenko G (2005) Maintaining the protective variant surface glycoprotein coat of African trypanosomes. Biochem Soc Trans 33: 981-982.

35. Mugnier MR, Cross GA, Papavasiliou FN (2015) The in vivo dynamics of antigenic variation in Trypanosoma brucei. Science 347: 1470-1473.

36. Stockdale C, Swiderski MR, Barry JD, McCulloch R (2008) Antigenic variation in Trypanosoma brucei: joining the DOTs. PLoS Biol 6: e185.

37. Hovel-Miner G, Mugnier M, Papavasiliou FN, Pinger J, Schulz D (2015) A Host-Pathogen Interaction Reduced to First Principles: Antigenic Variation in T. brucei. Results Probl Cell Differ 57: 23-46.

38. Pays E, Vanhollebeke B, Uzureau P, Lecordier L, Perez-Morga D (2014) The molecular arms race between African trypanosomes and humans. Nat Rev Microbiol 12: 575-584.

39. Harrington JM, Howell S, Hajduk SL (2009) Membrane permeabilization by trypanosome lytic factor, a cytolytic human high density lipoprotein. J Biol Chem 284: 13505-13512.

40. Greene AS, Hajduk SL (2016) Trypanosome Lytic Factor-1 Initiates Oxidation-stimulated Osmotic Lysis of Trypanosoma brucei brucei. J Biol Chem 291: 3063-3075.

41. De Greef C, Hamers R (1994) The serum resistance-associated (SRA) gene of Trypanosoma brucei rhodesiense encodes a variant surface glycoprotein-like protein. Mol Biochem Parasitol 68: 277-284.

42. Xong HV, Vanhamme L, Chamekh M, Chimfwembe CE, Van Den Abbeele J, et al. (1998) A VSG expression site-associated gene confers resistance to human serum in Trypanosoma rhodesiense. Cell 95: 839-846.

43. Stephens NA, Hajduk SL (2011) Endosomal localization of the serum resistance-associated protein in African trypanosomes confers human infectivity. Eukaryot Cell 10: 1023-1033.

44. Oli MW, Cotlin LF, Shiflett AM, Hajduk SL (2006) Serum resistance-associated protein blocks lysosomal targeting of trypanosome lytic factor in Trypanosoma brucei. Eukaryot Cell 5: 132-139.

45. Gibson W, Peacock L, Ferris V, Fischer K, Livingstone J, et al. (2015) Genetic recombination between human and animal parasites creates novel strains of human pathogen. PLoS Negl Trop Dis 9: e0003665.

46. Szempruch AJ, Sykes SE, Kieft R, Dennison L, Becker AC, et al. (2016) Extracellular Vesicles from Trypanosoma brucei Mediate Virulence Factor Transfer and Cause Host Anemia. Cell 164: 246-257.

47. Kieft R, Capewell P, Turner CM, Veitch NJ, MacLeod A, et al. (2010) Mechanism of Trypanosoma brucei gambiense (group 1) resistance to human trypanosome lytic factor. Proc Natl Acad Sci U S A 107: 16137-16141.

48. Capewell P, Cooper A, Clucas C, Weir W, Macleod A (2015) A co-evolutionary arms race: trypanosomes shaping the human genome, humans shaping the trypanosome genome. Parasitology 142 Suppl 1: S108-119.

49. DeJesus E, Kieft R, Albright B, Stephens NA, Hajduk SL (2013) A single amino acid substitution in the group 1 Trypanosoma brucei gambiense haptoglobin-hemoglobin receptor abolishes TLF-1 binding. PLoS Pathog 9: e1003317.

50. Capewell P, Clucas C, DeJesus E, Kieft R, Hajduk S, et al. (2013) The TgsGP gene is essential for resistance to human serum in Trypanosoma brucei gambiense. PLoS Pathog 9: e1003686.

51. Stijlemans B, Cnops J, Naniima P, Vaast A, Bockstal V, et al. (2015) Development of a pHrodo-based assay for the assessment of in vitro and in vivo erythrophagocytosis during experimental trypanosomosis. PLoS Negl Trop Dis 9: e0003561.

52. Naessens J (2006) Bovine trypanotolerance: A natural ability to prevent severe anaemia and haemophagocytic syndrome? Int J Parasitol 36: 521-528.

53. Gould SJ, Raposo G (2013) As we wait: coping with an imperfect nomenclature for extracellular vesicles. J Extracell Vesicles 2.

54. Valadi H, Ekstrom K, Bossios A, Sjostrand M, Lee JJ, et al. (2007) Exosome-mediated transfer of mRNAs and microRNAs is a novel mechanism of genetic exchange between cells. Nat Cell Biol 9: 654-659.

55. Coakley G, Maizels RM, Buck AH (2015) Exosomes and Other Extracellular Vesicles: The New Communicators in Parasite Infections. Trends Parasitol 31: 477-489.

56. Schwechheimer C, Kuehn MJ (2015) Outer-membrane vesicles from Gram-negative bacteria: biogenesis and functions. Nat Rev Microbiol 13: 605-619.

57. Brown L, Wolf JM, Prados-Rosales R, Casadevall A (2015) Through the wall: extracellular vesicles in Gram-positive bacteria, mycobacteria and fungi. Nat Rev Microbiol 13: 620-630.

58. Thery C (2015) Cancer: Diagnosis by extracellular vesicles. Nature 523: 161-162.

59. Zomer A, Maynard C, Verweij FJ, Kamermans A, Schafer R, et al. (2015) In Vivo imaging reveals extracellular vesicle-mediated phenocopying of metastatic behavior. Cell 161: 1046-1057.

60. Marti M, Johnson PJ (2016) Emerging roles for extracellular vesicles in parasitic infections. Curr Opin Microbiol 32: 66-70.

61. Mantel PY, Marti M (2014) The role of extracellular vesicles in Plasmodium and other protozoan parasites. Cell Microbiol 16: 344-354.

62. Twu O, de Miguel N, Lustig G, Stevens GC, Vashisht AA, et al. (2013) Trichomonas vaginalis exosomes deliver cargo to host cells and mediate hostratioparasite interactions. PLoS Pathog 9: e1003482.

63. Silverman JM, Clos J, Horakova E, Wang AY, Wiesgigl M, et al. (2010) Leishmania exosomes modulate innate and adaptive immune responses through effects on monocytes and dendritic cells. J Immunol 185: 5011-5022.

64. Silverman JM, Reiner NE (2011) Leishmania exosomes deliver preemptive strikes to create an environment permissive for early infection. Front Cell Infect Microbiol 1: 26.

65. Ghosh J, Bose M, Roy S, Bhattacharyya SN (2013) Leishmania donovani targets Dicer1 to downregulate miR-122, lower serum cholesterol, and facilitate murine liver infection. Cell Host Microbe 13: 277-288.

66. Regev-Rudzki N, Wilson DW, Carvalho TG, Sisquella X, Coleman BM, et al. (2013) Cell-cell communication between malaria-infected red blood cells via exosome-like vesicles. Cell 153: 1120-1133.

67. Mantel PY, Hoang AN, Goldowitz I, Potashnikova D, Hamza B, et al. (2013) Malaria-infected erythrocyte-derived microvesicles mediate cellular communication within the parasite population and with the host immune system. Cell Host Microbe 13: 521-534.

68. Garcia-Silva MR, das Neves RF, Cabrera-Cabrera F, Sanguinetti J, Medeiros LC, et al. (2014) Extracellular vesicles shed by Trypanosoma cruzi are linked to small RNA pathways, life cycle regulation, and susceptibility to infection of mammalian cells. Parasitol Res 113: 285-304.

69. Cocucci E, Meldolesi J (2015) Ectosomes and exosomes: shedding the confusion between extracellular vesicles. Trends Cell Biol 25: 364-372.

70. Harding CV, Heuser JE, Stahl PD (2013) Exosomes: looking back three decades and into the future. J Cell Biol 200: 367-371.

71. Harding C, Heuser J, Stahl P (1983) Receptor-mediated endocytosis of transferrin and recycling of the transferrin receptor in rat reticulocytes. J Cell Biol 97: 329-339.

72. Pan BT, Johnstone RM (1983) Fate of the transferrin receptor during maturation of sheep reticulocytes in vitro: selective externalization of the receptor. Cell 33: 967-978.

73. Bayer-Santos E, Aguilar-Bonavides C, Rodrigues SP, Cordero EM, Marques AF, et al. (2013) Proteomic analysis of Trypanosoma cruzi secretome: characterization of two populations of extracellular vesicles and soluble proteins. J Proteome Res 12: 883-897.

74. Silverman JM, Chan SK, Robinson DP, Dwyer DM, Nandan D, et al. (2008) Proteomic analysis of the secretome of Leishmania donovani. Genome Biol 9: R35.

75. Wood CR, Rosenbaum JL (2015) Ciliary ectosomes: transmissions from the cell's antenna. Trends Cell Biol 25: 276-285.

76. Silverman JM, Clos J, de'Oliveira CC, Shirvani O, Fang Y, et al. (2010) An exosome-based secretion pathway is responsible for protein export from Leishmania and communication with macrophages. J Cell Sci 123: 842-852.

77. Szempruch AJ, Sykes SE, Kieft R, Dennison L, Becker AC, et al. (2016) Extracellular Vesicles from Trypanosoma brucei Mediate Virulence Factor Transfer and Cause Host Anemia. Cell 164: 246-257.

78. da Silveira JF, Abrahamsohn PA, Colli W (1979) Plasma membrane vesicles isolated from epimastigote forms of Trypanosoma cruzi. Biochim Biophys Acta 550: 222-232.

79. Goncalves MF, Umezawa ES, Katzin AM, de Souza W, Alves MJ, et al. (1991) Trypanosoma cruzi: shedding of surface antigens as membrane vesicles. Exp Parasitol 72: 43-53.

80. Bayer-Santos E, Lima FM, Ruiz JC, Almeida IC, da Silveira JF (2014) Characterization of the small RNA content of Trypanosoma cruzi extracellular vesicles. Mol Biochem Parasitol 193: 71-74.

81. Garcia-Silva MR, Cabrera-Cabrera F, das Neves RF, Souto-Padron T, de Souza W, et al. (2014) Gene expression changes induced by Trypanosoma cruzi shed microvesicles in mammalian host cells: relevance of tRNA-derived halves. Biomed Res Int 2014: 305239.

82. Lambertz U, Oviedo Ovando ME, Vasconcelos EJ, Unrau PJ, Myler PJ, et al. (2015) Small RNAs derived from tRNAs and rRNAs are highly enriched in exosomes from both old and new world Leishmania providing evidence for conserved exosomal RNA Packaging. BMC Genomics 16: 151.

83. Cao M, Ning J, Hernandez-Lara CI, Belzile O, Wang Q, et al. (2015) Uni-directional ciliary membrane protein trafficking by a cytoplasmic retrograde IFT motor and ciliary ectosome shedding. Elife 4.

84. Truc P, Buscher P, Cuny G, Gonzatti MI, Jannin J, et al. (2013) Atypical human infections by animal trypanosomes. PLoS Negl Trop Dis 7: e2256.

85. Trocoli Torrecilhas AC, Tonelli RR, Pavanelli WR, da Silva JS, Schumacher RI, et al. (2009) Trypanosoma cruzi: parasite shed vesicles increase heart parasitism and generate an intense inflammatory response. Microbes Infect 11: 29-39.

86. Nogueira PM, Ribeiro K, Silveira AC, Campos JH, Martins-Filho OA, et al. (2015) Vesicles from different Trypanosoma cruzi strains trigger differential innate and chronic immune responses. J Extracell Vesicles 4: 28734.

87. Martins NO, Souza RT, Cordero EM, Maldonado DC, Cortez C, et al. (2015) Molecular Characterization of a Novel Family of Trypanosoma cruzi Surface Membrane Proteins (TcSMP) Involved in Mammalian Host Cell Invasion. PLoS Negl Trop Dis 9: e0004216.

88. Hassani K, Shio MT, Martel C, Faubert D, Olivier M (2014) Absence of metalloprotease GP63 alters the protein content of Leishmania exosomes. PLoS One 9: e95007.

89. Hassani K, Olivier M (2013) Immunomodulatory impact of leishmania-induced macrophage exosomes: a comparative proteomic and functional analysis. PLoS Negl Trop Dis 7: e2185.

90. Atayde VD, Aslan H, Townsend S, Hassani K, Kamhawi S, et al. (2015) Exosome Secretion by the Parasitic Protozoan Leishmania within the Sand Fly Midgut. Cell Rep 13: 957-967.

91. Geiger A, Hirtz C, Becue T, Bellard E, Centeno D, et al. (2010) Exocytosis and protein secretion in Trypanosoma. BMC Microbiol 10: 20.

92. Berardi R, Braconi C, Mantello G, Scartozzi M, Del Prete S, et al. (2006) Anemia may influence the outcome of patients undergoing neo-adjuvant treatment of rectal cancer. Ann Oncol 17: 1661-1664.

93. Berthier D, Breniere SF, Bras-Goncalves R, Lemesre JL, Jamonneau V, et al. (2016) Tolerance to Trypanosomatids: A Threat, or a Key for Disease Elimination? Trends Parasitol 32: 157-168.

Figures

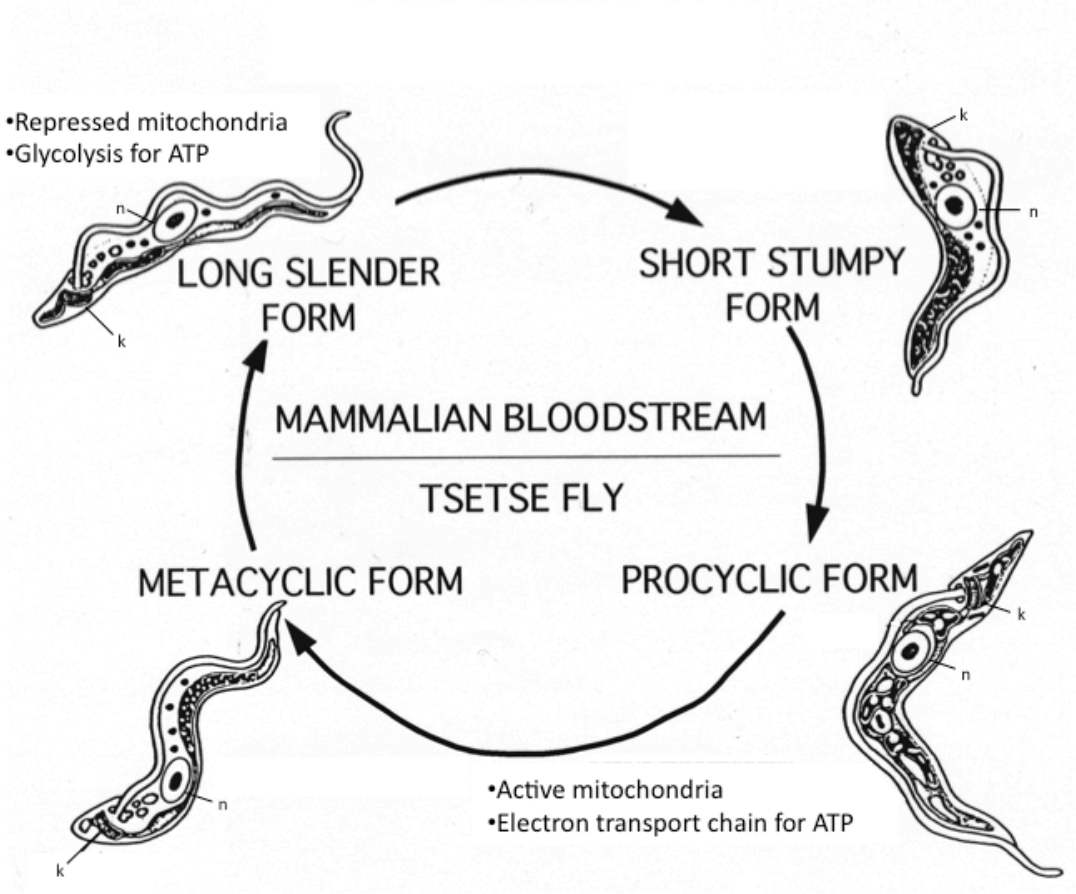

Figure 1.1. Biphasic lifecycle of *Trypanosoma brucei*. *T. brucei* cycles between an insect vector and mammalian host. During this life cycle progression these cells undergo morphological and biochemical changes. This diagram outlines major adaptations of the proliferative and infective forms of this parasite. Abbreviations: nucleus (n) and kinetoplast (k). (Adapted from Vickerman, *British Medical Bulletin*, 1985).

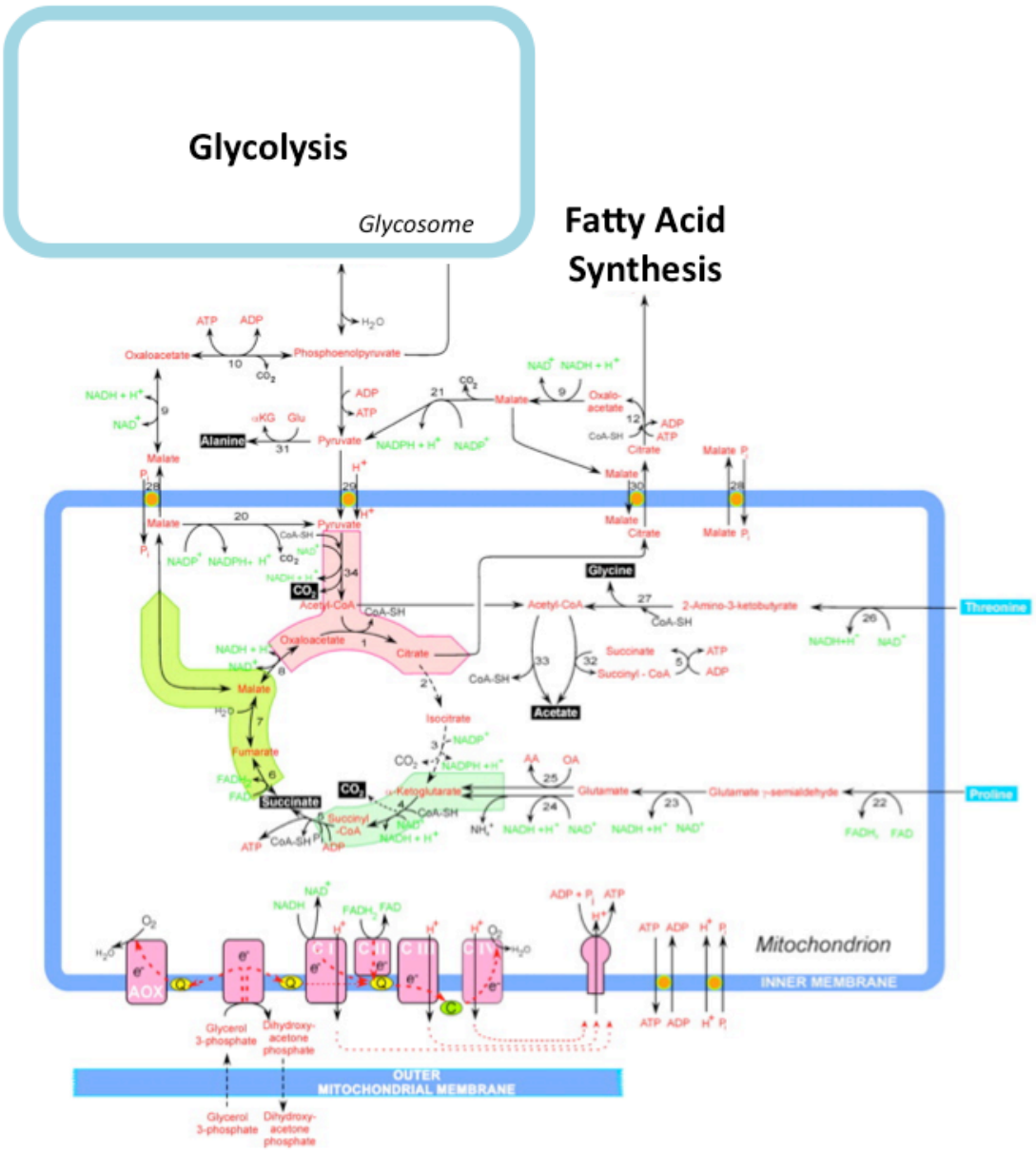

Figure 1.2. Diagram of metabolic pathways in procyclic form *T. brucei*. These cells have an active TCA cycle and rely on the proton gradient generated by the electron transport chain to produce ATP. In general this life cycle represses glycolysis and has fewer glycosomes in their cytoplasm. In contrast bloodstream form *T. brucei* rely on glycolysis for ATP generation, repress their TCA cycle function and instead hydrolyze ATP in the mitochondria to maintain a proton gradient for the import of RNAs and proteins. Abbreviations: alternative oxidase; NADH

dehydrogensase (CI); succinate dehydrogenase (CII); cytochrome bc1 (CIII); cytochorme c oxidase (CIV). (Adapted from van Weelden et al., *Journal of Biological Chemistry*, 2005).

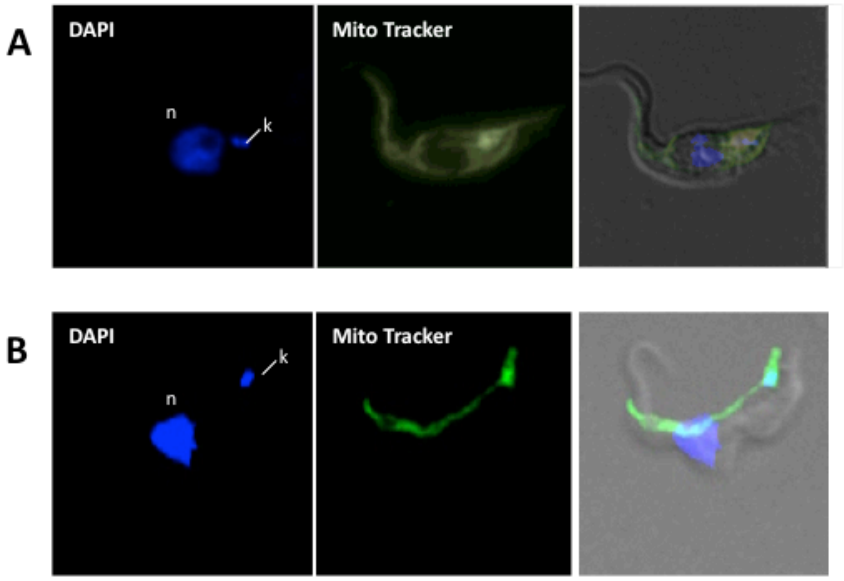

Figure 1.3. Mitochondrial developmental regulation between PF and BF *T. brucei.* In response to carbon source availability the different life cycle stages of *T. brucei* rely on different mechanisms for ATP production. **A)** In the PF stage cells use the mitochondrial electron transport chain to generate a proton gradient to drive the F_oF_1 ATPase for the generation of ATP. This results in a volumetric increase in the mitochondria and a complex branching cristae structure. **B)** In the BF stage cells instead rely on glycolysis in cytoplasmic glycosomes. This results in a reduction in mitochondrial volume and generation of a tubular structure. Abbreviations: nucleus (n) and kinetoplast (k).

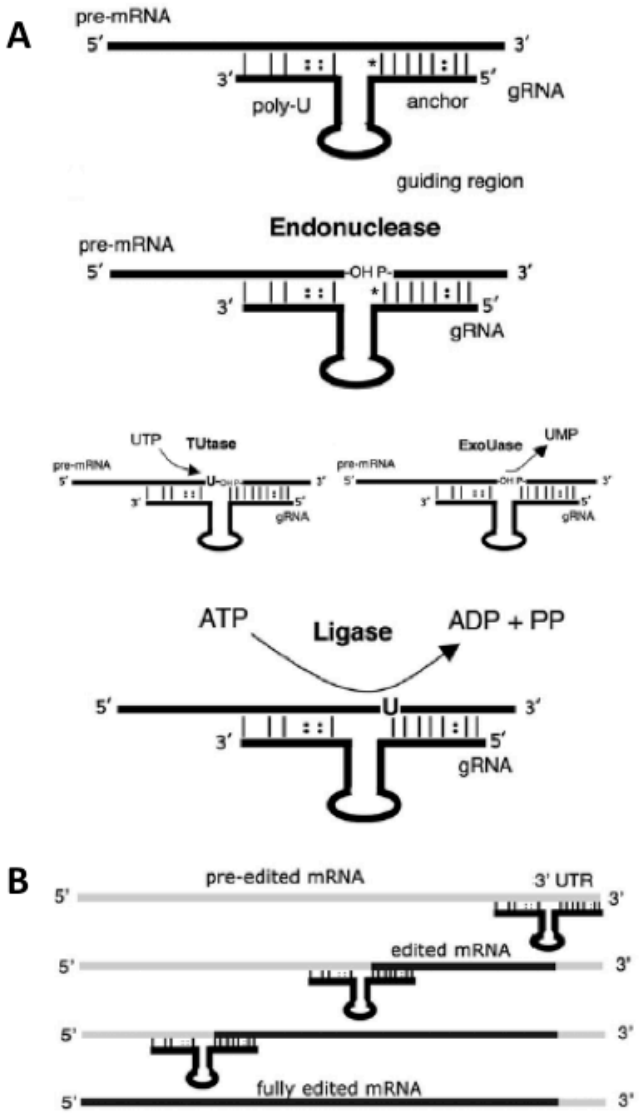

Figure 1.4. Diagram of mitochondrial uridine insertion/deletion RNA editing. **A)** Guide RNAs bind to their pre-mRNAs through the anchor duplex region. This pairing is facilitated through canonical nucleobase interactions (solid lines) and G:U pairings (dotted lines). The first mismatch between gRNA and pre-mRNA signals for endonuclealytic clevage of the pre-mRNA. After cleavage a uridine residue is added by a terminal uridylyl transferase (TUTase) during insertion editing. During deletion editing an exonuclease (ExoUase) removes one uridine residue from the pre-mRNA, after insertion or deletion the cleaved pre-mRNA ligated together by an

RNA ligase. **B)** The process of mRNA editing occurs in a 3' to 5' orientation on the pre-mRNA and initiates by a target gRNA binding in the 3' UTR of its target. (Adapted from Hajduk and Ochsenreiter, *RNA Biology*, 2010).

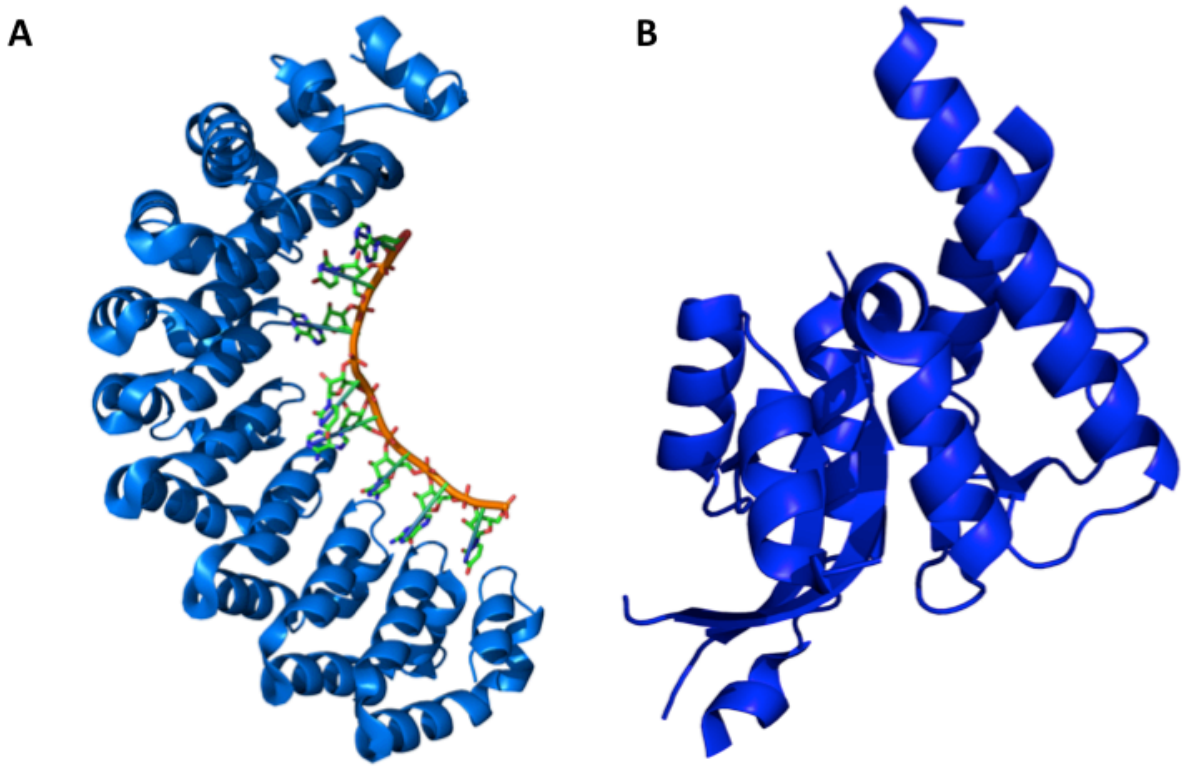

Figure 1.5. Artificial site-specific RNA endonucleases (ASRE). An ASRE is a engineered fusion enzyme which combines a single-stranded RNA sequence binding motif with an endonuclease domain. **A)** The Pumilio/FBF (PUF) domain recognizes 8-nucleotide single-stranded regions of RNA through amino acid contacts with the Watson Crick face of each nucleobase. **B)** The PIN endonuclease of SMG6 is a nonspecific endoribonuclease which cleaves the target substrat after binding. (PDB ID 2YJY and 2HWW).

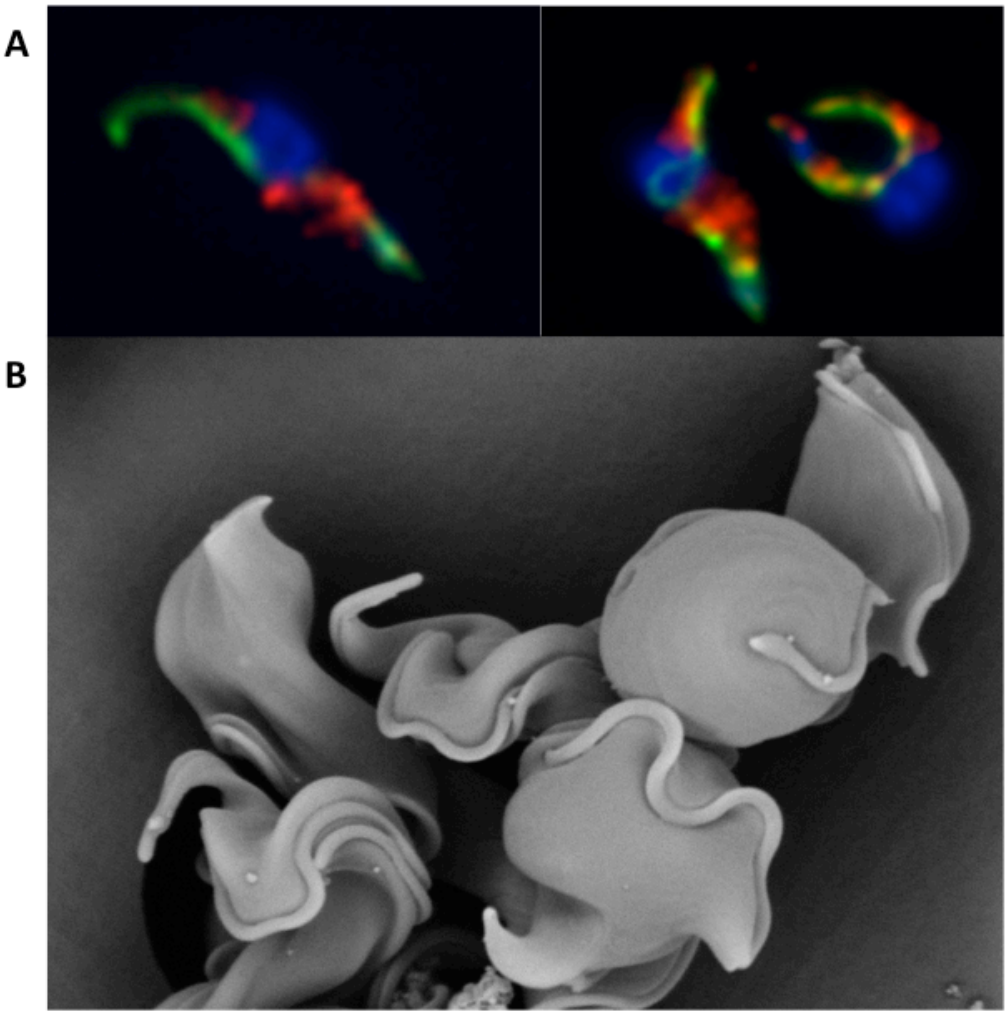

Figure 1.6. Bloodstream form (BF) *Trypanosoma brucei* repress the tricarboxylic acid cycle (TCA) while maintaining expression of three critical TCA cycle protein components of the alpha ketoglutarate dehydrogenase complex (α-KDE1, 2 and 3). **A)** Non-overlapping fluorescent localization of α-KDE1 (red) and its canonical binding partner protein α-KDE2 (green). Further analysis has shown that α-KDE1 localized to the glycosome while α-KDE2 was mitochondrial in BF *T. brucei*. **B) S**canning electron micrograph after 18hr RNAi induced knockdown of E1. Loss of E1 mRNA results in severe morphological changes caused by rapidly swelling of the flagellar pocket. (Adapted from Sykes et al., *Eukaryotic Cell*, 2015 Cover).

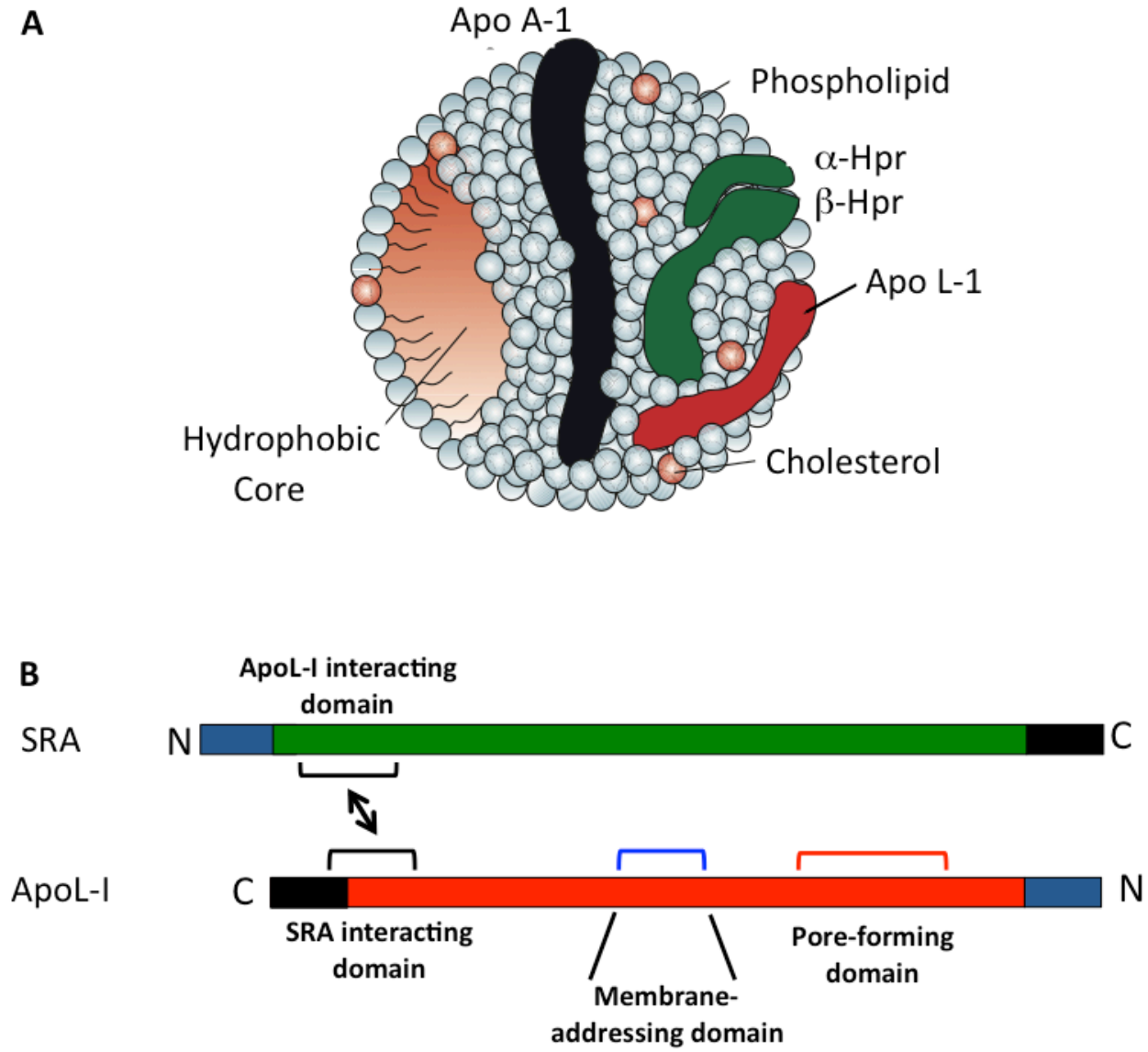

Figure 1.7. Mechanisms of defense for host infection and parasite persistence. **A)** Humans and higher primates are innately immune to African trypanosomes by virtue of circulating trypanosome lytic factors. TLF-1 is a high-density lipoprotein comprised of apolipoprotein A-1 (Apo A-1) and the primate specific haptoglobin related protein (HPR) and apolipoprotein L-1 (Apo L-1). The Apo L-1 protein is a pore-forming toxin that results in trypanosome killing. **B)** *Trypanosoma brucei rhodesiense* has evolved a mechanism to prevent the killing activity of Apo L-1 through the expression of the serum reissuance associate proteins (SRA). The N terminal

region of the SRA protein directly interacts with the C terminal portion of Apo L-1 blocking its insertion into membranes and facilitating its turn over.

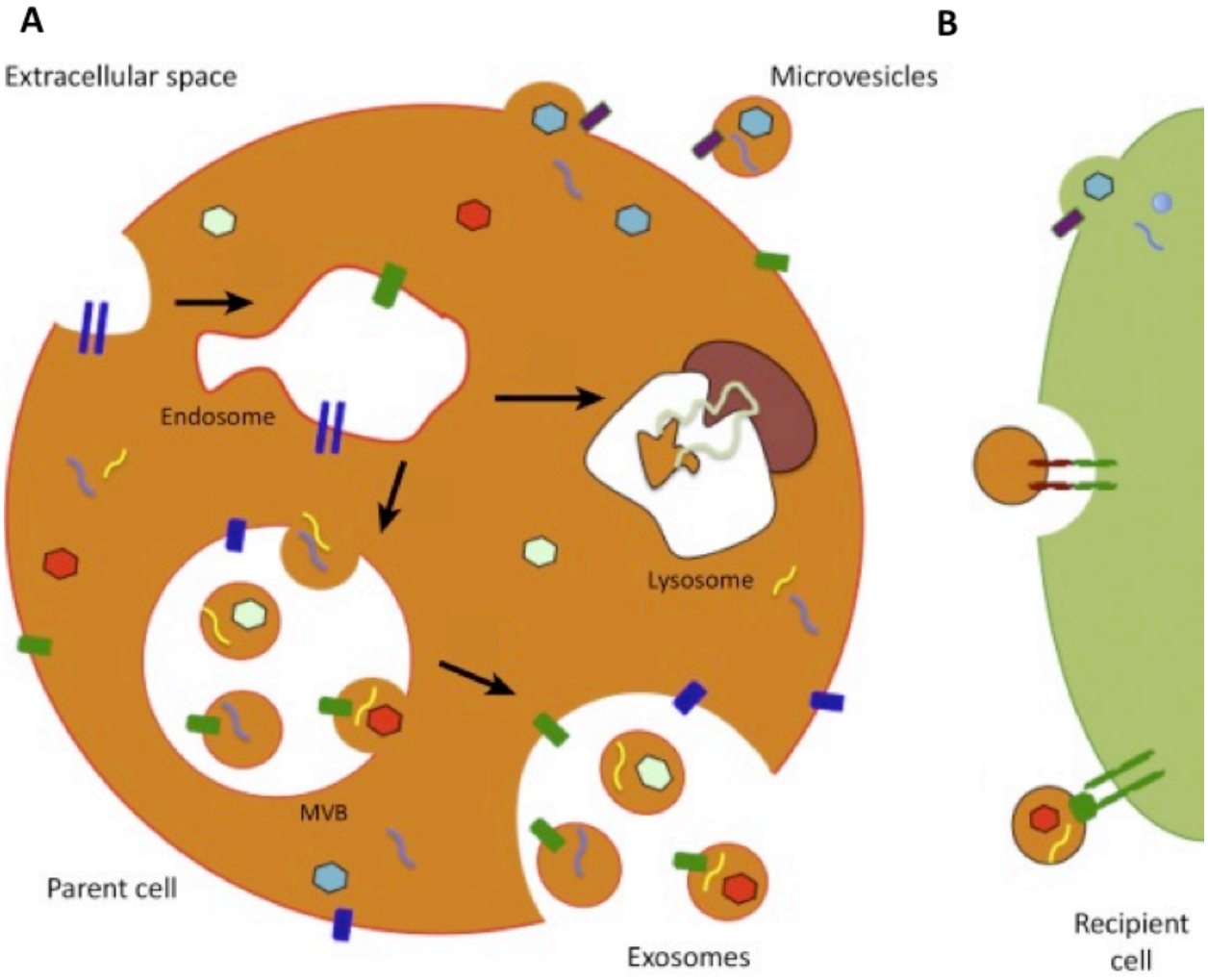

Figure 1.8. Extracellular vesicle secretion and interaction with recipient cells. **A)** EVs can be generated through shedding of the plasma membrane or by secretion from multi vesicular bodies (MVBs). EVs are enriched in cargo components including nucleic acids and proteins. **B)** EV interaction with recipient cells can be receptor mediated, receptor independent or through membrane fusion. (Adapted form Coakley et al., *Trends in Parasitology*, 2015).

Table 1.1. Alternatively Edited Mitochondrial Transcripts in *T. brucei* (Adapted from Ochsenreiter et al., *PLoS ONE*, 2008).

	ND7	ND8	ND9	COXIII	A6
# **Sequences/fully edited**	21/4	78/11	126/18	223/4	69/7
# **Alt. sequences**	1×G10, 1×N12	4×F04	6×F12	2×K12*	3×D08
Alt. editing sites	5	7	67	17	5
Alt. ORFs	2	2	1	1	1
Alt. start codon	Only AUG	UUG (ORF1)	GUG/UUG	UUG	UUG
		GUG (ORF2)			
Alt. stop codon/site	UAG 21nt downstream of *bona fide* UAG	UAA 34nt downstream *of bona fide* UAG	Uses the *bona fide* UAA	UAG 28nt downstream of *bona fide* UAA	Uses the *bona fide* UAG
Alt. gRNAs needed/identified	2/1	2/1	5/1	4/1	3/1
Type of alternative editing	AChange	TChange	ORFCreation	AChange	UTRChange
	TChange	XCreation		TChange	XCreation
				UTRChange	
				XCreation	

AChange, change in amino acid composition; TChange, change of termination codon; XCreation, creation of a junction sequence; UTRChange, change of UTR sequence; ORFCreation, creation of entire open reading frames by alternative editing.
*we have identified 31 cDNA sequences that form alternative open reading frames similar to K12 with minor amino acid changes in the junction region, these sequences are not identical to K12.

Table 1.2. Extracellular vesicles in the kinetoplastids *L. donovani*, *T. cruzi* and *T. brucei.*

	Leishmania donovani	Trypanosoma cruzi	Trypanosoma brucei
Disease	Kala azar	Chagas Disease	Human African trypanosomiasis
Transmission	Sand fly	Triatomine bugs	Tsetse fly
Host Recipient Cell Types	Macrophages, Monocytes and Hepatoma cells	Cardiac cells, Splenocytes	Erythrocytes
EV Formation Mechanism	Plasma membrane, Flagellar membrane and MVB	Plasma membrane, Flagellar membrane and MVB	Membrane Nanotubes
EV Interaction Mechanism	Unknown	Unknown	Membrane Fusion
Parasite Interaction Effects	Unknown	Differentiation	TLF Resistance
Host Interaction Effects	Immunomodulation and Dicer1 degradation	Immunomodulation	Anemia

CHAPTER 2

IN VIVO ANALYSIS OF TRYPANOSOME MITOCHONDRIAL RNA FUNCTION BY ARTIFICIAL SITE-SPECIFIC RNA ENDONUCLEASE MEDIATED KNOCKDOWN

Szempruch, A.J, Choudhury, R., Wang, Z., and S.L. Hajduk. RNA. 2015 Oct;21(10):1781-9. doi: 10.1261/rna.052084.115. Reprinted here with permission from the publisher.

Abstract

Trypanosomes possess a unique mitochondrial genome called the kinetoplast DNA (kDNA). Many kDNA genes encode pre-mRNAs that must undergo guide RNA directed editing. In addition, alternative mRNA editing gives rise to diverse mRNAs and several kDNA genes encode open reading frames of unknown function. To better understand the mechanism of RNA editing and the function of mitochondrial RNAs in trypanosomes, we have developed a reverse genetic approach using artificial site-specific RNA endonucleases (ASREs) to directly silence kDNA encoded genes. The RNA binding domain of an ASRE can be programmed to recognize unique 8-nucleotide sequences, allowing the design of ASREs to cleave any target RNA. Utilizing an ASRE containing a mitochondrial localization signal, we targeted the extensively edited mitochondrial mRNA for the subunit A6 of the F_0F_1 ATP synthase (A6) in the procyclic stage of *T. brucei*. This developmental stage, found in the midgut of the insect vector, relies on mitochondrial oxidative phosphorylation for ATP production with A6 forming the critical proton half channel across the inner mitochondrial membrane. Expression of an A6-targeted ASRE in procyclic trypanosomes resulted in a 50% reduction in A6 mRNA levels after 24 hours, a time dependent decrease in mitochondrial membrane potential ($\Delta\Psi m$) and growth arrest. Expression of the A6-ASRE, lacking the mitochondrial localization signal, showed no significant growth defect. The development of the A6-ASRE allowed the first *in vivo* functional analysis of an edited mitochondrial mRNA in *T. brucei* and provides a critical new tool to study mitochondrial RNA biology in trypanosomes.

Introduction

A member of the class Kinetoplastida, *Trypanosoma brucei* is a parasitic protist that causes human African sleeping sickness and Nagana in cattle. *T. brucei* cycles between an insect vector, the tsetse fly, and mammals undergoing dramatic changes in mitochondrial metabolism as a consequence of changes in expression of nuclear and mitochondrial genes (Matthews 2005). In the procyclic form (PF) of *T. brucei*, found in the midgut of the tsetse fly, ATP is mainly produced by the mitochondrial F_oF_1 ATPase driven by the mitochondrial membrane potential ($\Delta\Psi m$) generated by the electron transport chain (Bringaud et al., 2006; Coustou et al, 2003). Mitochondrial oxidative phosphorylation is repressed in bloodstream form (BF) *T. brucei* and these cells generate ATP by substrate level phosphorylation in peroxisome-like organelles called glycosomes (Gualdron-Lopez et al. 2012). Bloodstream form *T. brucei* lack functional respiratory complexes III and IV and ATP is hydrolyzed by the F_oF_1 ATPase driving the movement of protons out of the mitochondria. This catalytic reversal of the F_oF_1 ATPase establishes the $\Delta\Psi m$ needed for the fatty acid synthesis and the import of proteins and RNAs into the mitochondria of BF *T. brucei* (Brown et al. 2006; Schnaufer et al. 2005; Nolan and Voorheis 1992; Stephens et al. 2007).

A defining feature of all kinetoplastids is a unique mitochondrial genome known as the kinetoplast DNA (kDNA) (Jenson and Englund 2012; Lukes et al. 2002). *T. brucei* kDNA comprises ~10% of the total cell DNA and is organized as a large catenated network composed of two different circular DNA elements called maxicircles (~23kb) and minicircles (~1kb). There are approximately 50 maxicircles per kDNA network which encode the 9S and 12S ribosomal RNA, several mitochondrial unidentified open reading frames (MURFs) and 13 canonical

mitochondrial proteins including components of the electron transport chain and subunit 6 of the F_oF_1 ATP synthase (A6) (Aphasizhev and Aphasizheva 2011). However, the coding information in many maxicircle genes is incomplete because their precursor mRNAs (pre-mRNAs) need to be modified post-transcriptionally by a process called RNA editing. RNA editing in trypanosome mitochondria results in either the insertion or deletion of uridines at specific sites in the pre-mRNA, ultimately producing complete open reading frames (Hajduk and Ochsenreiter 2010; Aphasizhev and Aphasizheva 2011). Each kDNA network also contains thousands of minicircles encoding small guide RNAs (gRNAs) that specify the site and number of uridines added or deleted during the editing of pre-mRNAs (Blum and Simpson 1990; Pollard et al. 1990). The pre-mRNA editing proceeds through a series of complex RNA:RNA and RNA:protein interactions with the initial step being the formation of a short duplex between the gRNA and its cognate pre-mRNA immediately 3' to the first (3' most) editing site. This anchoring duplex region of RNA is followed by a region of mismatches between the gRNA and pre-mRNA that corresponds to insertion or deletion editing sites (Ochsenreiter et al. 2007). Mismatches within the pre-mRNA/gRNA produce secondary structural elements leading to the recruitment of the RNA editing core complex (RECC). The RECC is a large protein assembly of ~20S containing all the catalytic activities needed for mRNA editing (Aphasizhev and Aphasizheva 2011; Bohm et al. 2012; Goringer 2012). The processivity of mRNA editing is poorly understood. It is assumed that once a gRNA defined editing domain is complete the initiating gRNA will be displaced by a new gRNA annealing to the partially edited mRNA driving editing in a 3' to 5' direction along the partially edited mRNA. Recent data has shown that the mitochondrial RNA-binding complex 1 (MRB1) plays an essential role in the RNA editing process, allowing for iterative editing of a transcript and tethering editing to other RNA

processing within the mitochondria (Hashimi et al. 2013). All known protein components of the RECC, MRB1 and other mitochondrial editing complexes are nuclear encoded and traffic to the mitochondrion.

While maxicircles are homogeneous in sequence, minicircles are highly heterogeneous containing at least 300 sequence classes (Ochsenreiter et al. 2007). The sequence diversity and the number of minicircles per kDNA network suggests that the sequenced repertoire of gRNAs may be an underrepresentation (Hajduk and Ochsenreiter 2010). The number of gRNAs required to edit all known canonically edited mRNAs is ~200 (Corell et al. 1993). However, to date over 450 gRNAs have been identified, many lack known target sequences in mRNAs edited to encode canonical mitochondrial proteins (Ochsenreiter et al. 2007). This observation led to the discovery of an alternatively edited mRNA encoded by the maxicircle gene for cytochrome oxidase III (COIII) and the subsequent identification of a number of alternatively edited mRNAs that may encode proteins with unknown functions (Ochsenreiter et al. 2006; Ochsenreiter et al. 2008). A recent study sequenced the mitochondrial transcriptome of PF *T. brucei* and showed that among the more than 3 million sequence reads it was possible to identify ~640 major sequence classes of gRNAs (Koslowsky et al. 2014). This data suggests that the total number of unique gRNAs may greatly exceed the number of gRNAs required for canonical editing.

In order to better understand the mechanism of RNA editing, the function of MURFs, and alternatively edited mitochondrial RNAs, new *in vivo* genetic tools are needed. Here we describe the development of a method to specifically knock down mitochondrial RNAs in *T. brucei*, allowing functional analysis of individual mitochondrial encoded genes. Artificial Site-specific RNA Endonucleases (ASREs) combine a series of Pumilio/FBF (PUF) domains, Pumilio (from *Drosophila melanogaster*) and FBF (Fem-3 mRNA-Binding Factor from *Caenorhabditis*

elegans), engineered to specifically recognize and bind an 8-nucleotide single-stranded RNA target sequence, with the PIN domain of SMG6 which has non-specific endoribonuclease activity (Choudhury et al. 2012; Zhang et al. 2014). The single-stranded RNA binding domain (PUF domain) of the ASRE can be reprogrammed to recognize any 8-nucleotide sequence in principle (Cheong and Hall 2006; Dong et al. 2011) allowing the design of ASREs to cleave any target RNA.

To determine whether ASREs could be used to study mitochondrial RNA processing and function in trypanosomes, we targeted the canonically edited mRNA for the A6 subunit of the *T. brucei* mitochondrial F_oF_1-ATPase. This protein is essential in PF *T. brucei* as it couples the electrochemical potential generated by pumping of protons during electron transport to ATP synthesis (Bringaud et al. 2006; Hashimi et al. 2010; Dean et al. 2013). Our results showed that expression of an A6-ASRE, fused to a mitochondrial localization signal (MLS), specifically reduced A6 edited mRNA levels, interfered with proton movement through the F_O complex and was lethal to PF form *T. brucei*.

Results

A6-ASRE and A6-ASRE MLS$^{(-)}$ construct design and expression.

A trypanosome codon optimized ASRE was programmed to recognize the edited sequence, GUUAUUGG, (**Supplemental Figure 2.1A**) in the 3' UTR of A6 mRNA (**Supplemental Figure 2.1B**). This sequence is found only once within the mitochondria. The A6-ASRE contained a FLAG epitope tag and an N-terminal MLS from dihydroplipoyl dehydrogenase Tb11.01.8470 (**Figure 2.1A**). The 14 amino acid MLS has an internal cleavage site that results in the retention of five of the amino acids (Clayton et al. 1995). This short import sequence was selected to limit possible interference with the ASRE protein domains and because

it targets proteins to the mitochondrial matrix (Ochenreiter et al. 2008). Other MLS sequences that have been used successfully for mitochondrial import, such as the Riske iron-sulfur protein MLS, target heterologous proteins to *T. brucei* mitochondria membranes (Priest and Hajduk 1995). There are ~480 nuclear encoded RNAs that contain the A6-ASRE recognition sequence, in order to determine whether A6-ASRE phenotypes were a consequence of mitochondrial activities, a construct encoding the A6-ASRE but lacking the MLS (A6-ASRE $MLS^{(-)}$) was also prepared (**Figure 2.1A**). The A6-ASRE and A6-ASRE $MLS^{(-)}$ constructs were cloned into pLew100 for tetracycline inducible expression in stably transfected PF *T. brucei* (Lister 427 29-13) (Wirtz et al., 1999). Expression of the A6-ASRE following tetracycline induction was verified by northern blot hybridization with a probe specific for the coding sequence of the A6-ASRE (**Figure 2.1B**).

A6-ASRE protein import into mitochondria.

To determine whether the A6-ASRE protein was synthesized and imported into the mitochondrion, total cell lysates were prepared from *T. brucei* tranfectants and fractionated by differential centrifugation (Ochsenreiter et al., 2006; Sykes and Hajduk 2013). Total cell (T), cytosolic (C) and mitochondrial (M) protein fractions were prepared either before (uninduced) or 24 hours post-induction with tetracycline (induced) (**Figure 2.1C**). Mitochondria from induced cells were further fractionated into insoluble membrane (Mm) and soluble matrix fractions (Ma). All cell fractions were separated with SDS-PAGE (10%) and further examined using western blotting with an antibody against the FLAG epitope. Both total cell and cytoplasmic fractions from uninduced and induced cells showed a prominent 50kDa protein that cross-reacted with the FLAG antibody (asterisk). This cross-reacting protein, has previously been described in PF *T. brucei,* was restricted to cytosolic fractions (**Figure 2.1C**). In contrast, a ~60kDa α-FLAG

reacting protein, of the size expected for the A6-ASRE, was detected only following tetracycline induction. This protein fractionated with the mitochondrial matrix (Ma) suggesting the A6-ASRE was imported into PF *T. brucei* mitochondria (**Figure 2.1C**). While the FLAG-tagged A6-ASRE was reproducibly detected in the mitochondrial matrix fractions the levels were low relative to the cytoplasm. However, the FLAG-tagged A6-ASRE is unlikely to be a result of a contaminating cytoplasmic protein since the prominent cross-reactive 50kDa cytosolic protein is undetectable in the mitochondrial matrix. Fractionation of A6-ASRE MLS$^{(-)}$ cells before or 24 hours post-induction shows no ASRE present within the mitochondrial matrix (Ma) (**Supplemental Figure 2.2**).

The effects of A6-ASRE and A6-ASRE MLS$^{(-)}$ expression on PF *T. brucei* growth were analyzed (**Figure 2.1D and 2.E**). A6-ASRE induction resulted in a significant reduction in *T. brucei* growth after 48 hours, whereas growth of A6-ASRE MLS$^{(-)}$ was unaffected for up to six days post-induction. This difference in growth was not because of differences in expression of A6-ASRE and A6-ASRE MLS$^{(-)}$, since both proteins were expressed at comparable levels (**Figures 2.1D and 2.1E, insets**). Together these results indicated that A6-ASRE expression was lethal to PF *T. brucei* and that loss of mitochondrial targeting rescues the growth phenotype. Importantly, these results suggested that the possible off-target activity of the A6-ASRE against cytosolic RNAs does not contribute to the cell growth phenotype.

A6-ASRE knockdown of A6 edited mRNA.

The endoribonuclease cleavage activity of ASREs requires specific binding between the target RNA and the programmed PUF sequence (Choudhury et al. 2012). Analysis of the *T. brucei* mitochondrial RNAs allowed the design of ASRE targeting sequence specific for A6 edited mRNA. However, several nuclear encoded mRNAs were identified with a perfect 8-

nucleotide A6-ASRE target sequence. We used northern blot hybridization of total cellular RNA to evaluated the effect of A6-ASRE expression of mitochondrial A6 mRNA and a cytoplasmic mRNA containing the same 8-nucleotide targeting sequence. Total RNAs prepared from A6-ASRE PF *T. brucei* at 2, 4, 6, 8, 12, 18, 20 and 24 hours post-induction were fractionated by formaldehyde agarose gel electrophoresis and northern blotted. These early time points, prior to changes in cell growth, were chosen to avoid alterations in RNA levels that might be associated with downstream events caused by disrupted mitochondrial function rather than A6-ASRE directed knockdown. The ethidium bromide stained rRNA was used to verify equal RNA loading (**Figure 2.2A**). Levels of A6 edited, cytosolic eukaryotic translation initiation factor (eIF) and cytosolic β-tubulin mRNA was analyzed by northern blotting (**Figure 2.2A**). The relative level of A6-mRNA decreased to approximately 50% of uninduced levels at 18 hours and remained constant through 24 hours post-induction (**Figure 2.2A and 2.2B**). There was no detectable reduction in either the cytosolic eIF mRNA containing the 8-nucleotide A6-ASRE targeting sequence or the highly abundant cytosolic β-tubulin mRNA containing a part of the ASRE targeting sequence (6-nt) (**Figure 2.2A and 2.2B**). These results showed that the A6-ASRE recognized and cleaved the mitochondrial A6 edited mRNA but did not catalyze cleavage of cytoplasmic mRNAs containing perfect or near-perfect 8-nucleotide targets.

A6-ASRE specific knockdown of the A6 edited mRNA.

In order to determine whether the A6-ASRE knockdown was specific for the A6 mitochondrial mRNA and to ensure it was not due to non-specific mitochondrial RNA degradation, we analyzed the effect of the A6-ASRE and the A6-ASRE $MLS^{(-)}$ expression on several mitochondrial mRNAs by RT-qPCR. Total cell RNA, isolated from PF *T. brucei* prior to induction and 24 hours post-induction was used to prepare cDNA (**Figure 2.2C**). Specific

primers were designed for the analysis of edited A6 ATPase (8 of 8-nt ASRE targeting sequence), COIII (7of 8-nt ASRE targeting sequence), and cytochrome b (7 of 8-nt ASRE targeting sequence) mitochondrial mRNAs, as well as, cytosolic eIF (8 of 8-nt targeting sequence) and samples were normalized to the β-tubulin mRNA levels (**Supplemental Figure 2.1B**). Both the A6 edited mRNA and eIF mRNA contained the full 8-nucleotide A6-ASRE targeting sequence (**Figure 2.2C**) (**Supplemental Figure 2.1B**). Consistent with northern results we found a ~40% reduction ($p= 0.0058$) in A6 edited mRNA following 24 hours of A6- ASRE expression, whereas the expression of the A6-ASRE $MLS^{(-)}$ had no effect (**Figure 2.2C**). Neither the A6-ASRE nor the A6-ASRE $MLS^{(-)}$ caused a detectable decrease in eIF mRNA 24 hours post-induction. An additional six cytosolic transcripts containing the 8-nucleotide target sequence were analyzed by RT-qPCR (**Supplemental Figure 2.3**). These transcripts (Tb 427.10.3540; Tb427.10.12820; Tb427.10.3570; Tb427.10.13390; Tb427tmp03.0090; Tb427tmp02.0190) were selected because their orthologs have been shown to be lethal during RNAi (Alford et al. 2011). During 24 hour induction, A6-ASRE cells showed no decrease in the six cytosolic transcripts (**Supplemental Figure 2.3A**). Analysis of the six transcripts in A6-ASRE $MLS^{(-)}$ cells showed no decrease in mRNA levels, but there was an increase of ~40% for three transcripts (Tb427.10.12820; Tb427.10.13390 and Tb427tmp03.0090) (**Supplemental Figure 2.3B**). The lack of eIF and additional cytosolic transcript knockdown and apparent increase in three of the transcripts suggest that the A6-ASRE is inactive in the cytoplasm and may be due to the divalent cation requirement of the ASRE endonuclease. Both Mn^{2+} and Co^{2+} are largely sequestered in mitochondria and endoplasmic reticulum of eukaryotes with little available in the nucleus and cytoplasm (Gavin et al. 1992; Gunter et al. 2009). In order to test this possibility we attempted to supplement PF *T. brucei* growth media with Mn^{2+} to increase

cytosolic concentrations but even low levels of added Mn^{2+} were toxic to cells, possibly due to inhibition of RNA polymerase or oxidative damage of the cells by free Mn^{2+} (Trujillo et al. 2004; Park et al. 2012).

A6-ASRE induction alters mitochondrial function.

The hydrophobicity of A6 precludes direct analysis of the effect of A6-ASRE expression on protein levels. Consistent with the properties of other mitochondria encoded proteins, *T. brucei* A6 cannot be expressed as a recombinant protein and antibodies against the *T. brucei* A6 are unavailable. However, since the A6 plays a critical role in mitochondrial bioenergetics we examined the effects of A6-ASRE induction on the function of A6 in proton translocation and sensitivity to oligomycin. To determine whether reduced expression of the A6 mRNA disrupted mitochondrial $\Delta\Psi m$ we incubated cells with the cationic fluorescent rhodamine derivative tetramethylrhodamine methyl ester (TMRM) (Scaduto and Grotyohann 1999). Mitochondrial localization of this dye requires $\Delta\Psi m$ and initially we treated PF *T. brucei* with a proton half-channel inhibitor, oligomycin, to determine whether inhibition of the mitochondrial ATP synthesis affected membrane potential (**Figure 2.3A, left panel**). Oligomycin rapidly equilibrates into cells and after 5 minutes a small (~10%) but significant increase in $\Delta\Psi m$ was observed. This may reflect the interference of proton binding and movement from the mitochondrial intermembrane space through the A6 proton half channel into the matrix. Over time we observed a reduction of $\Delta\Psi m$ and after 24 hours of oligomycin treatment ~20% decrease in membrane potential. This is likely a consequence of an overall decrease in mitochondrial ATP synthesis. As a control, the TMRM signal was completely lost in depolarized mitochondria after treatment with 20μM of the membrane potential uncoupler carbonyl cyanide *m*-chlorophenyl hydrazone (CCCP). We next compared the relative mitochondrial $\Delta\Psi m$ for uninduced PF *T.*

brucei and 24 hours post-induction of A6-ASRE expression (**Figure 2.3A, right panel**). A6-ASRE induction resulted in a ~25% reduction in ΔΨm at 24 hours. Addition of 20μM CCCP at 24 hours completely collapsed the ΔΨm to ~1% of uninduced levels.

We anticipated that reduction in A6 levels, following A6-ASRE induction, would increase the sensitivity of PF *T. brucei* to oligomycin. To test oligomycin sensitivity, the growth of uninduced and A6-ASRE induced PF *T. brucei* was monitored in the presence of 0.03μM to 3μM oligomycin (**Figure 2.3B**). While both uninduced and A6-ASRE induced cells were oligomycin sensitive the A6-ASRE cells were ~ 100 fold more sensitive with 0.03μM oligomycin reducing survival by ~50% reduction in comparison to 3μM oligomycin for the uninduced cells. Together our results suggest that ASREs are an effective method to specifically knockdown the steady state levels of mitochondrial A6 edited mRNA and provides a new tool to study the function of other mitochondrial RNAs in trypanosomes.

Discussion

Here we report the development of a new genetic tool to study the function of mitochondrial RNAs in kinetoplastids. Using a nuclear encoded, mitochondria localized ASRE we have targeted a specific 8-nucleotide sequence in the edited mitochondrial mRNA for the A6 subunit of the F_1F_O ATPase in PF *T. brucei* (**Figure 2.1 A, B**). The A6-ASRE specifically reduced steady state A6 mRNA levels by ~40% but spares cytosolic RNA with the same target sequence. It may be possible to increase ASRE cleavage efficiency through the optimization of the mitochondrial localization signals, thus enhancing import efficiency and rate. Though we achieve a similar level of RNA knockdown as has been previously reported with ASREs, it may be possible to enhance knockdown by selecting target sequences with more than one site within the RNA of interest, or expressing ASREs against varied target sequences within a single RNA.

This approach may also help to limit the influence of RNA secondary structure which could inhibit ASRE binding and cleavage. In addition, it may be possible to enhance the specificity by expanding the Puf recognition domain of the ASRE, beyond the current 8-nucleotides (Filipovska et al. 2011). This modification may enhance binding affinity for the target RNA substrate and would also allow for the possibility of targeting nuclear encoded RNAs. The catalytic efficiency and activity in other cellular compartments may be improved by using a different RNA endonuclease, in place of the PIN nuclease. The edited A6 mRNA is the only mitochondrial RNA containing the full ASRE target sequence thus providing cleavage specificity within the mitochondrion. Other mitochondrial mRNAs, COIII and CyB, which contain near perfect target sequences (7 of 8 nucleotides) were not affected by A6-ASRE expression (**Figure 2.2**). This result is constant with previous findings showing 7-nucleotide matches were not sufficient for ASRE mediated cleavage (Choudhury et al. 2012) and confirms that non-sepcific RNA clevage does not contribute to A6 mRNA knockdown during A6-ASRE expression. Using the A6 ASRE we showed that the A6 subunit of the mitochondrial ATPase was essential for PF *T. brucei* growth (Figure 1C). Consistent with the critical role of A6 subunit in mitochondrial ATP synthesis we found that A6 mRNA knockdown resulted in increased sensitivity to the antibiotic oligomycin and a time dependent reduction in mitochondrial $\Delta\Psi m$ (**Figure 2.3**).

Until now genetic methods were not available for the functional analysis of specific kDNA encoded RNAs in kinetoplastids. Dyskinetoplastic trypanosomes, akin to petite mutants in yeast, have been studied and have provided limited specific information about the function of individual mitochondrial RNAs since dyskinetoplastic trypanosomes completely lack both

maxicircles and minicircles resulting in pleotropic phenotypes (Schnaufer et al. 2002; Dean et al. 2013). Cell lines carrying a single maxicircle gene mutation have not been reported.

There have been several attempts to study the function of trypanosome mitochondrial RNAs using RNAi knockdowns or gene knockouts of nuclear encoded proteins necessary for mitochondrial mRNA editing. These studies resulted in changes in the abundance of multiple mitochondrial mRNAs and lack specificity for individual mitochondrial RNAs. The knockdown of the kinetoplastid RNA editing protein 6 (KREPA6) was reported to reduce levels of ATPase 6 edited transcripts (Hashimi et al. 2010). Though the levels of ATPase 6 edited mRNA decrease following KREPA6 RNAi this cell line also showed a reduction in other mitochondrial mRNAs analyzed (COIII edited, CyB edited and MURF2 edited).

Another approach used to study the function of mitochondrial encoded proteins relied on the transfection and nuclear expression of a recoded mitochondrial gene (Ochenreiter et al. 2008). In this study a unique, short 60 amino acid hydrophilic portion of the AEP-1, protein encoded by an alternatively edited version of COIII mRNA was transfected into the ribosomal RNA locus within the nucleus of *T. brucei*. Nuclear expression and mitochondrial localization of this truncated version of AEP-1 resulted in a dominant negative phenotype leading to loss of kDNA organization (Ochenreiter et al. 2008). While these experiments successfully defined a function for AEP-1 the application of this approach is limited since most mitochondria encoded proteins are extremely hydrophobic and cannot be synthesized in the cytosol and imported into the mitochondrion. Other direct approaches, including mitochondrial gene knockouts and mitochondrial RNAi have been unsuccessful in trypanosomes.

The recent development of ASRE mediated RNA cleavage has allowed the disruption of specific mitochondrial transcripts to analyze function (Choudhury et al. 2012; Choudhury and

Wang 2014). Target sequence selection is critical since the sequence must be single-stranded and found exclusively on the RNA being targeted. In the studies reported here, we found that the A6-ASRE was specific for the mitochondrial A6 mRNA and did not cleave the cytosolic mRNAs for eIF containing the same 8-nucleotide targeting sequence (Figure 2). This is consistent with previous results that showed an ASRE directed against the mammalian mitochondria encoded NADH dehydrogenase subunit 5 (ND5) was specific and did not cleave cytosolic mRNAs containing the ND5 targeting sequence (Choudhury et al. 2012). This study showed that transfection of HEK293 cells with an ND5-ASRE lacking a mitochondrial localization sequence resulted in accumulation in the cytoplasm but had no effect on cell growth suggesting that nuclear encoded mRNAs were not targeted for cleavage by the ND5-ASRE. The lack of activity of ASREs outside the mitochondrion may be a consequence of the relatively high mitochondrial Mn^{2+} concentration and the metal ion selectivity of the PIN endoribonuclease (Choudhury et al. 2012).

Our studies show the feasibility of using ASREs to specifically target and cleave a mitochondrial mRNA in PF *T. brucei* that results in a loss of function phenotype consistent with the known function of the encoded protein. The results presented here provide the proof of concept to allow application of ASRE targeted knockdowns to investigate the function of other mitochondrial RNAs in trypanosomes.

Methods

Trypanosome cell culture

PF *T. brucei* (Lister 427 29-13) was grown in SM medium supplemented with 10% (v/v) heat inactivated fetal bovine serum at 27°C (Cunningham 1977). SM media was developed specifically to mimic the midgut of the tsetse fly. A previous study reported that a different line

of PF *T. brucei* (EATRO1125) grown in a different medium (SDM-79) with higher glucose concentrations (SDM-79, 11mM; SM, 3.9mM), were able to grow in the presence of oligomycin and that substrate level phosphorylation was sufficient for survival (Coustou et al. 2003). In our studies, PF *T. brucei* Lister 427 29-13 and another line of PF *T. brucei*, TREU 667, were highly susceptible to oligomycin when grown in SM medium thus allowing the effects of A6-ASRE knockdown on mitochondrial energetics to be evaluated (Figure 3)(data not shown).

A6 target sequence selection and ASRE reprogramming

Initially, ATPase A6 edited mRNA sequence was analyzed for potential secondary structure elements that may inhibit ASRE binding and cleavage. The A6 edited sequence was modeled using Mfold and the top lowest free energy models were compared to determine regions of single-stranded RNA (Zuker 2003). From the secondary structural analysis, a unique 8-nucleotide A6 edited mRNA sequence was identified. A6 edited mRNA target sequence, predicted to be single stranded, was compared with known edited and pre-edited transcripts as well as sequenced gRNAs and putative gRNAs derived from minicircle sequencing. From this analysis the GUUAUUGG sequence was selected within A6 mRNA editing site 1 and within the mitochondria is only present at this site. Reprogramming of the ASRE was achieved by altering the repeat helical regions, within the Puf domain, as previously described (Cheong and Hall 2006; Dong et al. 2011; Choudhury et al. 2012; Zhang et al. 2014). Each repeat was altered to recognize the appropriate target nucleotide, within the GUUAUUGG sequence (Supplemental Figure 1A). The A6-ASRE Puf domain was modeled using the template-based structure modeling web server for RaptorX (Källberg et al. 2012).

Inducible expression of A6-ASRE and A6-ASRE MLS$^{(-)}$

To generate inducible A6-ASRE and A6-ASRE MLS$^{(-)}$ constructs we used the previously characterized tetracycline inducible pLew100 vector. The ASRE sequence was amplified from GenArt plasmid pMA-T with ASRE specific primers containing *HindIII* and *BamHI* restriction sites. To generate the inducible A6-ASRE and A6-ASRE MLS$^{(-)}$ specific primers were used that either included or excluded the 14 amino acid MLS and contained *HindIII* and *BamHI* restriction sites. Both sequences were amplified by PCR and cloned into the pLew100 vector, thus generating a tetracycline inducible A6-ASRE and A6-ASRE MLS$^{(-)}$. After cloning into pLew100, the vector was linearized by digestion with *NotI* and was transfected by electroporation into PF *T. brucei* Lister 29-13. Clonal selection was carried out with phleomycin. The resulting clones were analyzed for A6-ASRE and A6-ASRE MLS$^{(-)}$ expression by induction with 1μg/ml tetracycline.

RNA extraction, cDNA synthesis and qPCR analysis

Total cell RNA was extracted from 4x10^8 PF *T. brucei*, uninduced or induced for the expression of A6-ASRE and A6-ASRE MLS$^{(-)}$. Cells were harvested by centrifugation and washed and re-pelleted twice, with phosphate buffered saline. RNA was extracted by Trizole following manufactures protocol. Extracted RNA was either used for analysis on formaldehyde agarose (1%) gels followed by northern blotting or was prepared for analysis by RT-qPCR. RNAs were treated with DNase I prior to cDNA synthesis. Synthesis of cDNAs was carried out with 5μg of DNase treated RNA using a mixture of random 9-mer and oligo dT primers in a 25 μl reaction, with (+RT) and without (-RT) *Avian Myeloblastosis Virus (AMV) reverse transcriptase* (Promega). cDNA was diluted 10-fold and 2.5 μl was used per 25 μl real time PCR reaction. Real time PCR reactions followed previously described methods (Carnes et al. 2005). In brief, 5 μl of forward and reverse primers (1.5 μM) along with 5μl +RT or –RT and 12.5 μL

of SYBR mix (Thermo) was used for a 25 μl reaction. Reaction conditions followed the following cycle parameters 50°C for 2 min and 95°C for 10 min, with 40 cycles of 95°C for 15s and 60°C for 1 min. Previously published primers for real time PCR were used (Carnes et al. 2005) and relative changes were analyzed using the Pfaffl method (Pfaffl 2001) with β-tubulin mRNA used for normalization.

Northern blot analysis

Total cellular RNA (5mg) extracted from induced and uninduced ASRE PF *T. brucei* cells was separated on a 7% formaldehyde 1% agarose gel and blot transferred to a nylon membrane. The membrane was interrogated using radiolabeled probes against edited A6, eIF and β-tubulin. The edited A6 probe was hybridized in an aqueous mix consisting of 20x SSC, 5x Denhardt's solution (Sigma), 1% SDS, 1mM sodium phosphate (pH 7.4), 1mM EDTA and 100 mg/ml salmon sperm DNA (Life Technologies) at 65°C overnight. The nylon membrane was washed three times for 30 min with 6x SSC at 60°C. Blots were reprobed with eIF and β-tubulin probes using a formamide based hybridization mix consisting of 50% formamide, 5x SSC, 5x Denhardt's solution, 1% SDS and 100ug/ml salmon sperm at 55°C overnight. Blots were washed three times with 1x SSC at 60°C for 30 min intervals. All blots were exposed to a storage phosphor screen (Molecular Dynamics) and analyzed using a Storm-860 PhosphorImager (GE Healthcare).

Cell fractionation and SDS-PAGE

Tetracycline induced and uninduced A6-ASRE expressing PF *T. brucei* were hypotonically lysed and mitochondria and cytosolic fractions were isolated as previously described (Harris et al. 1990). Purified mitochondria were further purified into membrane and matrix fractions as previously described (Sykes and Hajduk 2013). In brief, purified

mitochondria were incubated in 0.5% Triton X-100, 20mM HEPES-NaOH (pH 7.6) with protease inhibitor cocktail (Roche) on ice for 45 min. After permeabilization the insoluble membrane fraction was pelleted at 12,000 x g for 10 min at 4°C. Supernatant was retained as the matrix fraction. The insoluble membrane fraction was washed three times in extraction buffer. Induced and uninduced total cell, cytosol, total mitochondria, membrane and matrix samples for uninduced and induced samples were denatured using β-mercaptoethanol reducing SDS loading buffer. Samples were loaded based on cell equivalents ($1x10^7$-$1x10^8$ cells per lane) and analyzed by SDS-PAGE.

Mitochondrial membrane potential analysis

Trypanosome membrane potential was assessed as previously described (Seidman et al. 2012). Samples from A6-ASRE uninduced and induced cells were incubated with tetramethylrhodamine methyl ester (TMRM) (20nM) for 10 minutes allowing for mitochondrial accumulation in a membrane potential dependent manner (Scaduto and Grotyohann 1999). Cells were then washed and resuspended in fresh SM media and allowed to equilibrate for 30 min. After equilibration cells were again washed and resuspended in SM to a final concentration of $4x 10^6$/ml. Samples were analyzed using a Luminescence Spectrometer LS 55 (PerkinElmer) with an excitation wavelength of 548 nm and an emission wavelength of 573 nm.

Oligomycin sensitivity assay

PF *T. brucei* cells were cultured at a density of $1x10^5$/ml and treated with oligomycin at a concentration of 3μM, 0.3 μM or 0.03μM. Growth was then compared between uninduced and A6-ASRE induced cells over a 48h time course. Uninduced cells that were not treated with oligomycin were set as the 100% growth control.

Acknowledgments

We thank members of the Hajduk, Sabatini and Wang labs for helpful discussion and comments on the manuscript. This work was supported by NIH grants AI21401 (Hajduk) and CA158283 (Wang).

References

Alsford S, Turner DJ, Obado SO, Sanchez-Flores A, Glover L, Berriman M, Hertz-Fowler, Horn D. 2011. High-throughput phenotyping using parallel sequencing of RNA interference targets in the African trypanosome. *Genome Res* **21**:915–924.

Aphasizhev R, Aphasizheva I. 2011. Mitochondrial RNA processing in trypanosomes. *Res Microbiol* **162**: 655-663.

Blum B, Bakalara N, Simpson L. 1990. A model for RNA editing in kinetoplastid mitochondria: "Guide" RNA molecules transcribed from maxicircle DNA provide the edited information. *Cell* **60**: 189-198.

Bohm C, Katari VS, Brecht M, Goringer HU. 2012. Trypanosoma brucei 20 S editosomes have one RNA substrate-binding site and execute RNA unwinding activity. *J Biol Chem* **287**: 26268-26277.

Bringaud F, Riviere L, Coustou V. 2006. Energy metabolism of trypanosomatids: Adaptation to available carbon sources. *Mol Biochem Parasitol* **149**: 1-9.

Brown SV, Hosking P, Li J, Williams N. 2006. ATP synthase is responsible for maintaining mitochondrial membrane potential in bloodstream form Trypanosoma brucei. *Eukaryot Cell* **5**: 45-53.

Carnes J, Trotter JR, Ernst NL, Steinberg A, Stuart K. 2005. An essential RNase III insertion editing endonuclease in *Trypanosoma brucei. Proc Natl Acad Sci U S A* **102**: 16614-16619.

Cheong CG, Hall TM. 2006. Engineering RNA sequence specificity of Pumilio repeats. *Proc Natl Acad Sci U S A* **103**: 13635-13639.

Choudhury R, Tsai YS, Dominguez D, Wang Y, Wang Z. 2012. Engineering RNA endonucleases with customized sequence specificities. *Nat Commun* **3**: 1147.

Choudhury R, Wang Z. 2014. Manipulation of RNA using engineered proteins with customized specificity. *Adv Exp Med Biol* **825**: 199-225.

Clayton C, Hausler T, Blattner J. 1995. Protein trafficking in kinetoplastid protozoa. *Microbiol Rev* **59**: 325-344.

Corell RA, Feagin JE, riley GR, Strickland T, Guderian JA, Myler PJ, Stuart K. 1993. *Trypanosoma brucei* minicircles encode multiple guide RNAs which can direct editing of extensively overlapping sequences. *Nucl Acids Res* **21**: 4313-4320.

Coustou V, Besteiro S, Biran M, Diolez P, Bouchaud V, et al. 2003. ATP generation in *Trypanosoma brucei* procyclic form: cytosolic substrate level is essention but not oxidative phosphorylation. *J Biol Chem* **278**:49625-49635.

Cunningham, I. 1977. New culture medium for maintenance of tsetse tissues agrowth of trypanosomatids. *J. Protozool.* **24**: 325-329

Dean S, Gould MK, Dewar CE, Schnaufer AC. 2013. Single point mutations in ATP synthase compensate for mitochondrial genome loss in trypanosomes. *Proc Natl Acad Sci U S A* **110**: 14741-14746.

Dong S, Wang Y, Cassidy-Amstutz C, Lu G, Bigler R, Jezyk MR, Li C, Hall TM, Wang Z. 2011. Specific and modular binding code for cytosine recognition in Pumilio/FBF (Puf) RNA-binding domains. *J Biol Chem* **286**: 26732-26742.

Filipovska A, Razif MF, Nygard KK, Rackham O. 2011. A universal code for RNA recognition by PUF proteins. *Nat Chem Biol* **7**: 425-427.

Gavin CE, Gunter KK, Gunter TE. 1992. Mn2+ sequestration by mitochondria and inhibition of oxidative phosphorylation. *Toxicol Appl Pharmacol* **115**: 1-5.

Gnipova A, Panicucci B, Paris Z, Verner Z, Horvath A, Lukes J, Zikova A. 2012. Disparate phenotypic effects from the knockdown of various Trypanosoma brucei cytochrome c oxidase subunits. *Mol Biochem Parasitol* **184**: 90-98.

Goringer HU. 2012. 'Gestalt,' composition and function of the Trypanosoma brucei editosome. *Annu Rev Microbiol* **66**: 65-82.

Gualdron-Lopez M, Brennand A, Hannaert V, Quinones W, Caceres AJ, Bringaud F, Concepcion JL, Michels PAM. 2012. When, how and why glycolysis became compartmentalized in Kinetoplastea. A new look at an ancient organelle. I*nternat J Parasitol* **42**: 1-20.

Gunter TE, Gavin CE, Gunter KK. 2009. The case for manganese interaction with mitochondria. *Neurotoxicology* **30**: 727-729.

Hajduk S, Ochsenreiter T. 2010. RNA editing in kinetoplastids. *RNA Biol* **7**: 229-236.

Halbig K, Sacharidou A, De Nova-Ocampo M, Cruz-Reyes J. 2006. Preferential interaction of a 25kDa protein with an A6 pre-mRNA substrate for RNA editing in Trypanosoma brucei. *Int J Parasitol* **36**: 1295-1304.

Harris ME, Moore DR, Hajduk SL. 1990. Addition of uridines to edited RNAs in trypanosome mitochondria occurs independently of transcription. *J Biol Chem* **265**: 11368-11376.

Hashimi H, Benkovicova V, Cermakova P, Lai DH, Horvath A, Lukes J. 2010. The assembly of F(1)F(O)-ATP synthase is disrupted upon interference of RNA editing in Trypanosoma brucei. *Int J Parasitol* **40**: 45-54.

Hashimi H, Zimmer SL, Ammerman ML, Read LK, Lukes J. 2013. Dual core processing: MRB1 is an emerging kinetoplast RNA editing complex. *Trends Parasitol* **29**: 91-99.

Jensen RE, Englund PT. 2012. Network news: Thre replication of kinetoplast DNA. *Annu Rev Microbiol* **66**: 473-491.

Källberg M, Wang H, Wang S, Peng J, Wang Z, Lu H, Xu J. 2012. Template-based protein structure modeling using the RaptorX web server. *Nature Protocols* **7**, 1511–1522,

Koslowsky D, Sun Y, Hindenach J, Theisen T, Lucas J. 2014. The insect-phase gRNA transcriptome in Trypanosoma brucei. *Nucleic Acids Res* **42**: 1873-1886.

Lukes J, Guilbride DL, Votypka J., Zikova A, Benne, R, Englund PT. 2002. Kinetoplast DNA network: Evolution of an improbable structure. *Euk Cell* **1**: 495-502.

Matthews KR. 2005. The developmental biology of *Trypanosoma brucei. J Cell Sci* **118**: 283-290.

Nolan DP, Voorheis, HP. 1992. The mitochondrion in bloodstream forms of *Trypanosoma brucei* is energized by the electrogenic pumping of protons catalysed by the F1F0-ATPase. *Eur J Biochem* **209**: 207-216.

Ochsenreiter T, Hajduk SL. 2006. Alternative editing of cytochrome c oxidase III mRNA in trypaosome mitochondria generated protein diversity. *EMBO Rep* **7**: 1128-1133.

Ochsenreiter T, Anderson S, Wood ZA, Hajduk SL. 2008. Alternative RNA editing produces a novel protein involved in mitochondrial DNA maintenance in trypanosomes. *Mol Cell Biol* **28**: 5595-5604.

Ochsenreiter T, Cipriano M, Hajduk SL. 2007. KISS: the kinetoplastid RNA editing sequence search tool. *RNA* **13**: 1-4.

Park SH, Nguyen TN, Gunzl A. 2012. Development of an efficient in vitro transcription system for bloodstream form Trypanosoma brucei reveals life cycle-independent functionality of class I transcription factor A. *Mol Biochem Parasitol* **181**: 29-36.

Pfaffl MW. 2001. A new mathematical model for relative quantification in real-time RT-PCR. *Nucleic Acids Res* **29**: e45.

Pollard VW, Rohrer SP, Michelotti EF, Handcock K, Hajduk SL. 1990. Organization of minicircle genes for guide RNAs in *Trypanosoma brucei. Cell* **63**: 783-790.

Priest JW, Hajduk SL. 1995. The trypanosomatid Rieske iron-sulfur proteins have a cleaved presequence that may direct mitochondrial import. *Biochim Biophys Acta* **1269**: 201-204.

Scaduto RC, Jr., Grotyohann LW. 1999. Measurement of mitochondrial membrane potential using fluorescent rhodamine derivatives. *Biophys J* **76**: 469-477.

Schnaufer A, Clark-Walker GD, Steinberg AG, Stuart K. 2005. The F1-ATP synthase complex in bloodstream stage trypanosomes has an unusual and essential function. *EMBO J* **24**: 4029-4040.

Schnaufer A, Domingo GJ, Stuart K. 2002. Natural and induced dyskinetoplastic trypanosomatids: How to live without mitochondrial DNA. *Int J Parasitol* **32**: 1071-1084.

Seidman D, Johnson D, Gerbasi V, Golden D, Orlando R, Hajduk S. 2012. Mitochondrial membrane complex that contains proteins necessary for tRNA import in Trypanosoma brucei. *J Biol Chem* **287**: 8892-8903.

Stephens JL, Lee SH, Paul KS, Englund PT. 2007. Mitochondrial fatty acid synthesis in *Trypanosoma brucei*. *J Biol Chem* **282**: 4427-4436.

Sykes SE, Hajduk SL. 2013. Dual functions of alpha-ketoglutarate dehydrogenase E2 in the Krebs cycle and mitochondrial DNA inheritance in Trypanosoma brucei. *Eukaryot Cell* **12**: 78-90.

Trujillo M, Budde H, Pineyro MD, Stehr M, Robello C, Flohe L, Radi R. 2004. Trypanosoma brucei and Trypanosoma cruzi tryparedoxin peroxidases catalytically detoxify peroxynitrite via oxidation of fast reacting thiols. *J Biol Chem* **279**: 34175-34182.

Wirtz E, Leal S, Ochatt C, Cross GA. 1999. A tighly regulated inducible expression system for conditional gene knock-outs and dominant-negative genetics in *Trypanosoma brucei*. *Mol Biochem Parasitol* **99**: 89-101.

Zhang W, Wang Y, Dong S, Choudhury R, Jin Y, Wang Z. 2014. Treatment of type 1 myotonic dystrophy by engineering site-specific RNA endonucleases that target (CUG)(n) repeats. *Mol Ther* **22**: 312-320.

Zuker M. 2003. Mfold web server for nucleic acid folding and hybridization prediction. *Nucleic Acids Res* **31**: 3406-3415.

Figures

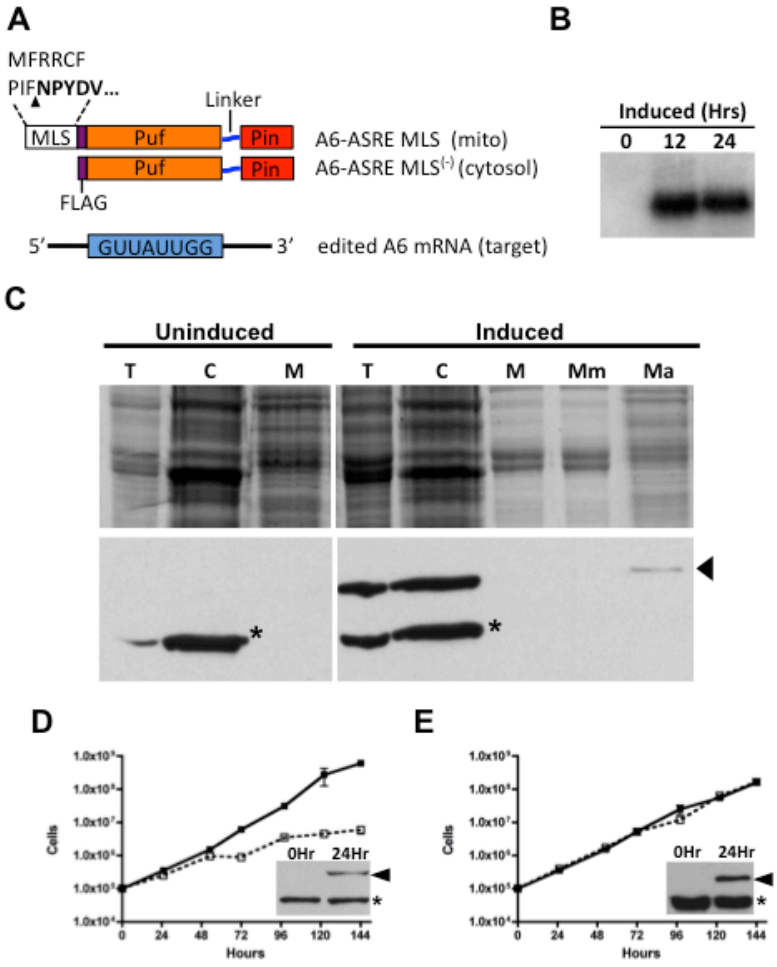

Figure 2.1. A6-ASRE and A6-ASRE MLS$^{(-)}$ expression and effect on PF *T. brucei*. growth. **(A)** A6-ASRE and A6-ASRE MLS$^{(-)}$ constructs were developed against GUUAUUGG sequence present in the 3' UTR of ATPase 6 edited mRNA. A6-ASRE construct contains and N-terminal 14 amino acid MLS from dihydroplipoyl dehydrogenase Tb11.01.8470. This sequence is recognized and cleaved upon import (arrow head) resulting in the retention of 5 amino acids (residues in bold). The MLS is followed by a FLAG epitope tag fused with a *T. brucei* codon optimized Puf –linker-PIN domains. The A6-ASRE MLS$^{(-)}$ lacks the mitochondrial localization signal. **(B)** Northern blot of total cell RNA from A6-ASRE cells taken at 0, 12, or 24 hours post

tetracycline induction (1 μg/ml) and hybridized with a probe specific for the A6-ASRE sequence. **(C)** Cell fractionation was carried-out on uninduced and induced (1 μg/ml tetracycline, 24 hours) cells. Total cellular (T), cytosolic (C), mitochondrial (M), mitochondrial membrane (Mm) and mitochondrial matrix (Ma) fractions were obtained. Cell equivalents were loaded at 1 x 10^7 for TC, C, M, Mm; while 1 x 10^8 was loaded for the Ma fraction. Samples were fractionated on SDS-PAGE (10%), and either coomassie stained (top panel) or transferred for western blotting and probed with α-FLAG (bottom panel). A cross-reacting band of 50kDa (asterisk) was seen in total cell and cytoplasmic fractions and absence from the mitochondrial fractions (M). An α-FLAG reactive band of ~60kDa was present in the A6-ASRE induced cell and fractionated with the mitochondrial matrix (Ma) (arrow head). **(D)** Growth of PF *T. brucei 29-13* A6-ASRE in the presence (open square) or absence (closed square) of tetracycline (1 μg/ml). Inset shows A6-ASRE expression at 24 hours post induction (arrow head) and presence of previously described ~50kDa cross-reacting band (asterisk). Each lane was loaded with 1 x 10^7 cell equivalents. **(E)** Growth of PF *T. brucei 29-13* A6-ASRE $MLS^{(-)}$ in the presence (open square) or absence (closed square) of tetracycline (1 μg/ml). Inset shows A6-ASRE $MLS^{(-)}$ expression at 24 hours post induction (arrow head) and presence of described ~50kDa cross-reacting protein (asterisk). Each lane was loaded with 1 x 10^7 cell equivalents.

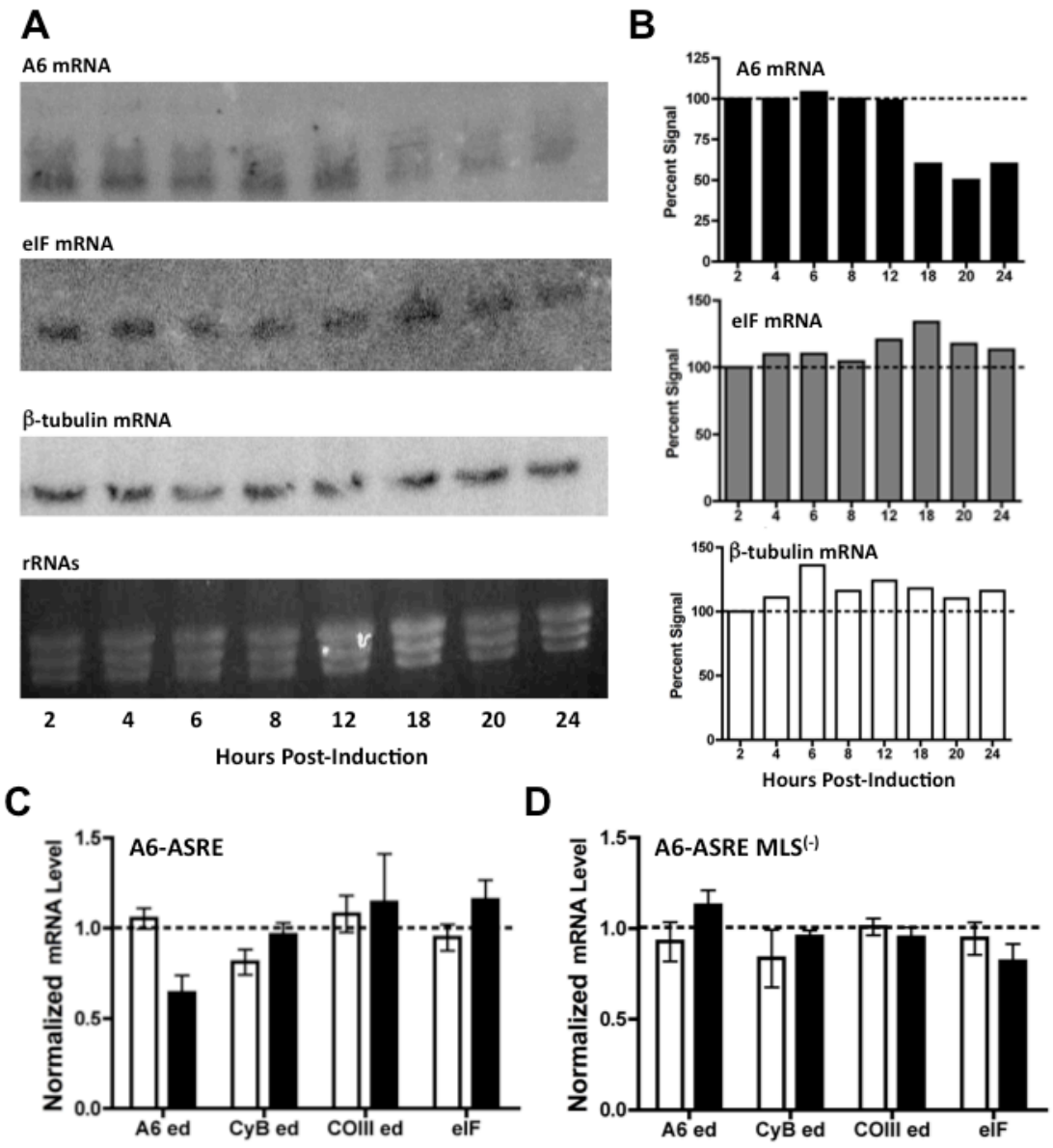

Figure 2.2. A6-ASRE mediated knockdown of A6 edited mRNA in PF *T. brucei*. (A) Total RNA was isolated from A6-ASRE PF *T. brucei* induced with tetracycline (1 μg/ml) for 2, 4, 6, 8, 12, 18, 20 or 24 hours and analyzed by northern blot. Samples were probed for A6 edited (top), eIF (middle) and β-tubulin (bottom) mRNA. Ethidium bromide stained formaldehyde agarose (1%) gel showing rRNA as loading control. **(B)** Quantitation of the northern blot hybridization results with A6 edited mRNA, eIF mRNA and β-tubulin mRNAs. **(C)** RT-qPCR analysis of A6

edited mRNA, CyB edited mRNA, COIII edited mRNA and the cytosolic eIF mRNA from uninduced (open bar) (n= 6) PF *T. brucei* and 24 hour post-induction (closed bar) (n= 5) with tetracycline (1 μg/ml). Normalized against β-tubulin mRNA. **(D)** RT-qPCR of samples from A6-ASRE MLS$^{(-)}$ uninduced (open bar) (n= 4) and 24 hour post-induction (closed bar) (n= 4) with etracycline (1 μg/ml). Normalized against β-tubulin mRNA.

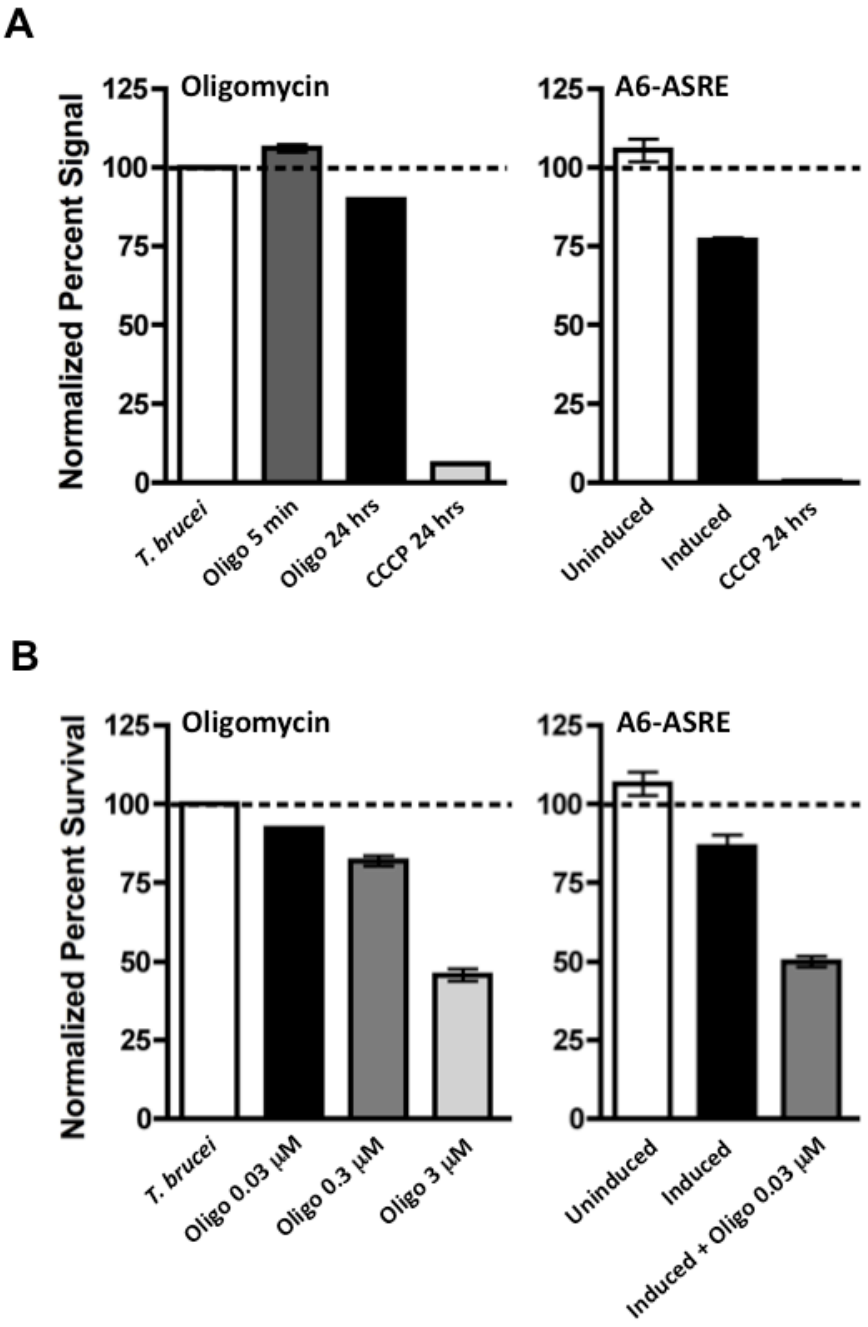

Figure 2.3. A6-ASRE expression alters mitochondria membrane potential and sensitivity to oligomycin. (A) Mitochondrial membrane potential from 2 x 10^6 cells measured by relative TMRM fluorescence (20nM) prior to treatment and 5 minutes and 24 hours following addition of 3 mM oligomycin. PF *T. brucei* containing A6-ASRE were left uninduced (n= 4), induced with

tetracycline (1 µg/ml) (n= 4) or uninduced and treated with 20µM of the membrane potential uncoupler CCCP (n= 4). Mitochondrial membrane potential was measured at 0 and 24 hours post addition of tetracycline or CCCP. **(B)** Growth of PF *T. brucei* in the presence of the ATPase proton half-channel inhibitor oligomycin. A6-ASRE PF *T. brucei* cultures were started at a density of 1 x 10^5 cells/ml and left uninduced, induced with tetracycline (1 µg/ml), treated with 3µM oligomycin or induced with tetracycline (1 µg/ml) and treated with 0.03µM oligomycin (n= 3 for all samples). Cell numbers were determined at 24 hours post treatment and used to calculate the relative percent survival against the uninduced control.

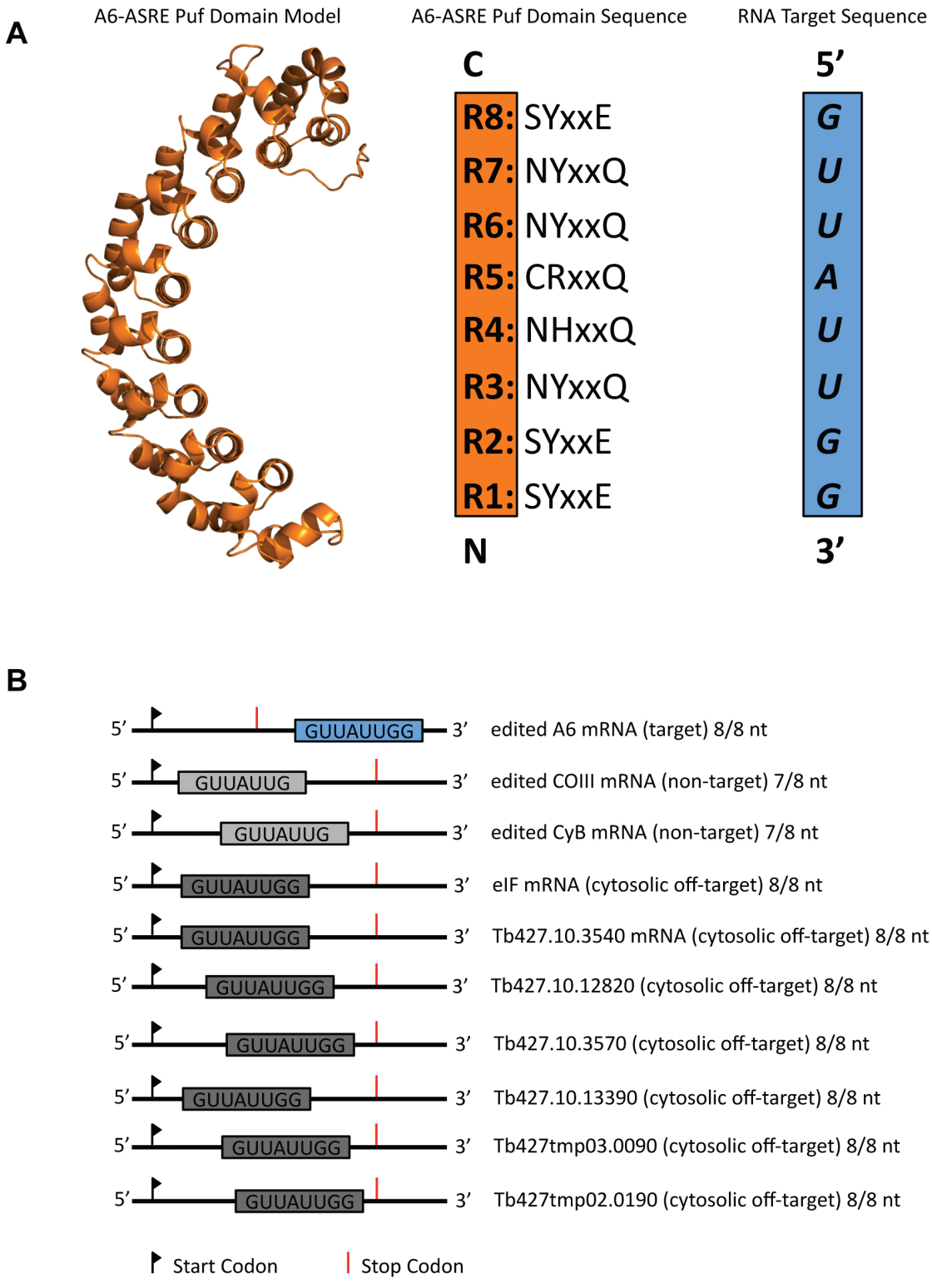
A
A6-ASRE Puf Domain Model
A6-ASRE Puf Domain Sequence
RNA Target Sequence
C
R8: SYxxE
R7: NYxxQ
R6: NYxxQ
R5: CRxxQ
R4: NHxxQ
R3: NYxxQ
R2: SYxxE
R1: SYxxE
N
5’
G
U
U
A
U
U
G
G
3’
B
5’ GUUAUUGG 3’ edited A6 mRNA (target) 8/8 nt
5’ GUUAUUG 3’ edited COIII mRNA (non-target) 7/8 nt
5’ GUUAUUG 3’ edited CyB mRNA (non-target) 7/8 nt
5’ GUUAUUGG 3’ eIF mRNA (cytosolic off-target) 8/8 nt
5’ GUUAUUGG 3’ Tb427.10.3540 mRNA (cytosolic off-target) 8/8 nt
5’ GUUAUUGG 3’ Tb427.10.12820 (cytosolic off-target) 8/8 nt
5’ GUUAUUGG 3’ Tb427.10.3570 (cytosolic off-target) 8/8 nt
5’ GUUAUUGG 3’ Tb427.10.13390 (cytosolic off-target) 8/8 nt
5’ GUUAUUGG 3’ Tb427tmp03.0090 (cytosolic off-target) 8/8 nt
5’ GUUAUUGG 3’ Tb427tmp02.0190 (cytosolic off-target) 8/8 nt
Start Codon
Stop Codon

Supplemental Figure 2.1. A6-ASRE programming and RNA targets. (A) Structure model, as predicted by RaptorX, of A6-ASRE Puf domain. Amino acid sequences are given for each repeat 1-8 (orange box) used for recognize the adjacent target nucleotide the A6 sequence (blue box). **(B)** Orientation of start and stop codons in relation to full (8-nt) or partial (7-nt) A6 target sequence for RNAs analyzed in this study. Target A6 sequence, non-target mitochondria encoded mRNAs with less than perfect target sequences and cytosolic off-target nuclear encoded mRNAs with perfect target sequences.

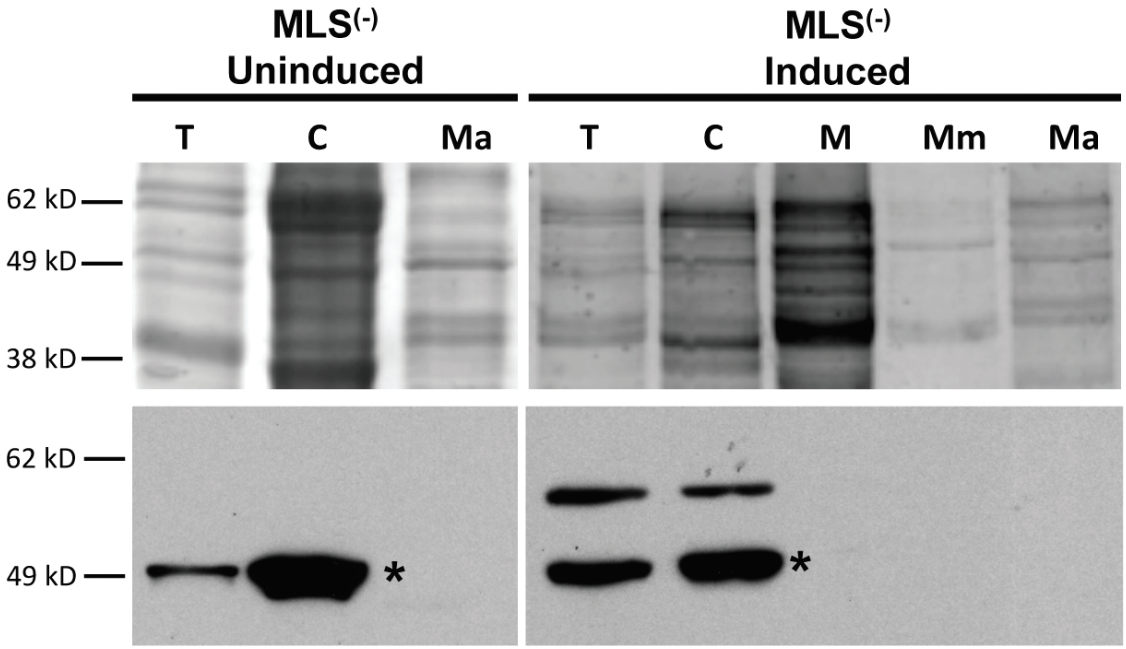

Supplemental Figure 2.2. A6-ASRE MLS$^{(-)}$ mitochondrial fractionation. Cell fractionation was carried-out on uninduced and induced (1 µg/ml tetracycline, 24 hours) A6-ASRE MLS$^{(-)}$ cells. Total cellular (T), cytosolic (C), mitochondrial (M), mitochondrial membrane (Mm) and mitochondrial matrix (Ma) fractions were obtained. Cell equivalents were loaded at 1 x 10^7 for T, C, M, Mm; while 1 x 10^8 was loaded for the Ma fraction. Samples were fractionated on SDS-

PAGE (10%), and either coomassie stained (top panel) or transferred for western blotting and probed with α-FLAG (bottom panel). A cross-reacting band of 50kDa (asterisk) was seen in total cell and cytoplasmic fractions and absence from the mitochondrial fractions (M). The ~60kDa α-FLAG reactive band, which corresponds to the A6-ASRE$^{(-)}$ was detected in the total cellular (T) and cytosolic (C) fractions but not within the mitochondrial matrix (Ma).

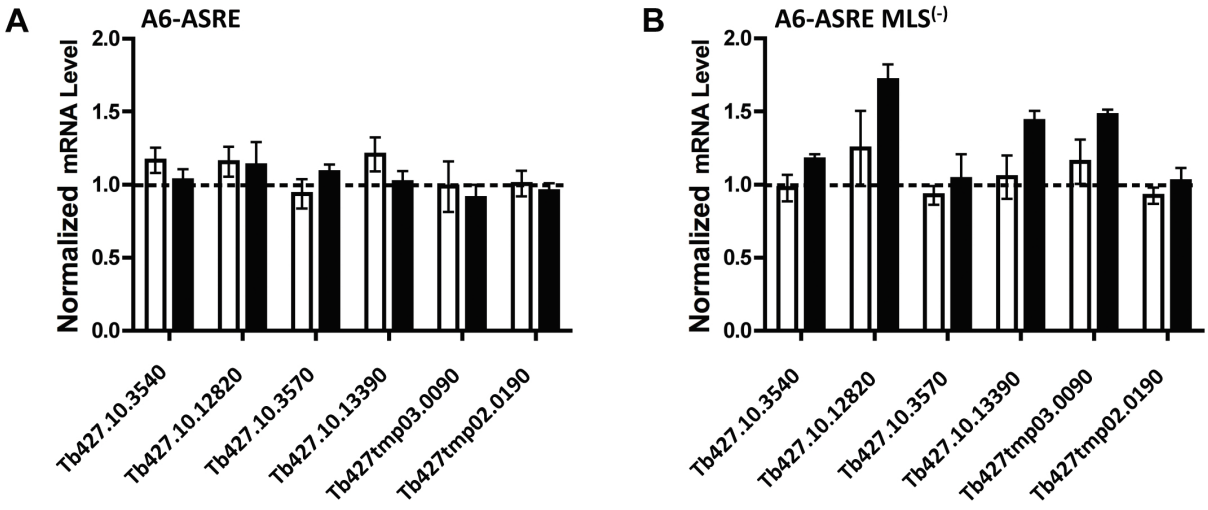

Supplemental Figure 2.3. A6-ASRE induction does not reduce cytosolic transcript levels. **(A)** RT-qPCR analysis of Tb 427.10.3540; Tb427.10.12820; Tb427.10.3570; Tb427.10.13390; Tb427tmp03.0090; Tb427tmp02.0190 from uninduced (open bar) (n= 3) PF *T. brucei* and 24 hour post-induction (closed bar) (n= 3) with tetracycline (1 μg/ml). Normalized against β-tubulin mRNA. **(B)** RT-qPCR of samples from A6-ASRE MLS$^{(-)}$ Uninduced (open bar) (n= 3) and 24 hour post-induction (closed bar) (n= 3) with tetracycline (1 μg/ml). Normalized against β-tubulin mRNA.

CHAPTER 3

THE KREBS CYCLE ENZYME α-KETOGLUTARATE DECARBOXYLASE IS AN ESSENTIAL GLYCOSOMAL PROTEIN IN BLOODSTREAM AFRICAN TRYPANOSOMES

Szempruch, A. [*], Sykes, S. [*] and S. Hajduk. . Eukaryotic Cell. 2015 Mar;14(3):206-15. doi: 10.1128/EC.00214-14. [*] These authors contributed equally to this work. Reprinted with permission from the publisher.

Abstract

The α-ketoglutarate decarboxylase (a-KDE1) is a Krebs cycle enzyme found in the mitochondrion of the procyclic form (PF) *Trypanosoma brucei*. The bloodstream form (BF) of *T. brucei* lacks a functional Krebs cycle and relies exclusively on glycolysis for ATP production. Despite the lack of a functional Krebs cycle α-KDE1 was expressed in BF *T. brucei* and RNAi knockdown of α-KDE1 mRNA resulted in rapid growth arrest and killing. Cell death was preceded by progressive swelling of the flagellar pocket as a consequence of recruitment of both flagella and plasma membranes into the pocket. Bloodstream form *T. brucei* expressing an epitope tagged copy of α-KDE1 showed localization to glycosomes and not the mitochondrion. We used a cell line transfected with a reporter construct containing the N-terminal sequence of α-KDE1 fused to GFP to examine the requirements for glycosome targeting. We found that the N-terminal 18 amino acids of α-KDE1 contained overlapping mitochondria and peroxisome targeting sequences and was sufficient to direct localization to the glycosome in BF *T. brucei*. These results suggest that α-KDE1 has a novel moonlighting function outside the mitochondrion in BF *T. brucei*.

Introduction

The protozoan parasite *Trypanosoma brucei* causes human African sleeping sickness and the chronic wasting disease nagana in cattle (1-3). *T. brucei* has a complex life cycle within an insect vector, the tsetse fly (*Glossina* spp.), and in the blood, lymphatics and central nervous systems of mammals (4). During development the parasite undergoes changes in both morphology and metabolism in response, in part, to the carbon source available for energy production. In mammals, the bloodstream form (BF) *T. brucei* has an ample supply of glucose and exclusively utilizes glycolysis for energy production (5, 6). Most of the glycolytic enzymes

are localized to the glycosome, a peroxisome-like organelle, which catalyzes the conversion of glucose to glyceraldehyde 3-phosphate (7, 8). Consistent with the central role of glycolysis in ATP production, the mitochondrion of BF *T. brucei* is reduced to a simple, tubular, acristate organelle lacking both respiratory cytochromes and a functional Krebs cycle (4). This developmental stage of *T. brucei* is unable to carry out mitochondrial oxidative phosphorylation.

In the midgut of the tsetse fly, amino acids from digested bloodmeals replace glucose as the primary carbon source available to procyclic form (PF) *T. brucei*. Procyclic form *T. brucei* retain glycosomes but the role of glycolysis in ATP production is reduced and a large, branched mitochondrion with numerous inner membrane cristae develops shortly after ingestion by the fly (4). Several Krebs cycle enzymes have been shown to be essential for energy metabolism in PF trypanosomes but an intact Krebs cycle, catalyzing the degradation of glucose and amino acids to CO_2, is not operative (9). Rather, internalized amino acids, primarily proline and glutamate, are degraded by the Krebs cycle enzymes α-ketoglutarate dehydrogenase (α-KD) and succinyl-CoA synthetase to succinate (9). Despite the non-cyclic nature of the pathway, the Krebs cycle enzymes still provides high-energy electrons, via NADH and $FADH_2$, to the electron transport chain that generates the electrochemical proton gradient necessary for mitochondrial oxidative phosphorylation.

α-ketoglutarate dehydrogenase is a large enzyme complex that catalyzes the conversion of α-ketoglutarate to succinyl-CoA. Multiple copies of the α-ketoglutarate decarboxylase (α-KDE1) (2-oxoglutarate dehydrogenase E1, Tb11.01.1740), dihydrolipoyl succinyltransferase (α-KDE2) and dihydrolipoamide dehydrogenase (α-KDE3) subunits are arranged for efficient substrate transfer between active sites (10). The reaction initiates with α-KDE1 mediated oxidative decarboxylation of α-ketoglutarate and the subsequent release of CO_2. Succinyl

formed from this step is transferred to CoA by the lipoyl group of α-KDE2 followed by the regeneration of the lipoic acid by the reduction of NAD^+ via E3 (11). The α-KD is a vital component of energy metabolism in most aerobic prokaryotes and eukaryotes. In *T. brucei,* α-KDE1, α-KDE2 and α-KDE3 mRNAs are constitutively expressed in both BF and PF trypanosomes yet a functional Krebs cycle and α-KD activity are only present in the PF trypanosomes (12). We showed that α-KDE2 is a bifunctional protein that localized to the mitochondrion of BF *T. brucei* but was not involved in energy production. Cell fractionation studies showed that α-KDE2 was tightly associated with the trypanosome mitochondrial genome, the kinetoplast DNA (kDNA) and was required for equal segregation of mitochondria and kDNA to daughter cells at cytokinesis (12). Other metabolic enzymes, including the Krebs cycle enzyme aconitase, have been shown to "moonlight" carrying out multiple functions in other organisms (13, 14).

Here we report that α-KDE1 is also essential to BF *T. brucei*. RNA interference (RNAi) knockdown of α-KDE1 mRNA levels results in rapid growth arrest, morphological changes and cell death within 24 hours. Following α-KDE1RNAi induction, the flagellar pocket rapidly swells to eventually occupy much of the cell. Electron microscopy showed that recruitment of both cell surface and flagella membranes facilitated the formation of the swollen flagellar pocket. Furthermore, we found that α-KDE1 was undetectable in the BF mitochondrion but rather localized to glycosomes suggesting that this canonical Krebs cycle enzyme can be differentially targeted in BF *T. brucei* and has a unique, essential function.

Methods

Cell culture. Bloodstream form *T. brucei* (TREU667 and 427) were grown at 37° C in 5% CO_2 in HMI-9 medium containing 10% fetal bovine serum (FBS) (Gemini Bioproducts,

West Sacramento, CA) and Serum Plus supplement (SAFC Biosciences, Lenexa, KS). The α-KDE1 RNAi cell line was maintained in the same medium but with tetracycline-free FBS (10%).

Construction of cell lines. Two 580 and 439 bp partial α-KDE1 (Tb11.01.1740) products were amplified from BF *T. brucei* 9013 genomic DNA using primers 5'-CCCTCGAGTGGCGCAGAGTCACTTATTG-3' and 5'-CCAAGCTTAATGGGACACTGAAAGGCAC-3' and 5'-CTCGAGGCCCACCGTGTAAATATGGA-3' and 5'-AAGCTTACACGCGATTCAACGTGATA-3' respectively and ligated into the inducible pZJM RNAi vector to produce the α-KDE1 RNAi cell lines (15). The construct was linearized using NotI for transfection. For the HA-tagged cell lines primers 5'-CCCCTCGAGCCGTGAATCCAACAACTGTGG-3' and 5'-CCCCTCGAGTGAAAATACGCATTCGCAAA-3' were used to amplify a partial α-KDE1 sequence (301 bp) from BF *T. brucei* TREU 667 genomic DNA and was ligated into the modified pMOTag2H in-situ tagging vector (16). The vector was linearized with a unique restriction site and transfected into wild-type BF TREU 667 *T. brucei*. The transfections were carried out using the nucleofector system (Lonza, Walkersville, MD).

Northern analysis. Total RNA was extracted from cells using TriPure Isolation Reagent (Roche, Indianapolis, IN, USA) and transcripts were separated on a 7% formaldehyde, 1% agarose gel. RNAs were transferred to a membrane and hybridized with radiolabeled probes prepared from ORFs specific for α-KDE1 and β-tubulin using Prime-It random primer labeling kit (Stratagene, Santa Clara, CA, USA). Radiolabeled probes were hybridized with the trypanosome RNAs in a buffer containing 50% (vol/vol) formamide, 5x SSC, 5x Denhardt's solution (Sigma, St. Louis, MO, USA), 1% (w/v) SDS and 100 μg/ml salmon sperm DNA (Life

Technologies, Grand Island, NY, USA) at 55°C overnight. Blots were washed three times at 30 minute intervals in 0.2x SSC containing 0.1% SDS at 68°C, exposed to a storage phosphor screen (Molecular Dynamics), and analyzed on a STORM-860 PhosphorImager (GE Healthcare).

Concanavalin A binding assay. RNAi cells were induced with 1 μg/ml of doxycycline for 6, 12, and 18 hours and washed with ice cold HMI9 without serum proteins. For concanavalin A-FITC (Con A-FITC) (Sigma) binding, cells were resuspended in 3°C serum free, HMI9 containing 1% BSA and 5 μg/ml Con A-FITC and incubated for 15 minutes. Cells were further incubated on ice for 5 minutes and washed in ice-cold serum free HMI9 and prepared for fluorescence microscopy.

α-KDE1- eGFP fusion construct and colocalization. The 17 amino acid N-terminal signal sequence from α-KDE1 was fused to enhanced (e)GFP to test localization. Fusion was carried out using a primer containing the α-KDE1 signal sequence (italicized in primer) and regions specific for eGFP with forward primer 5'-GATCAAGCTT*ATGATGCGAAGGCTCAGTCCTGTGAACGGTTCGGTGGTTTCGCCCAATGT C*ATGAGTAAAGGAGAAGAACTTTTC-3' and reverse primer specific for eGFP 5'-GATCGGATCCTTATTTGTATAGTTCATCCATGCC-3'. The α-KDE1-eGFP fusion gene was cloned into the BamHI/HindIII site of the pLew100 vector (17). Bloodstream form *T. brucei* 9013 cells were transfected and used for expression and co-localization studies.

Fluorescence microscopy. Bloodstream form *T. brucei* were smeared on a microscope slide, rapidly air dried and fixed in methanol (-20°C) for 10 minutes. Slides were rinsed and blocked using 20% FBS in PBS for 30 minutes. α-KDE1 RNAi or α-KDE1-HA cells respectively, were used to localize the RNAi induced posterior vacuole or to localize α-KDE1. Antibodies against PFR (1:500) was used in combination with 4′,6′-diamidino-2-phenylindole

(DAPI) staining to localize the flagellar pocket. The localization of α-KDE1-HA in BF *T. brucei* was determined by staining with MitoTracker (Life Technologies, Grand Island, NY, USA), antibodies against the HA epitope (1:100; Abcam, Cambridge, MA), and antibodies against the *T. brucei* aldolase (James Morris, Clemson University) (14). All antibodies were diluted in blocking buffer and cells were incubated with the primary antibody for one hour. Slides were then washed with PBS and incubated with appropriate secondary antibody (1:500) for 30 minutes in the same blocking buffer. Following incubation with the secondary antibody, slides were washed with PBS and coated with DAPI containing the antifade reagent ProlongGold (Life Technologies). Images were acquired using a Zeiss Axio Observer inverted microscope equipped with an AxioCam HSm and evaluated with AxioVision v4.6 software (Zeiss).

Scanning and transmission electron microscopy. Induced BF *T. brucei* α-KDE1 RNAi cells were fixed in 2.5% glutaraldehyde, 2% paraformaldehyde, 2 mM $CaCl_2$, and 100 mM cacodylate (pH 7) in a 1:1 ratio (cell media to fixative) for 30 minutes at 25^{o}C. Cells were pelleted twice in serum free HMI9, washed for 1 hour in a buffer containing 200 mM sucrose and 100 mM cacodylate (pH 7.4), and postfixed with 1% OsO_4 in 100 mM cacodylate buffer for 1 hour. Fixed cells were washed in dH_2O and dehydrated through a graded ethanol series. Cell pellets were embedded in epon resin, sections were prepared and stained using uranyl acetate and lead citrate. Images were taken using a JEOL-JEM 1210 transmission electron microscope (JEOL). For SEM, 2.5% glutaraldehyde fixed cells were dehydrated on a 0.22 μm membrane, critical point dried, sputter coated with gold and viewed using a Zeiss 1450EP scanning electron microscope (Zeiss).

Western blot analysis. Total cell protein from wild-type and α-KDE1-HA *T. brucei* were denatured in reducing SDS loading buffer and fractionated by a SDS-PAGE. Proteins from

gel were transferred to a membrane, blocked with 5% (wt/vol) milk TBS-T (150 mM NaCl, 10 mM Tris-HCl, pH 8, 0.05% [vol/vol] Tween 20) and incubated overnight with primary antibodies against HA (1:2000; Abcam) epitopes. The blot was then washed, incubated with horseradish peroxidase secondary antibody (1:5000) for 1 hour, washed again with TBS-T and developed.

Results

α-KDE1 is essential in BF *T. brucei*. Previous analysis of α-KDE1, α-KDE2 and α-KDE3 steady state mRNA levels showed constitutive expression in both PF and BF *T. brucei* despite the lack of a functional Krebs cycle in BF developmental stages of this parasite (12, 18). To examine the function of α-KDE1 in BF *T. brucei* an inducible RNAi cell line was prepared. Treatment with doxycycline resulted in rapid growth arrest, within 6 hours, followed by a decrease in cell number indicating a cytocidal effect of the α-KDE1 RNAi (**Figure 3.1A**). Northern blot analysis revealed a slight decrease in α-KDE1 mRNA 6 hours post induction and a further reduction, ~55% of pre-induction levels, after 24 hours (**Figure 3.1B**). However, after 24 hours of RNAi approximately 90% of the cells were dead. The lethality was not due to off target effects of the RNAi since similar effects were observed when another, non-overlapping, sequence in the α-KDE1 mRNA was targeted for RNAi silencing (**Supplemental Figures 3.1 & 3.2**). These results are consistent with the findings of Alsford et al. 2011, where a minimal reduction in α-KDE1 mRNA resulted in a loss of fitness in all BF cell conditions. A minimal reduction in RNA levels, resulting in in a loss of fitness for ~70 other BF mRNAs in these experiments (19).

Morphological and motility changes in α-KDE1 RNAi cells. Accompanying the RNAi induced growth arrest was the formation of a 1-2 μm vacuole at the posterior end of the

cell within 6 hours. This vacuole progressively expanded until it occupied much of the cytoplasm of cells after 18-24 hours (**Figure 3.1C; Supplemental Figure 3.2**). Live cell imaging of RNAi induced cells also showed that α-KDE1 RNAi knockdown resulted in the loss of rapid tumbling motility characteristic of BF *T. brucei*. Motility was severely restricted by 6 hours post RNAi induction and correlated with the formation of the posterior vacuole and inclusion of actively moving flagella within the vacuole at 12 to 18 hours post induction (**Supplemental Figure 3.3**). Scanning electron microscopy of α-KDE1 RNAi *T. brucei* also showed time dependent changes to the overall morphology with progressive cell swelling originating from the posterior end of the cell (**Figure 3.1D**). Together these results showed that α-KDE1 was essential for the survival of BF *T. brucei* and that even small changes in steady state levels of α-KDE1 mRNA resulted in the rapid arrest of cell growth and dramatic changes in motility and morphology. Since the Krebs cycle is inoperative in BF *T. brucei* these results suggested an alternative function for α-KDE1.

In order to better define the morphological changes induced by α-KDE1 RNAi we used fluorescence microscopy to examine the position of the RNAi induced vacuole relative to 1) the kDNA which is located adjacent to the basal bodies at the base of the flagellum; 2) ConA reactive mannose residues which are only found exposed on the *T. brucei* surface in the flagellar pocket; and 3) the paraflagellar rod (PFR) protein which is associated the flagellum axoneme after the flagellum exits the flagellar pocket. Thus, based on these markers the flagellar pocket can be defined as the area between the kDNA and the PFR that binds ConA. At 6 hours post induction, a small posteriorly located vacuole was visible that co-localized with ConA staining and was positioned between the kDNA and the PFR stained portion of the flagellum (**Figure 3.2A**). The enlarged vacuole seen by DIC microscopy at 12 and 18 hours post-induction retained its position relative to the kDNA and PFR but only a small portion of the vacuole stained with

ConA (**Figure 3.2B and 3.2C**). The non-uniform distribution of the ConA staining over time made it difficult to determine whether the vacuole was the product of the swelling of a single flagellar pocket or rather a collection of closely packed vacuoles.

Depletion of α-KDE1 results in an enlarged flagellar pocket. Vesicular trafficking in African trypanosomes is highly polarized with the flagellar pocket serving as the site for all secretion and endocytosis (20, 21). The swollen posterior vacuoles seen in the α-KDE1 RNAi cells (**Figure 3.1C and Figure 3.2B-C**) resembled the swollen flagellar pocket in BF *T. brucei* following RNAi silencing of genes encoding proteins involved in endocytosis (22-26). However, we observe no change to endocytosis rates of ConA (**Supplemental Figure 3.4 A-B**).

We used TEM to examine thin sections of fixed cells taken at 6, 12, 18, and 24 hours post induction in order to determine if the vacuole in α-KDE1 RNAi cells was the flagellar pocket. By 18 hours most cells had a prominent cytosolic vacuole (**Figure 3.3A**). During a time course of α-KDE1 RNAi the vacuole increased in size until it occupied much of the cytoplasm after 18-24 hours (**Figure 3.3A-F**). Most cells contained a single vacuole, even when it had expanded to occupy much of the cell, and the presence of flagella confirmed that α-KDE1 RNAi resulted in swelling of the flagellar pocket.

Abnormal morphology of α-KDE1 RNAi cells. A girdle of subpellicular microtubules is closely juxtaposed to the cytosolic face of the plasma membrane of trypanosomes. This unusual structure contributes to the maintenance of overall shape and cellular motility. A space in the subpellicular microtubules array corresponds to the opening of the flagellar pocket where the flagellum emerges and leaves the pocket membrane free of subpellicular microtubules. The absence of subpellicular microtubules at the flagellar pocket is an important structure feature of trypanosomes and is likely necessary to allow vesicle transport between the cell and external

environment (27, 28). The mechanism excluding the assembly of subpellicular microtubules at the flagellar pocket is not known, however, in α-KDE1 RNAi cells we found that patches of the expanded flagellar pocket membrane contained subpellicular microtubules suggesting that plasma membrane, from outside the pocket, may be recruited to the rapidly expanding flagellar pocket upon RNAi induction or that subpellicular microtubules are no longer excluded from this region (**Figure 3.4A**).

The dynamic changes to the flagellar pocket membrane were accompanied by changes to the overall appearance of the flagellum in the α-KDE1 RNAi cells. At the light microscope level, the flagellum often appeared to be coiled within the flagellar pocket or associated with the cytoplasm of the trypanosome (**Figure 3.2; Supplemental Figure 3.5**). When viewed by TEM several alterations to the flagellum were observed in α-KDE1 RNAi *T. brucei* including the presence of flagella axoneme, bare of surrounding membranes, in the cytoplasm (**Figure 3.4B-C**). In addition, the cysolic axonemes often contained associated PFR structures suggesting a selective stripping of the specialized flagella membrane as the axoneme moved into the cytoplasm (**Figure 3.4B-C; Supplemental Figure 3.6A**). Further evidence of dynamic changes at the flagella membrane in the α-KDE1 RNAi cells was the presence of a large number of flagella that appear to contain multiple axonemes and PFR complexes (**Figure 3.4C; Supplemental Figure 3.6 B-E**). The overall recruitment of both plasma and flagella membranes correlates with the rapid expansion of the flagellar pocket suggesting that sequestration of membrane components from these contiguous sites may allow the rapid expansion of the flagellar pocket.

Association of KDE1 with *T. brucei* glycosomes. Electron microscopy of α-KDE1 RNAi *T. brucei* revealed other unexpected features. We observed α-KDE1 RNAi cells appeared

to contain clustered putative glycosomes with a single membrane (**Figure 3.5; Supplemental Figure 3.7 A-E**). The glycosomes in the α-KDE1 RNAi *T. brucei* were often concentrated near the flagellar pocket (**Figure 3.5 B-C**) and many were abnormally elongate and bilobed in structure (**Figure 3.5A-B**). To investigate whether the changes in glycosome abundance and morphology were a direct consequence of α-KDE1 RNAi we first examined the cellular localization of cells expressing an epitope tagged copy of α-KDE1-HA. To establish the specificity of the HA antibody, total cell lysates from wild type and α-KDE1-HA cell lines were prepared, fractionated by SDS-PAGE and analyzed by Western blotting with anti-HA (**Figure 3.6A**). The anti-HA did not react with proteins from non-transfected, wild type *T. brucei* and a single 116 kDa immunoreactive band, the expected size for *T. brucei* α-KDE1- HA, was observed in the transfected cell lysates. The localization of α-KDE1-HA was investigated using Mitotracker to identify the BF *T. brucei* mitochondrion and immunofluorescence microscopy, with anti-HA, to identify KDE1-HA (**Figure 3.6B**). α-KDE1-HA was distributed throughout the cytoplasm as small punctate structures and did not appear to co-localized with the mitochondrion. This is in contrast to the mitochondrial localization of α-KDE2 in BF *T. brucei* (12). The punctate cytoplasmic localization of α-KDE1-HA was reminiscent of the distribution of glycosomes in *T. brucei* (29, 30). Immunofluorescence microscopy with an antibody against the glycolytic enzyme, aldolase, confirmed that α-KDE1-HA was localized to glycosomes in BF *T. brucei* (**Figure 3.6C**). These results suggest that α-KDE1 has an unknown function within the glycosome of BF *T. brucei*. Further, our findings suggest that the trypanocidal effects and morphological changes associated with RNAi knockdown of the α-KDE1 are a consequence of loss of this function.

α-KDE1 contains overlapping N-terminal mitochondrial and glycosomal signal sequences. The unexpected localization of α-KDE1 to BF *T. brucei* glycosomes raised the question of how this protein was differentially targeted to mitochondria and glycosomes. Studies on the import of proteins into trypanosome glycosomes and mitochondria has led to the identification of amino acid sequences that can specifically target both organelles. The mitochondrial targeting signals (MTS) are largely, but not exclusively, restricted to N-terminal amino acids that can be as short as five residues in trypanosomes (31-33). *T. brucei* proteins require either C-terminal peroxisomal targeting signals-1 (PTS1) or N-terminal peroxisomal targeting signals-2 (PTS2) sequences for import into glycosomes (34-37). α-KDE1 has a highly conserved N-terminal MTS (MMRRL-), lacks the characteristic tripeptide C-terminal PTS1 sequence but contains an N-terminal sequence, overlapping the MTS, containing residues conserved in glycosome and peroxisome PTS2 sequences (MMR**RL**SP**V**NGS**V**) with a highly conserved basic amino acid (arginine) at position 4 and hydrophobic residues at positions 5, 8 and 12 (38) (**Figure 3.7A**). To determine whether the N-terminal sequence from α-KDE1 functioned as a glycosome targeting sequence the first 18 amino acids were fused to the coding sequence for the reporter protein eGFP and cloned into a tetracycline regulated vector to allow expression in BF *T. brucei* (**Figure 3.7B**). The localization of α-KDE1-eGFP was determined by fluorescence microscopy in a stable cell line. Consistent with the localization of the full length, α-KDE1-HA, α-KDE1-eGFP localized exclusively to glycosomes of BF *T. brucei* indicating that the N-terminal 18 amino acids of α-KDE1 contained a functional PTS2 (**Figure 3.7C-D**).

Discussion

Organisms use a wide array of mechanisms to compensate for a seeming limitless need for biological diversity in the face of rather limited genetic potential. Generation of functionally

distinct proteins from a single gene by genetic recombination, alternative mRNA processing and post translational modifications contributes to changes in all organisms in response to environmental and developmental cues (39-43). In addition, a small but significant number of proteins can carry out multiple functions without sequence or post-translation change. The moonlighting functions of several canonical metabolic enzymes have been described in mammals, fungi, plants and protozoa (12, 13, 44). Identifying moonlighting activities for essential proteins is difficult since conventional loss of function analyses generally cannot distinguish a single versus multiple activities for a protein. We have begun to investigate potential moonlighting activities for mitochondrial proteins in African trypanosomes. The developmental regulation of mitochondrial carbohydrate metabolism in *T. brucei* allowed us to initially investigate the function of the enzyme components of the inoperative Krebs cycle in BF *T. brucei*. We previously reported that the dihydrolipoyl succinyltransferase, α-KDE2, was expressed in BF *T. brucei* and was associated with the kDNA network and mitochondrial membrane. This protein was essential for the maintenance of the kDNA during cell division (12). The studies reported here show that α-ketoglutarate decarboxylase, α-KDE1, is also essential in BF *T. brucei* since RNAi knockdown resulted in growth arrest and caused death within 24 hours. Furthermore, we observed morphological changes to the α-KDE1 RNAi *T. brucei* that included extensive and rapid swelling of the flagellar pocket, which was mediated by sequestering of both flagella and plasma membrane into the pocket. The function of α-KDE1 in BF *T. brucei* was addressed by examining the intracellular localization of the protein by immunofluorescence microscopy. Unexpectedly we found that α-KDE1exclusively localized to glycosomes in BF *T. brucei* and we showed that the N-terminal 18 amino acids of α-KDE1 contained overlapping mitochondrial and glycosomal targeting sequences. Together these results

showed that α-KDE1was preferentially targeted to glycosomes in BF *T. brucei* and while the function of α-KDE1 in glycosome is unknown it is essential.

The knockdown of α-KDE1 mRNA by RNAi resulted in the rapid expansion of the flagellar pocket. The resultant cells, after 12-18 hours of induction, resembled the "big eye" cells that were first observed in clathrin and later in dynamin-like protein RNAi knockdowns (22, 25). In both cases the expansion of the flagellar pocket was explained by decreased endocyctosis since secretion was unaffected. In the α-KDE1 RNAi cells, endocytosis was not affected and the expansion of the pocket appeared to result from the recruitment of membrane from both the plasma membrane outside the pocket and the flagella membrane. While we do not know the role that α-KDE1plays in maintenance of the flagellar pocket our results suggest that even small changes in α-KDE1 mRNA dramatically alter membrane dynamics in these organisms. It is possible that the high fluidity of the BF *T. brucei* plasma membrane contributes to membrane mobilization in the a-KDE1 RNAi cells. Rapid lateral mobility of GPI anchored molecules is necessary to allow clearance of antibodies against the VSG preventing early killing of BF trypanosomes (45). It is possible that the high fluidity of BF *T. brucei* membranes requires positive regulatory mechanisms to maintain functional subdomains within the contiguous membrane systems of the plasma, flagellum and flagellar pocket. It is difficult to predict the role of α-KDE1 in such a pathway because of the complexity of the metabolic and biosynthetic pathways in glycosomes, however, analysis of α-KDE1 associated proteins in BF *T. brucei* may provide additional insight.

The localization of α-KDE1 to the BF *T. brucei* glycosome was explained by the identification of an N-terminal PTS2 consensus sequence (38). Peroxisomal import of both PTS1 and PTS2 containing proteins requires a family of proteins, peroxins (PEX) that recognize

PTS1 or PTS2 and allow import (46). Several homologues of the PEX proteins have now been identified in trypanosomes and have been shown to be necessary for protein import into the glycosome (47-50). The exclusive localization of α-KDE1to the glycosome of BF *T. brucei* suggests that the PTS2 dominates targeting in the BF while the MTS directs localization to PF mitochondria when a-KDE1 assembles into a functional Krebs cycle enzyme complex (12). Dual targeting of peroxisomal proteins has been described for a range of eukaryotes and the mechanism of targeting to different organelles can be the result of alternative transcription start sites, polyadenylation or splicing giving rise to proteins with distinct targeting sequences (51, 52). Proteins that are dual targeted to mitochochondria and peroxisomes may have an N-terminal MTS and C-terminal PTS1. In the case of type II NAD(P)H dehydrogenases (ND) in *Arabidopsis* the intracellular distribution of NDs is dependent of the affinity of the NDs for the mitochondrial or peroxisomal receptors (53). Differential phosphorylation at serines near a PTS2 can also interfere with peroxisomal targeting (54).

There are several potential mechanisms for the differential targeting of α-KDE1to the mitochondrion of PF *T. brucei* and to the glycosomes of BF cells. While lacking cis-splicing all trypanosome mRNAs are processed by the addition of a 39nt RNA at the 5' end by trans-splicing. Recent studies have shown that alternative trans-spliced mRNAs can be translated to isoforms of proteins that are differentially localized to the mitochondrion, nucleus or cytosol (55). However, analysis of the transcriptome data for the 5' ends of PF and BF *T. brucei* mRNAs did not reveal heterogeneity at the 5' end of α-KDE1 mRNAs that could alter MTS or PTS2 sequences (55). Rather, it seems likely that the differential localization of α-KDE1 is a consequence of the relative efficiencies of the import of α-KDE1 into the glycosome and mitochondrion of BF and PF *T. brucei*.

It is tempting to speculate that since the BF *T. brucei* lack cytochrome mediated electron transport that the energetic state of the BF and PF may differ and selectively influence protein import. However, the mitochondrial membrane potential in PF and BF *T. brucei* has been measured to be nearly identical (130-140mV) and import of proteins into BF *T. brucei* mitochondria has been shown to be dependent on a membrane potential (56, 5). In contrast to α-KDE1, α-KDE2 remains targeted to the mitochondrion in BF (although then having a different, moonlighting function in that organelle), thus the use (expression and routing) of these proteins, which usually are part of a single mitochondrial complex, is uncoupled in BF cells (12). Reduced mitochondrial α-KDE1 was also not a consequence of a deficiency in the general protein import machinery since both mitochondria and glycosomes import a number of proteins constitutively during development. While we do not know the molecular basis for the selective targeting of α-KDE1 to the PF mitochondria and the BF glycosome an analogous situation has been described for the distribution of catalase A in yeast (56). Catalase A is a peroxisomal protein necessary for the detoxification of oxygen radicals and serves as a scavenger of H_2O_2 produced by peroxisomal enzymes. However, when cultivated under respiratory growth conditions, where reactive oxygen species accumulate in mitochondria, yeast import catalase A into both peroxisomes and mitochondria. The changes we have observed in the distribution of α-KDE1 during *T. brucei* development mirrors the metabolic state of the mitochondrion suggesting that metabolic sensing may play a role in establishing the cellular distribution of this and other moonlighting proteins.

Acknowledgments

We thank Jim Morris (Clemson University) for antibodies against trypanosome aldolase, Anzio Gartrell, John Shields and Mary Ard (University of Georgia) for assistance with electron microscopy and Torsten Ochsenreiter (Bern University) for insight into mechanisms of protein

diversification in trypanosomes. We also wish to thank members of the Hajduk and Sabatini labs for helpful discussion and comments on the manuscript. This work was supported by NIH grants AI21401 and AI39033.

References

1. **Simarro PP, Diarra A, Postigo JAR, Franco JR, Jannin JG.** 2011. The human African trypanosomiasis control and surveillance programme of the World Health Organization 2000-2009: The way forward. PLoS Negl. Trop. Dis. **5**: e1007

2. **Van den Bossche P, de La Rocque S, Hendrickx G, Bouyer JA**. 2010. Changing environment and the epidemiology of tsetse-transmitted livestock trypanosomiasis. Trends Parasitol. **26**: 236–243

3. **Wolburg H, Mogk S, Acker S, Frey C, Meinert M, Lazarus M, Urade Y, Kubata BK, Duszenko M.** 2012. Late Stage Infection in Sleeping Sickness. PLoS ONE **7**: e34304.

4. **Matthews KR**. 2005. The developmental cell biology of *Trypanosoma brucei*. J. Cell. Sci. **118**:283-290

5. **Bringaud F, Riviere L, Coustou V.** 2006. Energy metabolism of trypanosomatids: Adaptation to available carbon sources. Mol. Biochem. Parasitol. **149**:1–9.

6. **Timms MW, van Deursen FJ, Hendricks EF, Matthews KR**. 2002. Mitochondrial development during life cycle differentiation of African trypanosomes: evidence kinteoplast-dependent differentiation control point. Mol. Boil. Cell **13**:3747-3759.

7. **Parsons M.** 2004. Glycosomes: parasites and the divergence of peroxisomal purpose. Mol. Microbiol. **53**: 717-24.

8. **Michels PAM, Bringaud F, Herman M, Hannaert V.** 2006. Metabolic functions of glycosomes in trypanosomatids. Biochim. et Biophy. Acta **1763**:1463-1477.

9. **van Weelden SW, Fast B, Vogt A, van Der Meer P, Saas J, van Hellemond JJ, Tielens AGM, Boshart M.** 2003. Procyclic *Trypanosoma brucei* do not use Krebs cycle activity for energy generation. J. Biol. Chem. **278**: 12854-63.

10. **Perham RN.** 1991. Domains, motifs, and linkers in 2-oxo acid dehydrogenase multienzyme complexes: a paradigm in the design of a multifunctional protein. Biochem. **30**: 8501-12.

11. **Perham RN.** 2000. Swinging arms and swinging domains in multifunctional enzymes: catalytic machines for multistep reactions. Annu. Rev. Biochem. **69**: 961-1004.

12. **Sykes SE, Hajduk SL.** 2013. Dual functions of α-ketoglutarate dehydrogenase E3 in the Krebs cycle and mitochondrial DNA inheritance in *Trypanosoma brucei*. Euk. Cell 12: 78-90.

13. **Jeffery CJ** 2009. Moonlighting proteins- an update. Mol BioSyst. **5**: 345-350.

14. **Chen XJ, Wang X, Kaufman BA, Butow RA.** 2005. Aconitase couples metabolic regulation to mitochondrial DNA maintenance. Science **307**:714–717.

15. **Wang, Z., J. C. Morris, M. E. Drew, and P. T. Englund**. 2000. Inhibition of Trypanosoma brucei gene expression by RNA interference using an integratable vector with opposing T7 promoters. J Biol Chem **275**:40174-4017.

16. **Oberholzer M, Morand S, Kunz S, Seebeck T.** 2006. A vector series for rapid PCR-mediated C-terminal in situ tagging of *Trypanosoma brucei* genes. Mol. Biochem. Parasitol. **145**:117-120.

17. **Wirtz E Leal S, Ochatt C, Cross GAM.** 1999. A tightly regulated inducible expression system for conditional gene knock-outs and dominate-negative genetics in *Trypanosoma brucei*. Mol. Biochem. Parasitol. **99**: 89-101.

18. **Nilsson, D., K. Gunasekera, J. Mani, M. Osteras, L. Farinelli, L. Baerlocher, I. Roditi, and T. Ochsenreiter**. 2010. Spliced leader trapping reveals widespread alternative splicing patterns in the highly dynamic transcriptome of *Trypanosoma brucei*. PLoS Pathog **6**:e1001037.

19. **Alsford,S., Turner D. J., Obado S. O., Sanchez-Flores A., Glover L, Berriman M., Hertz-Fowler C. and D. Horn.** 2011. High-throughput phenotyping using parallel sequencing of RNA interference targets in the African trypanosome. Genome Res. **21**: 915-924.

20. **Field MC, Carrington M.** 2009. The trypanosome flagellar pocket. Nat. Rev. Microbiol. **7**:775-786.

21. **Silverman JS, Bangs JD.** 2012. Form and function in the trypanosomal secretory pathway. Curr. Opin Microbiol. **15**: 463-8.

22. **Allen CL, Goulding D, Field MC.** 2003. Clathrin-mediated endocytosis in essential in *Trypanosoma brucei*. EMBO J. **22**: 4991-5002.

23. **Ali M, Leung KF, Field MC**. 2014. The ancient small GTPase Rab21 functions in intermediate endocytic steps in trypanosomes. Eukaryot. Cell **13**:304-319.

24. **Hall B, Allen CL, Goulding D, Field MC.** 2004. Both of the Rab5 subfamily small GTPases of *Trypanosoma brucei* are essential and required for endocytosis. Molec. Biochem. Parasitol. **138**: 67-77.

25. **Chanez AL, Hehl AB, Engsler M, Schneider A.** 2006. Ablation of the single dynamin of *T. brucei* blocks mitochondrial fission and endocytosis and leads to precise cytokinesis arrest. J Cell Sci. **119**: 2968-2974.

26. **Garcia-Salcedo J, Perez-Morga D, Gijon P, Dibeck V, Pays E, Nolan DP.** 2004. A differential role for actin during the life cycle of *Trypanosoma brucei*. EMBO J. **23**: 780-789.

27. **Gadelha C, Rothery S, Morhew M, MeIntosh JR, Severs NJ, Gull K.** 2009. Membrane domains and flagellar pocket boundaries are influenced by the cytoskeleton in African trypanosomes. Proc. Natl. Acad. Sci. **106**: 17425-17430.

28. **Balber, AE.** 1990. The pellicle and membrane of the flagellum, flagellar adhesion zone and flagellar pocket: functionally discrete surface domains in the bloodstream form of African trypanosomes. CRC critical reviews in immunology **10**:177-201.

29. **Clayton CE, Michels P.** 1996. Metabolic compartmentation in African trypanosomes. Parasitol. Today **12**: 465-471.

30. **Guerra-Giraldez C, Quijada L, Clayton CE.** 2002. Compartmentation of enzymes in a microbody, the glycosome, is essential in *Trypanosoma brucei*. J. Cell Sci. **115**: 2651-2658.

31. **Priest JW, Hajduk SL.** 1995. The trypanosomatid Rieske iron-sulfur proteins have a cleaved presequence that may direct mitochondrial import. Biochim Biophys Acta **1269**:201-201.

32. **Hausler T, Stierhof YD, Blattner J, Clayton C.** 1997. Conservation of mitochondrial targeting sequence function in mitochondrial and hydrogenosomal proteins from the early-branching eukaryotes *Crithidia, Trypanosoma and Trichomonas*. Eur J. Cell. Biol. **73**:240-251.

33. **Schneider A, Bursac D, Lithgow T**. 2008. The direct route: a simplified pathway for protein import into the mitochondrion of trypanosomes. Trends Cell Biol. **18**:12-18.

34. **Gould SJ, Keller GA, Hosken n, Wilkinson J, Subramini S**. 1989. A conserved tripeptide sorts proteins to peroxisomes. J. Cell Biol. 108: 1657-1664.

35. **Tsukamoto, Hata S, Yokota S, Fujiki Y, Hijkata M, Miyazawa S, Hashimoto T, Osumi T**. 1994. Characterization of the signal peptide at the amino terminus of the rat peroxisomal 3-letpacyl-CoA thiolase precursor. J. Biol. Chem. **269**: 6001-6010.

36. **Colasante C, Ellis M, Ruppert T, Voncken F.** 2006. Comparative proteomics of glycosomes from bloodstream form and procyclic culture form *Trypanosoma brucei brucei.* Proteomics **6**:3275-3293.

37. **Chudzik DM, Michels PA, De Walque S, Hol WGJ** 2000. Structures of type-2 peroxisomal targeting signals in two trypanosomatid aldolases. J. Molec. Biol. **300**: 697-707.

38. **Petriv OI, Tang L, Titorenko VI, Rachubinski RA**. 2004. A new definition for the consensus sequence of the peroxisome targeting signal type 2. J. Molec. Biol. **341**: 119-134.

39. **Graveley BR.** 2001. Alternative splicing: increasing diversity in the proteomic world. Trends Genet **17**:100-107.

40. **Cooper MD, Alder MN**. 2006. The evolution of adaptive immune systems. Cell, **124**: 815-822.

41. **Moore MJ, Proudfoot NJ**. 2009. Pre-mRNA processing reaches back to transcription and ahead to translation. Cell **136**:688-700.

42. **Schmucher D.** 2007. Molecular diversity of Dscam: recognition of molecular identity in neuronal wiring. Nat. Rev. Neurosci. **8**: 915-920.

43. **Ochsenreiter T, Hajduk SL.** 2006. Alternative editing of cytochrome c oxidase III mRNA in trypanosome mitochondria generates protein diversity. EMBO Rep. **7**:1128–1133

44. **Daphne HEW, Huberts IJ, van der Klei J.** 2010. Moonlighting proteins: An intriguing mode of multitasking. Biochim. et Biophys. Acta **1803**: 520-525.

45. **Engstler M, Pfohl T, Herminghaus S, Boshart M, Wiegertjes G, Heddergott N, Overath P.** 2007. Hydrodynamic flow-mediated protein sorting on the cell surface of trypanosomes. Cell, **131**, 505-515.

46. **Galland N, Michels PA.** 2010. Comparison of the peroxisomal matrix protein import

system of different organisms. Exploration of possibilities for developing inhibitors of the import system of trypanosomatids for anti-parasite chemotherapy. Eur. J. Cell Biol. **89**:621–637.

47. **Galland N, Demeure F, Hannaert V, Verplaetse E, Vertommen D, Van der Smissen P, Courtoy PJ, Michels PA**. 2007. Characterization of the role of the receptors PEX5 and PEX7 in the import of proteins into glycosomes of *Trypanosoma brucei*. Biochim. Biophys. Acta **1773**:521–535.

48. **Verplaetse E, Rigden DJ, Michels PA.** 2009. Identification, characterization and essentiality of the unusual peroxin 13 from Trypanosoma brucei. Biochim. Biophys. Acta **1793**:516–527.

49. **Krazy H, Michels PA.** 2006. Identification and characterization of three peroxins—PEX6, PEX10 and PEX12—involved in glycosome biogenesis in *Trypanosoma brucei*. Biochim. Biophys. Acta **1763**:6–17.

50. **Kessler PS, Parsons M.** 2005. Probing the role of compartmentation of glycolysis in procyclic form *Trypanosoma brucei*: RNA interference studies of PEX14, hexokinase, and phosphofructokinase. J. Biol. Chem. **280**:9030–9036

51. **Ast J, Stiebler AC, Freitag J, Bolker M.** 2013. Dual targeting of peroxisomal proteins. Frontiers Physiol. **4**: 1-8.

52. **Petrova VY, Drescher D, Kujumdzieva AV, Schmitt MJ.** 2004. Dual targeting of yeast catalase A to peroxisomes and mitochondria. Biochem. J. **380**:393-400.

53. **Carrie C, Murcha MW, Kuehn K, Duncan O, Barthet M, Smith PM.** 2008. Type II NAD(P)H dehydrogenases are targeted to mitochondria and chloroplasts or peroxisomes in *Arabidopsis thalina*. FEBS Lett. **582**:3073-3079.

54. **Jung S, Marelli M, Rachubinski RA, Goodlett DR, Aitchinson JD.** 2010. Dynamic

changes in the subcellular distribution of Gpd1p in response to cell stress. J. Biol. Chem. **285**:6739-6749.

55. **Nilsson D, Gunasekera K, Mani J, Osteras M, Farinelli L, Baerlocher L, Roditi I, Ochsenreiter T.** 2010. Spliced leader trapping reveals widespread alternative splicing patterns in the highly dynamic transcriptome of *Trypanosoma brucei.* PLoS Pathog. **6**:e1001037.

56. **Vercesi AE, Docampo R, and Moreno SNJ.** 1992. Energization-dependent Ca2+ accumulation in *Trypanosoma brucei* bloodstream and procyclic trypomastigotes mitochondria. Mol. Biochem. Parasitol. **56**, 251-258.

57. **Williams S, Saha L, Singha UK, Chaudhuri M.** 2008. *Trypanosoma brucei*: differential requirement of membrane potential for import of proteins into mitochondria in two developmental stages**.** Exp. Parasitol.**118**: 420-33.

Figures

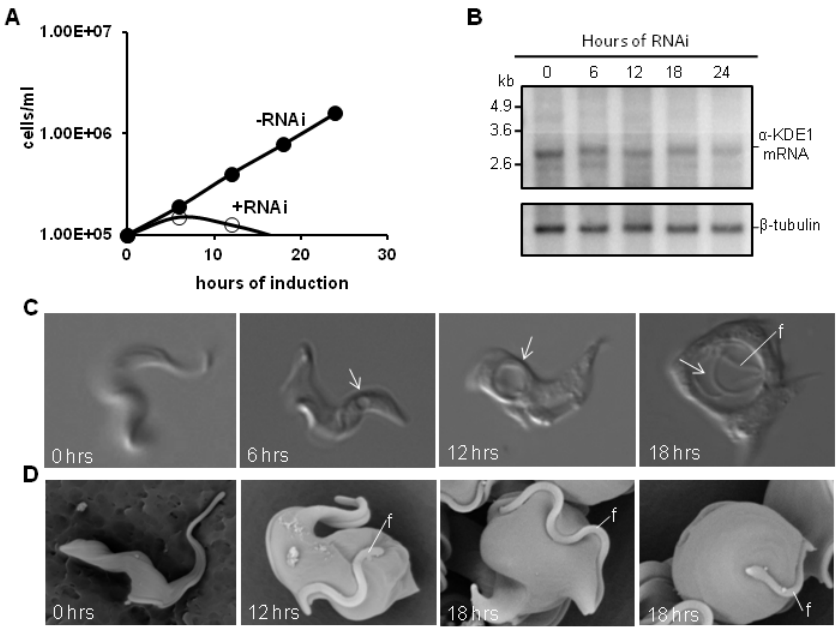

Figure 3.1. α-KDE1 is essential in BF *T. brucei*. Effect of α-KDE1RNAi knockdown on growth and morphology of BF *T. brucei*. (A) Growth of α-KDE1 RNAi cells in culture at 37°C in the presence (+) or absence (-) of doxycycline. (B) Northern blot analysis of the levels of α-KDE1 and β-tubulin mRNA. Total cell RNA was isolated following induction with doxycycline, fractionated on agarose gels and hybridized with specific radioactively labeled probes for α-KDE1 and tubulin. (C) DIC images taken from videos of α-KDE1 RNAi cells following induction with doxycycline for 0, 6, 12, and 18 hours. The position of the expanding posterior

vacuole is indicated (arrow) (D) Scanning electron microscopy of α-KDE1 RNAi *T. brucei* following treatment with doxycycline. The position of the flagella (f) is indicated.

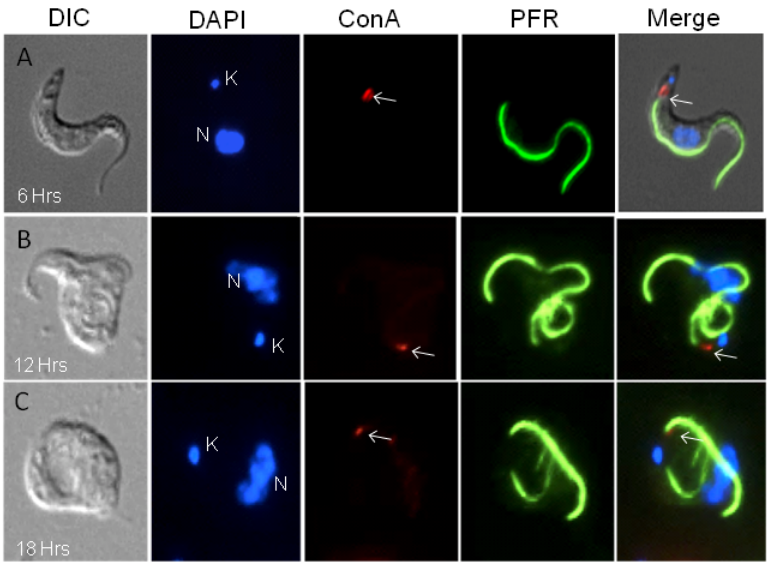

Figure 3.2. Localization of the α-KDE1RNAi induced vacuole. (A-C) Following induction with doxycycline for 6, 12 or 18 hours α-KDE1RNAi cells were incubated at 3°C with Con A-FITC then fixed and incubated with antibodies against PFR and stained with DAPI. The position of the DAPI stained kinetoplast (K) and nucleus (N) are indicated as is bound ConA (arrow).

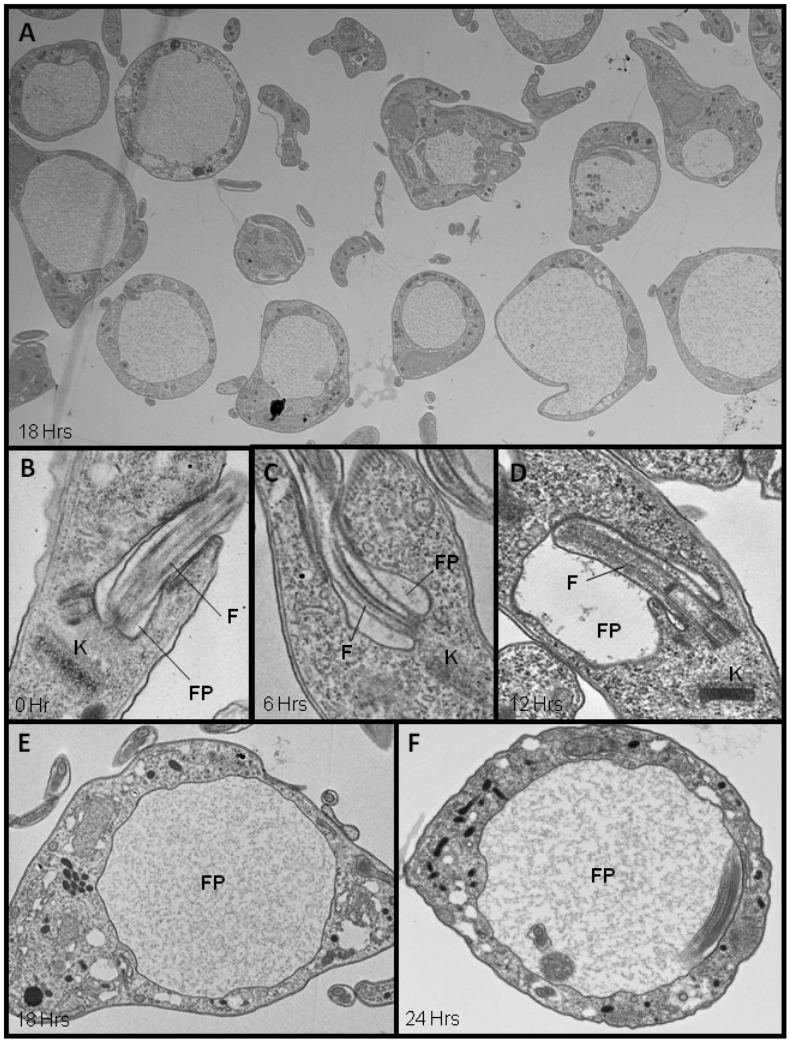

Figure 3.3. α-KDE1 RNAi cause flagellar pocket swelling. Transmission electron microscopy of BF *T. brucei* α-KDE1RNAi. (A) Low magnification image of a field of cells 18 hours after RNAi induction showing a high percentage of cells having a large intracellular vacuole. α-KDE1RNAi treated cells taken at the time of doxycycline induction (B) and after 6 hours (C), 12 hours (D), 18 hours (E) and 24 hours (F). The position of the flagellar pocket (FP), flagellum (F) and kinetoplast (K) are indicated.

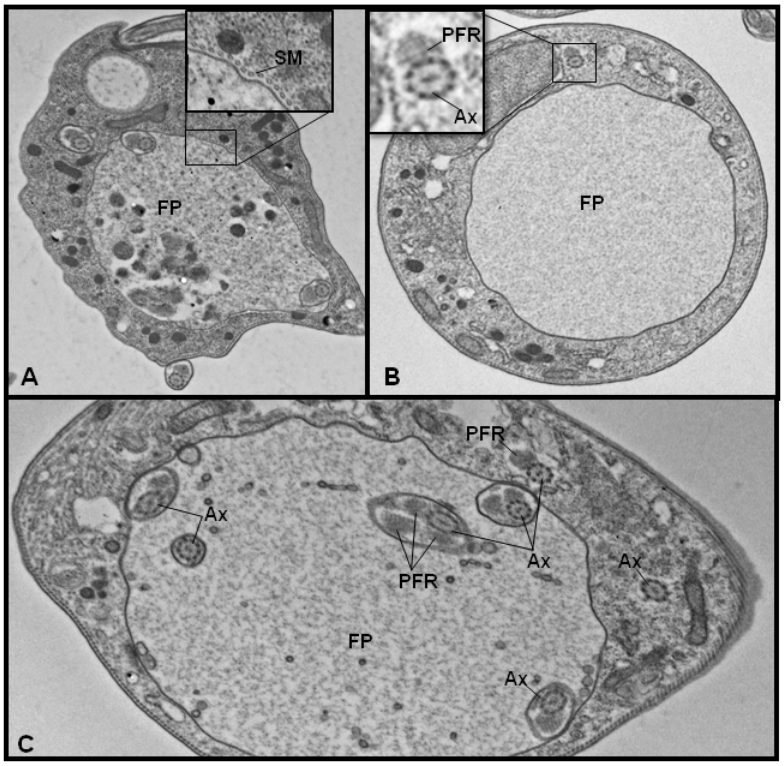

Figure 3.4. Flagellar and plasma membrane are recruited to form the expanding flagellar pocket. Transmission electron microscopy of BF *T. brucei* following induction of α-KDE1 RNAi with doxycycline. (A) Plasma membrane associated pellicular microtubules are found on the membrane of the expanding flagellar pocket . Inset is a higher magnification of a portion of flagellar membrane with associated subpellicular microtubules. (B) Both axoneme and PFR, stripped of flagellar membrane, are displaced to the cytoplasm of α-KDE1 RNAi cells. Inset is a higher magnification view of a stripped axoneme and associated PFR in the cytoplasm.

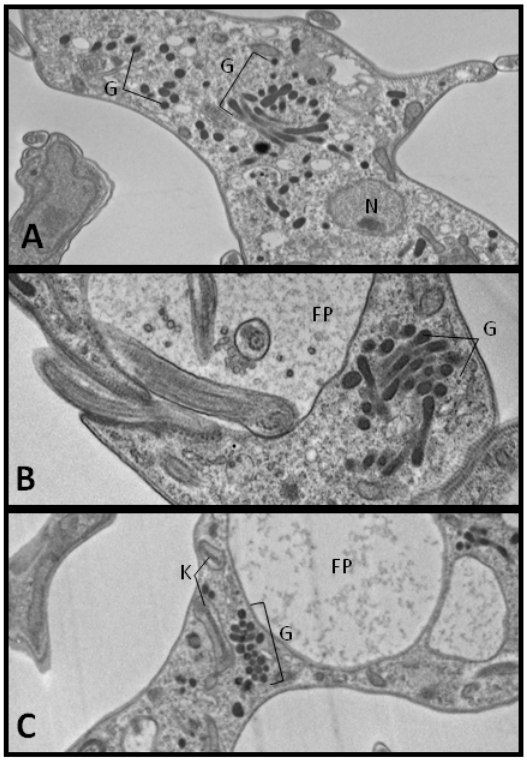

Figure 3.5. Morphological changes to glycosomes in α-KDE1 RNAi *T. brucei.* Transmission electron microscopy of BF *T. brucei* following induction of α-KDE1 RNAi with doxycycline. (A-C) 18 hours after induction of α-KDE1 RNAi revealed clusters of elongated glycosomes throughout the cytoplasm but predominately near the flagellar pocket. The position of the flagellar pocket (FP), glycosomes (G), kinetoplast (K) and nucleus (N) are indicated.

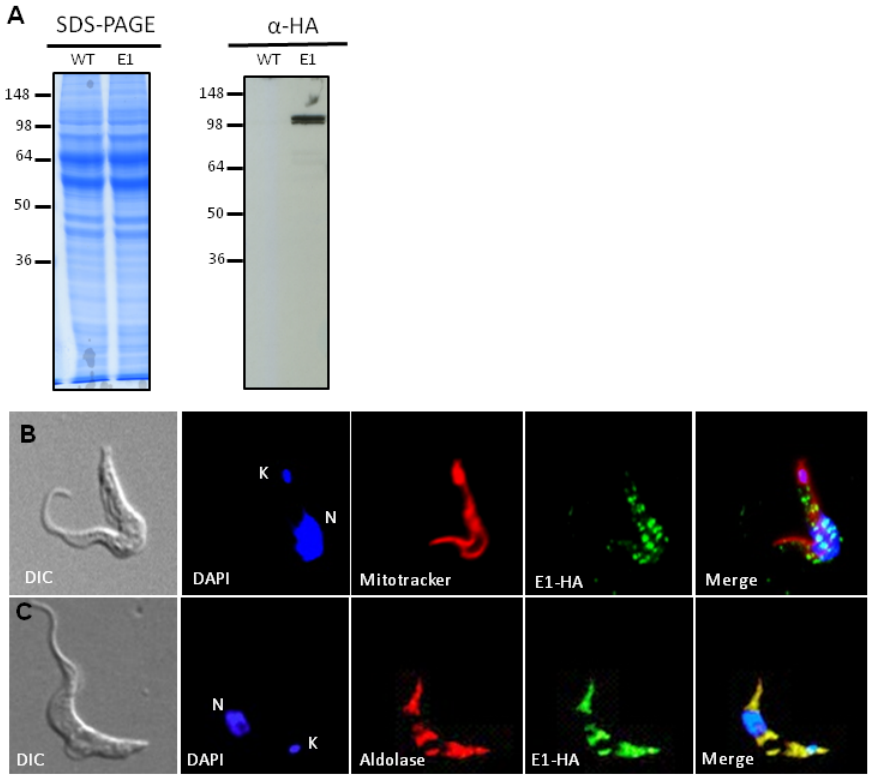

Figure 3.6. Localization of α-KDE1 to the glycosome of BF *T. brucei*. α-KDE1 was tagged with a C-terminal HA epitope and was used to prepare a constitutively expressing α-KDE1-HA cell line. (A) Total cell protein from wild type and α-KDE1-HA cells was fractionated by SDS-PAGE and analyzed by western blot. On the left is the Coomassie stained gel and on the right the blot following incubation with anti-HA. (B, C) The localization of α-KDE1-HA by immunofluorescence microscopy relative to the mitochondrion stained with MitoTracker (B) and aldolase (C). The positions of the nucleus (N) and kinetoplast (K) are indicated.

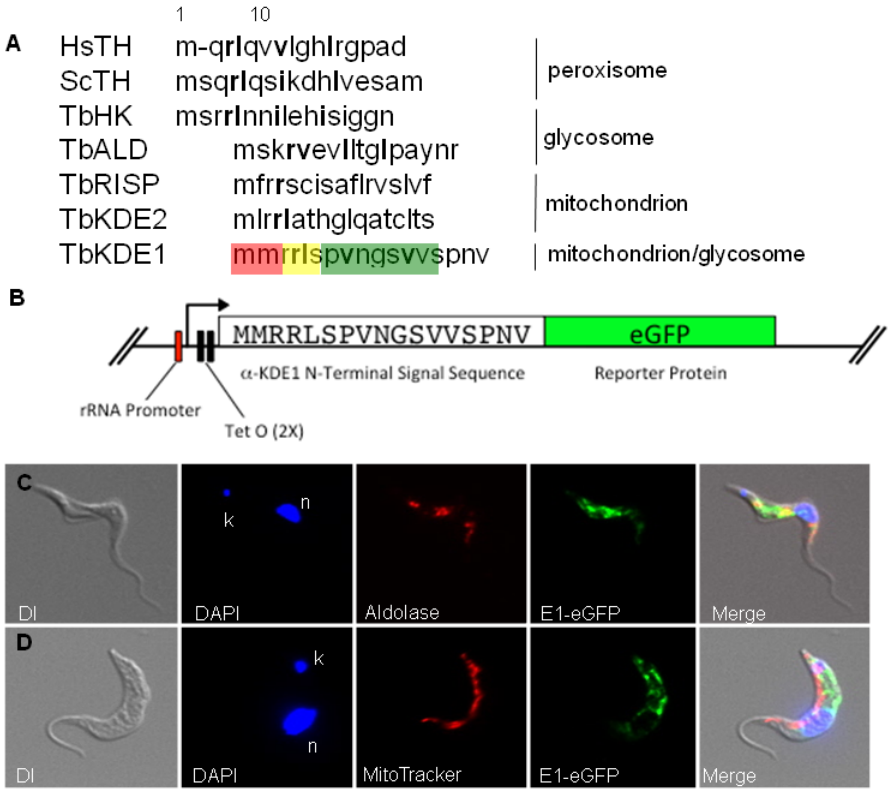

Figure 3.7. α-KDE1 contains an N-terminal glycosome targeting signal. (A) Alignment of N-terminal amino acid sequences of α-KDE1, human and yeast peroxisomal, trypanosome glycosomal and trypanosome mitochondrial proteins. The proposed trypanosome α-KDE1 MTS sequence (red) and PTS2 sequences (green). The arginine at position 4 and the leucine at position 5 (yellow) overlap in the predicted MTS and PTS2 sequences. Highly conserved residues in all PTS2 sequences are indicated in bold (positions 4, 5,8, 12 in α-KDE1). (B) A fusion construct used to produce an α-KDE1-eGFP reporter contains the N-terminal 18 amino acids of α-KDE1 and the coding sequence for eGFP. (C-D) Following induction eGFP localization was determined by fluorescence microscopy with cells stained with anti-aldolase (C) and Mitotracker (D). The positions of the nucleus (N) and kinetoplast (K) are indicated.

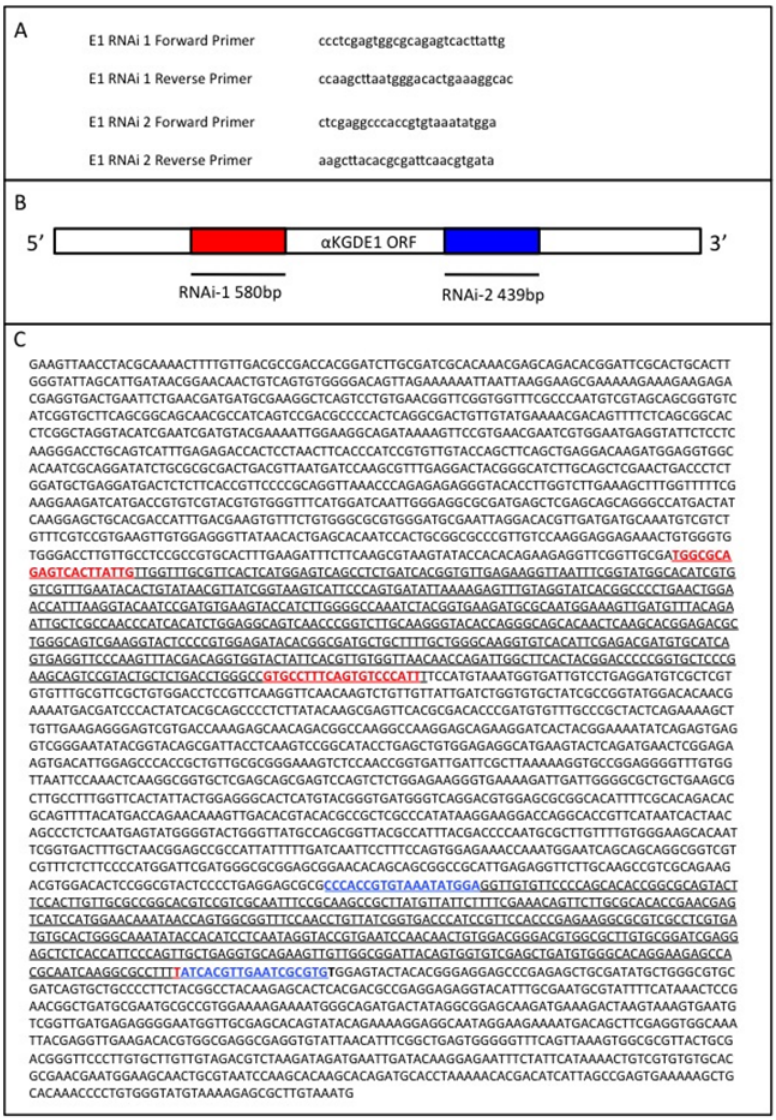

Supplemental Figure 3.1. Amplification of two α-KDE1 sequences for RNAi (A) Forward and reverse primer pairs for preparation of two α-KDE1 RNAi constructs. The complete primer sequence is shown. (B) Relative location and size of the two products from the α-KDE1 open reading frame (ORF). (C) Coding sequence of the α-KDE1. The sequences complementary to the PCR primers are indicated in red and blue.

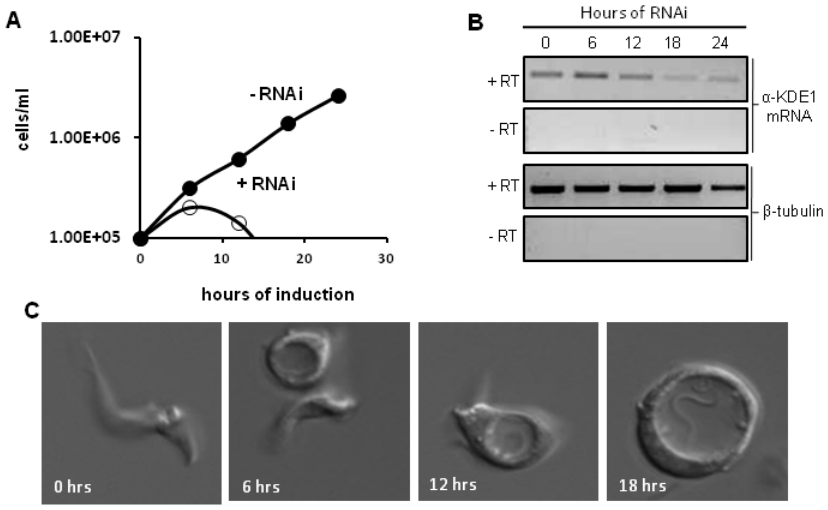

Supplemental Figure 3.2. Effects on BF *T. brucei* following α-KDE1RNAi knockdown with second RNAi sequence. (A) Growth of α-KDE1RNAi cells in culture at 37C in the presence (+) or absence (-) of doxycycline. (B) RT-PCR analysis of α-KDE1 and β-tubulin mRNA. Cellular RNA was extracted during time course induction with doxycycline, cDNA was prepared and used for PCR amplification, with (+) and without (-) reverse transcriptase (RT) to ensure no contaminating DNA was present from RNA preparation. PCR products were ran on agarose gels and imaged. (C) DIC images taken from videos of α-KDE1 RNAi cells following induction with doxycycline for 0, 6, 12, and 18 hours. The expanding posterior vacuole and internalized flagellum are visible.

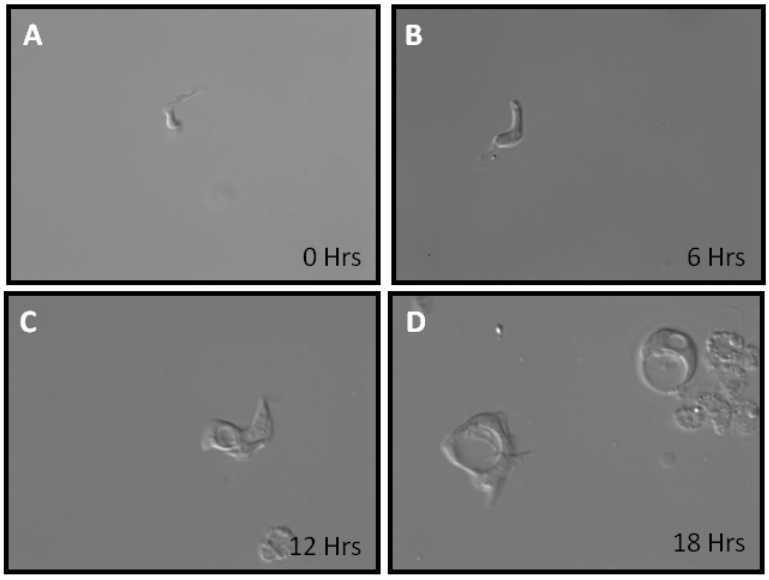

Supplemental Figure 3.3. Motility of BF *T. brucei* is altered by α-KDE1RNAi. (A-D)Videos of cells by DIC at the time of induction (0 hours) and 6, 12, 18 hours post induction.

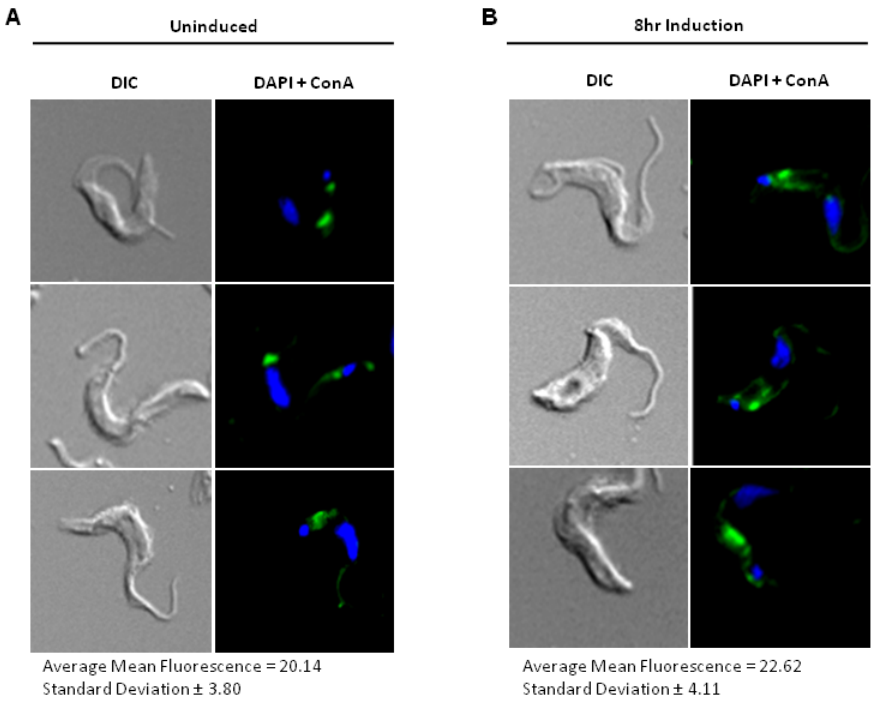

Supplemental Figure 3.4. Endocytosis during α-KDE1 RNAi induction. (A) Endocytosis of ConA was carried out for uninduced cells and internalized ConA signal was quantified using

ImageJ softwear. (B) ConA endocytosis was also carried out after 8 hours of induction with doxycycline and internalized ConA signal was quantified with ImageJ softwear.

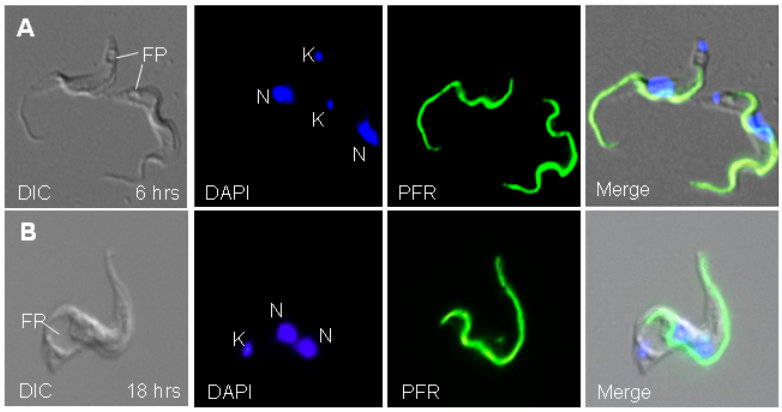

Supplemental Figure 3.5. Localization of the posterior vacuole in α-KDE1RNAi *T. brucei*. Position of the vacuole relative to the kinetoplast (K) and paraflagella rod (PFR). (A) 6hours post induction. (B) 18 hours post induction.

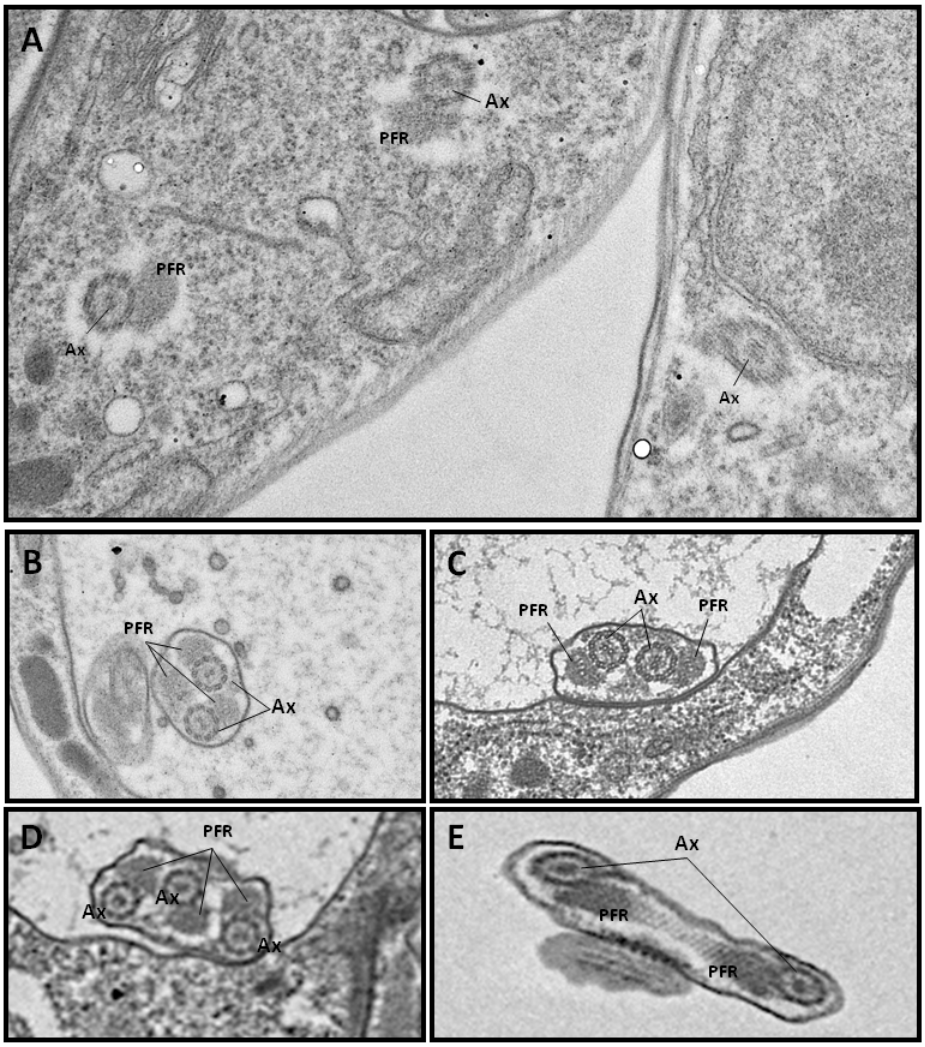

Supplemental Figure 3.6. Morphological changes to the flagellum in α-KDE1 RNAi *T. brucei.* Transmission electron microscopy of BF *T. brucei* following induction of α-KDE1 RNAi with doxycycline. (A-E) 18 hours after induction of α-KDE1 RNAi revealed flagellar axonemes (Ax) and paraflagellar rod (PFR) stripped of flagellar membrane in the cytoplasm. Flagella were also observed in the flagellar pocket and outside the cell that contained multiple Ax and PFR complexes.

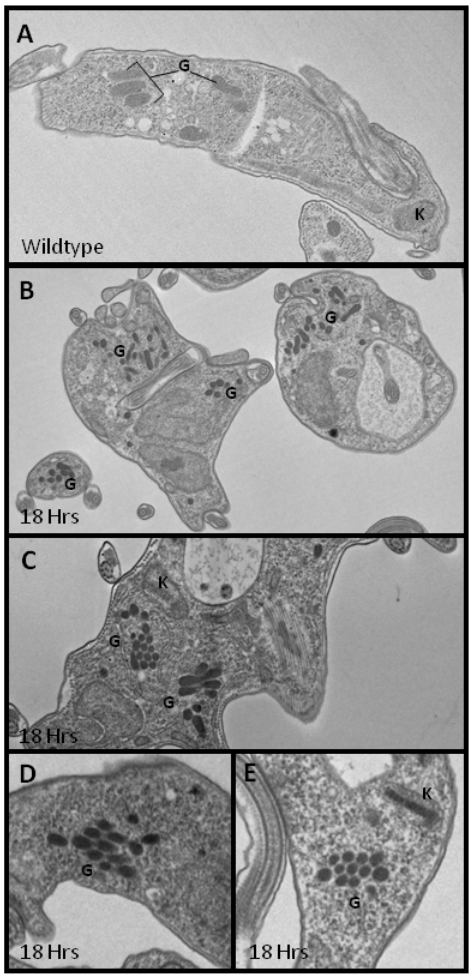

Supplemental Figure 3.7. Morphological changes to glycosomes in α-KDE1 RNAi *T. brucei.* Transmission electron microscopy of BF *T. brucei* following induction of α-KDE1 RNAi with doxycycline. (A) Representative untreated wild type BF *T. brucei*. (B-E) BF *T. brucei* 18 hours after induction of α-KDE1 RNAi revealed clusters of elongated glycosomes throughout the cytoplasm but predominately near the flagellar pocket. The position of the flagellar pocket (FP), glycosomes (G), kinetoplast (K) and nucleus (N) are indicated.

CHAPTER 4

EXTRACELLULAR VESICLES FROM *TRYPANOSOMA BRUCEI* MEDIATE VIRULENCE FACTOR TRANSFER AND CAUSE HOST ANEMIA

Szempruch A.J.[*], Sykes S.E.[*], Kieft R., Dennison L.W., Becker A.C., Gartrell A., Martin W.J., Nakayasu E.S., Almeida I.C., Hajduk S.L. and J.M. Harrington. Cell. 2016 Jan 14;164(1-2):246-57. doi: 10.1016/j.cell.2015.11.051. [*] These authors contributed equally to this work. Reprinted with permission from the publisher.

Abstract

Intercellular communication between parasites and with host cells provides mechanisms for parasite development, immune evasion and disease pathology. Bloodstream African trypanosomes produce membranous nanotubes that originate from the flagellar membrane and disassociate into free extracellular vesicles (EVs). Trypanosome EVs contain several flagellar proteins that contribute to virulence and *Trypanosoma brucei rhodesiense* EVs contain the serum resistance-associated protein (SRA) necessary for human infectivity. *T. b. rhodesiense* EVs transfer SRA to non-human infectious trypanosomes allowing evasion of human innate immunity. Trypanosome EVs can also fuse with mammalian erythrocytes resulting in rapid erythrocyte clearance and anemia. These data indicate that trypanosome EVs are organelles mediating non-hereditary virulence factor transfer and causing host erythrocyte remodeling inducing anemia.

Introduction

Bacteria and eukaryotic cells use extracellular vesicles (EVs) as vehicles for delivery of modulatory proteins, lipids and nucleic acids to neighboring cells (Schorey et al., 2015; Yanez-Mo et al., 2015). Extracellular vesicles generally fall into two classes: 1) exosomes produced in the exocytic pathways and generally associated with the formation of multivesicular bodies (MVBs) and 2) ectosomes formed by budding of the plasma membrane. Both carry effector proteins and nucleic acids (Schorey et al., 2015; Wood and Rosenbaum, 2015). Functions proposed for EVs include transfer of drug resistance, growth regulation, quorum sensing, immune regulation, developmental modulation and neurotransmission (Remis et al., 2014). In addition, several human diseases including cancer, atherosclerosis, neurodegeneration, as well as

viral and parasite infections are affected by EV production. A clear and defining function of EVs is the delivery of modulatory molecules to other cells within and between species. The range of functions attributed to EVs is reflected in diverse mechanisms of EV biogenesis and composition (Schorey et al., 2015).

The kinetoplastidae is a diverse group of eukaryotic microbes responsible for several important human and animal diseases including African sleeping sickness (*Trypanosoma brucei rhodesiense* and *Trypanosoma brucei gambiense*), Chagas disease (*Trypanosoma cruzi*), Kala azar (*Leishmania donovani*) and Nagana in cattle (*Trypanosoma brucei brucei*). *T. cruzi* and *Leishmania* spp. have been shown to release EVs that interact with host cells and modulate immune responses (Marcilla et al., 2014). Other eukaryote pathogens also produce EVs. EVs derived from *Plasmodium falciparum*-infected erythrocytes promote parasite differentiation and regulate immune cells within the mammalian host (Mantel et al., 2013; Regev-Rudzki et al., 2013). The urogenital tract parasite *Trichomonas vaginalis* produces EVs that alter adherence to host cells and modulate the host immune response to infection (Twu et al., 2013).

Humans and other higher primates are innately immune to many African trypanosomes by virtue of circulating trypanosome lytic factors (TLF). Human pathogenic *T. b. rhodesiense* circumvents TLF activity through expression of a virulence factor, the serum-resistance associated protein (SRA) (De Greef and Hamers, 1994). The mechanism of SRA involves binding to apolipoprotein L-1 (ApoL-1), a pore forming toxin within TLF (Vanhamme et al., 2003). Binding, uptake and intracellular trafficking of TLF to early endosomes of *T. b. rhodesiense* leads to co-localization of SRA and TLF facilitating the neutralization of ApoL-1 activity(Stephens and Hajduk, 2011). Transfection of *T. b. brucei* with the gene encoding SRA or co-infection of tsetse flies with *T. b. rhodesiense* and *T. b. brucei* allows for transfer of the gene

encoding *SRA* to *T. b. brucei* and confers resistance to TLF (Gibson et al., 2015; Xong et al., 1998). Direct transfer of this virulence protein between trypanosomes has not been reported.

Like many extracellular pathogens, African trypanosome infection initially elicits a type 1 immune response that includes expression of inflammatory cytokines and activation of myeloid cells. These host immune responses have been implicated in the pathology of trypanosomiasis-associated anemia (Stijlemans et al., 2015). Anemia is markedly severe during acute infection and is the major cause of cattle death due to Nagana (Naessens, 2006). Recently, erythrophagocytosis by activated liver and spleen myeloid cells has been identified as a major contributor to erythrocyte clearance. In addition, the lipid composition of erythrocytes is altered during trypanosome infection and these erythrocytes are preferentially phagocytosed by the host's myeloid cells (Stijlemans et al., 2015). While host responses that contribute to anemia have been characterized, the parasite factors that elicit erythrocyte clearance are unknown.

Here we describe a dynamic class of membrane nanotubes that bud from the trypanosome flagellar membrane and vesicularize to form EVs. The proteome of these EVs is enriched for specific flagellar membrane proteins and contains a number of proteins implicated in virulence and persistence within the host. Functionally we show that *T. brucei* EVs fuse with target lipid bilayers, including the flagellar pocket of neighboring trypanosomes, resulting in transfer and internalization of lipids and proteins. Transferred proteins retain activity since *T. b. rhodesiense* EVs transfer SRA to *T. b. brucei* resulting in resistance to TLF. *T. brucei* EVs are also highly fusogenic with host erythrocyte membranes, altering the physical properties of the membrane and causing erythrocyte clearance from circulation. We postulate that this causes anemia during animal and human infection by African trypanosomes. Our findings show that EVs contribute to

the complexity of African trypanosomiasis through the transfer of virulence factors between parasites and inadvertent interaction with host cells, which has a profound effect on disease.

Results

Flagellar membrane budding gives rise to nanotubes and EVs in *T. brucei*

Exchange of metabolites, nucleic acids and proteins in bacteria can take place over short and long distances via the formation of membrane nanotubes between individual bacterium and production and delivery of EVs (Dubey and Ben-Yehuda, 2011). Cell-cell communication occurs in the eukaryotic pathogen *T. b. brucei* as demonstrated by quorum sensing-mediated differentiation into the tsetse fly transmissible short-stumpy developmental form in the mammalian bloodstream (Mony et al., 2014) and social motility exhibited by procyclic forms in the insect vector midgut (Oberholzer et al., 2010). The molecular mechanisms underlying these communication processes in African trypanosomes have not yet been identified.

Visualization of bloodstream form (BF) *T. b. brucei* by differential interference contrast (DIC) video microscopy revealed the presence of highly dynamic filamentous structures (2-20 μm) extending from the posterior end of some cells (**Figure 4.1A**). These structures resembled previously described thread-like appendages, later called plasmanemes, associated with BF African trypanosomes (Babudieri and Tomasini, 1962; Schepilewsky, 1912; Vickerman and Luckins, 1969). Occasionally filaments appeared to make connections with the posterior ends of other trypanosomes and if unattached become highly branched (**Figure 4.1A**). These structures were largely disregarded due to lack of detection from blood of infected mice (Ellis et al., 1976; Wright et al., 1970). To determine if these structures were physiologically relevant we performed DIC video microscopy of infected mouse blood. Similar filamentous structures were also visible on *T. brucei* in the blood of infected mice (**Figures 4.1B and S4.1A**). The formation of the

filaments *in vitro* was stimulated by stress from RNAi against an essential BF protein or by addition of complement active serum to growth medium (**Figure S4.1B**) (Sykes et al., 2015). These induction mechanisms allowed us to investigate filament biogenesis.

Live imaging of BF *T. brucei* labeled with the membrane binding dye octadecyl rhodamine B (R18) suggested that filaments were bounded by a lipid membrane and led us to rename the plasmanemes "membrane nanotubes" to better reflect their structure and composition (**Figure 4.1C, Movie S4.1 and S4.2**). Observations of nanotubes connecting cells showed these interactions were stable over long distances (>20 μm) and highly dynamic, releasing and forming new connections with several cells over time (**Figure 4.1D and Movie S4.3**). When visualized by negative stain transmission electron microscopy (TEM), nascent nanotubes showed a continuous membrane (**Figure 4.1E and Figure S4.1C**), consistent with previous observations using negative stain and thin section TEM (Frevert and Reinwald, 1988; Vickerman and Luckins, 1969). Though it has been shown previously that short stumpy *T. brucei* produce "secretory-filaments" we restricted our studies to exponentially growing long slender BF *T. brucei* (Ellis et al., 1976). Nanotubes were restricted to the cell posterior, suggesting a polarized point of origin. TEM of thin sections revealed membrane budding from the flagellum, with similar characteristics to the adjacent flagellar membrane (**Figure 4.1F and Figure S4.1D**) and three-dimensional reconstruction of serial sections showed that protrusion of the flagellar membrane gave rise to a tubular structure lacking the axoneme and paraflagellar rod **(Figure 4.1G and Movie S4.4**). These observations suggested that *T. brucei* nanotubes developed from budding of the flagellar membrane and extended for at least a short distance parallel to the flagellum. Longitudinal sections through nanotubes revealed repeating spherical units resembling "beads on a string" outside the flagellar pocket at the cell surface (**Figure 4.2A**). The average

diameter of a "bead" was approximately 100 nm (**Figure 4.2B**). The vesicular appearance of trypanosome nanotubes resembles the vesicle chains that dissociate to produce free EVs in the bacterium *Myxococcus xanthus* (Dubey and Ben-Yehuda, 2011). These observations are similar to previous reports from trypanosomes (Babudieri and Tomasini, 1962; Ellis et al., 1976; Frevert and Reinwald, 1988; Schepilewsky, 1912). Indeed, scanning electron microscopy revealed trypanosome-associated vesicles consistent in size with nanotube beads (**Figure 4.2C**). Using DIC video microscopy, we observed the dynamics of formation, release and disassociation of a nanotube into diffusible EVs (**Figure 4.2D and Movie S4.5**). Release from nanotubes allowed us to purify, characterize and investigate the cellular interactions of trypanosome EVs derived from exponentially growing cells, that have not been stimulated for nanotube formation.

The EV proteome is enriched in flagellar membrane proteins and parasite virulence factors

When viewed by negative stain TEM purified EVs appear as unilamellar vesicles approximately 70-80 nm in diameter, consistent with the size of nanotube associated beads (**Figure 4.2E upper panel**). TEM thin section analysis of purified EVs revealed membrane-bound vesicles of ~80 nm in size with a 10 nm thick membrane (**Figure 4.2E lower panel and Figure S4.1E**) with similar characteristics to cell plasma membrane (**Figure S4.1F**). Nanoparticle tracking analysis revealed a major population of vesicles with a mean diameter of 81 nm and a minor population 165 nm in diameter (**Figure 4.2F**). Purified EVs showed a different SDS-PAGE protein profile than total cell (**Figure 4.2G**). Proteomic analysis of EVs revealed 156 proteins from diverse functional classes (**Table S4.1**) and several were confirmed by western blotting, including the expressed variant surface glycoprotein (VSG 221), Hsp-70, glycerol kinase and aldolase (**Figure 4.2H**). Similar to observations from *Leishmania* spp. we detected ribosomal proteins in the *T. brucei* EV proteome (Silverman et al., 2010). Although it is

not uncommon to screen out proteins based on high isoelectric point, removing many ribosomal proteins, we performed an analysis on the complete/unfiltered 156 proteins (**Figure 4.2I, Table S4.1 and Table S4.2**) (Broadhead et al., 2006). Comparison of the EV proteome with that of the flagellar surface and flagellar matrix showed significant overlap (**Figure 4.2I**) (Oberholzer et al., 2011). Our analysis showed that 50 of 156 EV proteins were either flagellar matrix or membrane proteins representing 32% of the EV proteome. In addition, we found only minor similarity with the glycosome (2%) and mitochondrial (2%) proteomes (Guther et al., 2014; Panigrahi et al., 2009) (**Figure 4.2I and Table S4.2**), which is proportionally similar when compared to the total proteome; therefore, EVs from *T. b. brucei* BFs are not enriched with proteins from these two organelles. Ten of these proteins have previously been co-localized by fluorescence microcopy and were shown to be flagellar/flagellar-associated (**Table S4.2**). While the EVs appear homogeneous in size and morphology they may be derived from multiple mechanisms of origin. Enrichment of EVs with flagellar proteins is consistent with a population of EVs being derived from nanotubes that form by budding of the flagellar membrane. We observed that in addition to abundant proteins such as VSG more than 20% of the EVs composition was from low abundance proteins (**Table S4.2**) (Jensen et al., 2014). Among these minor proteins were several flagellar proteins, including calflagin (CF), adenylate cyclase (GRESAG4), glycosylphosphatidylinositol phospholipase C (GPI-PLC) and metacaspase 4 (MCA4), that contribute to the virulence of *T. brucei* in the mammalian host (**Table S4.2**) (Emmer et al., 2010; Proto et al., 2011; Salmon et al., 2012; Webb et al., 1997). We next determined whether African trypanosomes expressing SRA, a well-characterized virulence factor, release EVs containing this protein. Extracellular vesicles were purified from a *T. b. brucei* line expressing a Ty-epitope tagged SRA (*T. b. brucei*$^{SRA\text{-}Ty}$) (Oli et al., 2006) and western blots demonstrated the presence of SRA in these preparations

(**Figure 4.2J**). The diversity of virulence factors detected in the EV proteome suggests that the flagellum may serve as part of a sorting pathway for delivery of biologically active molecules to neighboring cells.

T. b. rhodesiense EVs transfer SRA to *T. b. brucei* and confers resistance to TLF

The observation that SRA was present in EVs led us to investigate whether SRA could be transferred to TLF susceptible *T. b. brucei*. We used flow cytometry to determine whether EVs from *T. b. brucei*$^{SRA\text{-}Ty}$ bound and were taken-up by wild type *T. b. brucei* (**Figures 4.3A and 4.3B**). *T. b. brucei* were incubated with SRA-Ty containing EVs at 37°C, washed to remove unbound EVs and fixed with paraformaldehyde. Fixed cells were either treated directly with anti-Ty antibody and a fluorescent secondary antibody (**Figure 4.3A**) or first treated with low concentrations of detergent (0.1% Triton X-100) to permeabilize the cells prior to addition of antibodies (**Figure 4.3B**). EV treated wild type *T. b. brucei* became SRA-Ty positive after detergent treatment. Suggesting that EVs delivered SRA-Ty which accumulated in an intracellular location that was accessible to antibodies only following detergent permeabilization. Immunofluorescence microscopy indicated that SRA-Ty delivered by EVs was internalized by wild type *T. b. brucei* and co-localized with concanavalin A (ConA) a marker for the trypanosome endocytic pathway (**Figure 4.3C and S4.2A-C**). Together these data indicated that SRA from EVs was deposited in the endolysosomal system of recipient trypanosomes. Since SRA localizes to endosomes in *T. b. rhodesiense* and *T. b. brucei*$^{SRA\text{-}Ty}$ these observations suggested EV transfer of SRA may protect recipient *T. b. brucei* from TLF killing (Stephens and Hajduk, 2011).

There have been a number of reported human infections by non-human infectious species of trypanosomes (Truc et al., 2013). While these may represent either misidentification of the

parasite or genetic acquisition of TLF resistance, an alternative possibility is transfer of SRA to TLF susceptible trypanosomes during a dual infection with *T. b. rhodesiense*. Our discovery that SRA was transferred by EVs to *T. b. brucei* and localized to an endolysosomal compartment led us to ask whether co-cultivation of *T. b. brucei* $^{SRA\text{-}Ty}$ or *T. b. rhodesiense* with wild type *T. b. brucei* conferred TLF resistance (**Figures 4.3D-F and S4.2D**). Co-cultivation of *T. b. brucei* $^{SRA\text{-}Ty}$ and *T. b. brucei*^{Hyg} allowed selection of a small (20%) but reproducible fraction of cells showing dual resistance to TLF and hygromycin (**Figure S4.2D**). In order to avoid the long selection time needed for the outgrowth of hygromycin resistant cells, recipient *T. b. brucei* were cultured in a transwell system separated by a 0.2 μm filter from either *T. b. brucei* $^{SRA\text{-}Ty}$ or *T. b. rhodesiense*. The transwell membrane prevented direct contact between the donor and recipient cells but allowed diffusion of EVs into the compartment containing the recipient *T. b. brucei* (**Figure 4.3D**). Co-cultivation of *T. b. brucei* opposite *T. b. brucei* $^{SRA\text{-}Ty}$ or *T. b. rhodesiense* in transwells led to an increase in TLF resistant *T. b. brucei* with the percentage of cells surviving overnight incubation with TLF approaching levels observed for untreated cells (**Figures 4.3E and 4.3F**).

While these co-cultivation studies were consistent with EV transfer of SRA to recipient cells they did not exclude the possibility that diffusible, non-EV-associated SRA could cross the transwell membrane conferring TLF resistance to the recipient cells. To exclude this possibility purified EVs were added directly to wild type *T. b. brucei* (**Figure 4.3G**). Addition of EVs from *T. b. brucei*$^{SRA\text{-}Ty}$ or *T. b. rhodesiense* but not EVs from wild type *T. b. brucei* increased TLF resistance of recipient *T. b. brucei* in a dose-dependent manner (**Figures 4.3H, 4.3I and S4.2E**). These data indicated that functional SRA was transferred by EVs to co-cultured trypanosomes leading to resistance to TLF.

Trypanosome EVs are highly fusogenic and rapidly transfer proteins and lipids to recipient trypanosomes

Internalization of EV-associated SRA by recipient *T. b. brucei* could be by receptor-mediated or fluid-phase endocytosis of EVs or may reflect direct fusion of EVs with the trypanosome plasma membrane. To determine the site of interaction and subsequent fate of EV proteins we labeled purified trypanosome EVs with Alexa-Fluor594 and followed the binding and localization of these proteins in *T. brucei*. When endocytosis was blocked, by maintaining cells at 3°C, EV proteins accumulated in the flagellar pocket as indicated by co-localization with ConA (**Figure 4.4A**). Binding of EVs to the trypanosome flagellar pocket was nonsaturable, suggesting a receptor-independent process (**Figure S4.3A**). This *T. brucei* EV binding could not be competed away with unlabeled BF *T. brucei* EVs (**Figure S4.3B-C**) or with EVs from a different life cycle stage (**Figure S4.3D-E**), related kinetoplastid *Leishmania tarentolae* (**Figure S4.3F-G**) or with human erythrocyte microvesicles (**Figure S4.3H-K**). After warming to 37°C, to allow endocytosis, both ConA and labeled EV proteins localized within endolysosomal vesicles (**Figure 4.4B**). *T. b. brucei* EVs bound and were taken up independent of the expressed VSG (**Figure S4.4A**) and subspecies of *T. brucei* (**Figure S4.4B**).

Since EV binding and uptake by *T. b. brucei* was receptor-independent and because EVs from other cell types have been shown to fuse with target cell membranes (Evans et al., 2012; Vidal and Hoekstra, 1995), we asked whether *T. brucei* EVs were fusogenic. Trypanosome EVs were purified and labeled with a self-quenching concentration of the lipophilic fluorophore octadecyl rhodamine B (R18). When R18-labeled EVs were incubated with *T. brucei*, a time-dependent increase in fluorescence was observed, indicating dilution of the fluorophore and suggesting fusion of the EVs with *T. brucei* membranes (**Figure 4.4C**). When visualized by

ImageStream flow-cytometry, the R18 signal appeared initially localized to the posterior ends of cells and subsequently spread over the entire surface of the cell (**Figures. 4.4D, 4.4E and S4.4C**). These data are consistent with EVs fusing to the flagellar pocket membrane and rapid equilibration of EV lipids throughout the trypanosome membranes.

Trypanosome EVs are fusogenic with artificial liposomes and mammalian erythrocytes

To determine whether EV fusion was due to unique features of the flagellar pocket membrane of trypanosomes, purified R18-labeled *T. b. brucei* EVs were incubated with unlabeled 1-palmitoyl-2-oleoyl-sn-glycero-3-phosphocholine (POPC) large unilamellar liposomes (LUV). A time-dependent increase in fluorescence was observed as R18 was diluted into the unlabeled LUV membranes due to fusion (Figure 4.5A). Trypsinization of EVs ablated fusion, but EVs retained R18 loading requiring detergent treatment for R18 release, indicating that a(n) exposed EV protein(s) was necessary for membrane fusion (Figure 4.5A).

Since *T. b. brucei* is an extracellular parasite within the circulatory system, host erythrocytes would present abundant target membranes for EV fusion. Therefore we investigated whether *T. b. brucei* EVs fuse with mammalian erythrocytes. Purified EVs, but not POPC LUV, fused with human erythrocyte ghosts and fusion was ablated by trypsinization of the EV (**Figure 4.5B**). Flow cytometry indicates that EVs fuse with intact erythrocytes and transfer R18 from EVs to erythrocytes (**Figure 4.5C**). Fluorescence microscopy of R18-EV treated erythrocytes revealed a diffuse R18 signal spread over the surface of the cell (**Figure 4.5D**). Fusion also resulted in transfer of Alexa-Fluor labeled EV proteins to erythrocytes (**Figure 4.5E**). Therefore, EVs facilitate transfer of trypanosome lipid and protein to host erythrocytes. To further address this possibility, BF *T. b. brucei* were labeled with R18, incubated with erythrocytes separated in 0.2 μm transwells and erythrocytes analyzed by flow cytometry (**Figure 4.5F**). Consistent with

T. b. brucei EVs transfer, we found that erythrocytes became labeled with R18 under these conditions.

T. b. brucei EV fusion modifies erythrocytes and causes anemia

Rifkin demonstrated that membrane-form VSG was transferred to erythrocytes co-cultured with *T. b. brucei* (Rifkin and Landsberger, 1990). Based on the presence of VSG in EVs and transfer of EV proteins to erythrocytes, we asked whether VSG is present on EV treated erythrocytes. Immunofluorescence microscopy showed VSG on the surface of erythrocytes treated with *T. b. brucei* EVs (**Figure 4.6A**). This result was recapitulated when erythrocytes were co-incubated with *T. b. brucei* separated in transwells, again consistent with the biogenesis and fusion of EVs (**Figure 4.6B**). Based on these results we postulate that fusogenic trypanosome EVs may serve as vehicles for pathogen-to-host cell transfer of membrane proteins.

Because EV fusion incorporates exogenous proteins and lipids into erythrocytes, we investigated whether the physical properties of the plasma membrane were altered. Human erythrocytes treated with EVs were less sensitive to osmotic lysis (**Figure 4.6C**). To more specifically define the EV-mediated changes to erythrocyte membranes, we probed plasma membrane lipid packing. Human erythrocytes incubated with EVs showed an increase in membrane rigidity as indicated by a narrowing and shift of the emission spectra of Laurdan towards shorter wavelengths (**Figure 4.6D**). Recently it has been shown that erythrocyte lipid composition was altered during trypanosomiasis, and these cells were preferentially phagocytosed by myeloid cells (Stijlemans et al., 2015). Incorporating parasite lipid via EV fusion may explain altered erythrocyte lipid composition.

Trypanosome infection elicits a severe loss of erythrocytes during acute phase infection that is independent of B-cell response or IgM (Magez et al., 2008). We found that during acute

infection mice exhibited a level of anemia that correlates to parasitemia (**Figures 4.6E and 4.6F**). These data suggested that anemia during the acute phase was a response to a density dependent trypanosome factor. We reasoned that EVs would be present at concentrations dependent on parasite density and that EV altered erythrocytes would be cleared from circulation. To test whether EV fusion causes clearance we incubated GFP-expressing mouse erythrocytes with *T. brucei* EVs and intravenously injected these cells into naive mice. Similar to human erythrocytes, EVs fuse with mouse erythrocytes and acquire VSG, lipid and increased rigidity (**Figure S4.5A-D**). Clearance occurred rapidly, within 1 hour, and the remaining EV treated erythrocytes became stable in circulation after 24 hr (**Figure 4.6G**). Finally, we tested whether circulating EVs stimulated a loss of erythrocytes. Injection of EVs into the tail vein of BALB/c or C57BL/6 mice resulted in increased erythrocyte volume (**Figure S4.5E**), which may be a consequence of lipid incorporation into the plasma membrane via EV-fusion, and a mean 5.3 % and 10.6 % decrease of erythrocytes (normalized to control injections) 1 hr post-injection (**Figure 4.6H**). These decreases correspond to a loss of 3.0×10^8 and 7.1×10^8 erythrocytes in BALB/C and C57BL/6 mice, respectively. Greater loss of erythrocytes in C57BL/6 is consistent with more severe anemia in trypanosome infected C57BL/6 than BALB/c mice (Magez et al., 2008). These data combined suggest that the fusogenic properties of trypanosome EVs directly alter the physical properties of erythrocytes and likely contribute to anemia associated with both cattle and human trypanosomiasis.

Discussion

It has become increasingly clear that most cells communicate within their immediate environment by the formation of membrane nanotube-like extensions and by the release of EVs (Remis et al., 2014; Schorey et al., 2015). Extracellular vesicles derived from “donor cells” can

have profound effects on “recipient cells” by altering gene expression and modulating signaling pathways resulting in developmental changes and modulation of immune response. EVs have also been shown to transfer virulence factors from infectious microbes to host cells, transmit infectious prion proteins and HIV and contribute to cancer and cardiovascular disease progression (Fevrier et al., 2004; Zomer et al., 2015). Here we report the discovery of EVs formed by the budding and subsequent vesicularization of long membrane nanotubes from the flagellum of African trypanosomes. In these studies we observed that *T. b. brucei* EVs contained several proposed trypanosome virulence factors. Furthermore, we showed that during co-cultivation EVs from *T. b. rhodesiense* facilitated the transfer of the virulence factor SRA to *T. b. brucei* where it localized within an endolysosomal compartment and conferred resistance to TLF. The formation of EVs was enhanced under stress conditions or with the addition of complement active serum and we postulate that EV delivery of virulence factors, including but not limited to SRA, might be advantageous to the parasite in immune competent hosts. We also found that trypanosome derived EVs are highly fusogenic with mammalian erythrocytes, resulting in physical changes to the erythrocyte membrane and rapid clearance in a mouse model. Anemia is associated with both human and cattle trypanosomiasis contributing to pathology and death. Several proposed *T. b. brucei* virulence factors were found in the EV proteome, including the flagellar proteins GPI-PLC, calflagins, and metacaspase 4. While these proteins contribute to parasite virulence their mechanisms are unknown (Emmer et al., 2010; Proto et al., 2011; Webb et al., 1997). We found that nanotubes and EVs associated with trypanosomes have a thick VSG coat consistent with budding from the flagellar membrane; however purified EVs have a sparse coat suggesting activation of the EV associated GPI-PLC (Figures 2E and S1D, E). This may have implications in fusion of EVs with target membranes. *T. b. brucei* EVs also contained a

flagellar adenylate cyclase (GRESAG4) previously proposed to increase the levels of cAMP in host immune cells, which in turn activates the host cell protein kinase A (PKA) (Salmon et al., 2012). The activation of host cell PKA reduced production of TNF-alpha sparing trypanosomes from host innate immunity (Salmon et al., 2012). While an appealing model, it was unclear how trypanosome adenylate cyclase could be transferred to host cells in an active state. Our discovery that highly fusogenic *T. b. brucei* EVs contain this enzyme raises the possibility that transfer of active GRESAG4 via EVs increased the levels of cAMP in recipient host cells.

The expression of SRA is necessary for human infectivity by *T. b. rhodesiense* and can be transferred to *T. b. brucei* during sexual crosses of the two subspecies in the tsetse fly vector (Gibson et al., 2015). This has important implications in the generation of new genetic variants of human infective trypanosomes. Parasite co-infection in tsetse flies is dependent on dual infection of the blood meal from the mammalian host with the two subspecies. While both *T. b. rhodesiense* and *T. b. brucei* can infect cattle and wild game it has been largely held that *T. b. brucei* cannot infect primates. We have shown that co-culturing the two subspecies resulted in transfer of SRA to *T. b. brucei* and the transmission of nonhereditary resistance to human TLF. This may have important implications in establishing dual infections in the tsetse fly and the generation of genetic diversity during epidemics of sleeping sickness when humans would represent a significant reservoir of the parasites.

Anemia is a consistent symptom of human and veterinary trypanosomiasis and a major cause of morbidity (Naessens, 2006). The role of anemia in the pathology of trypanosomiasis cannot be overstated and it has been argued that the ability to resist anemia is more important for survival and reproduction than the ability to control parasitemia (Naessens, 2006). A pronounced anemia that is associated with a type 1 inflammatory response and erythrophagocytosis occurs

during the acute phase of infection, whereas the significant, yet less severe anemia during the chronic phase coincides with a type 2 macrophage status and presence of the anti-inflammatory cytokine IL-10. The host responses that result in anemia are well characterized (Stijlemans et al., 2015). Our studies show that trypanosome EVs fuse with mammalian erythrocytes and cause changes to the physical properties of the membrane. We propose that our animal studies show that these changes lead to erythrophagocytosis and is the cause of anemia during acute trypanosomiasis. This discovery opens the possibility of identifying inhibitors of EV fusion with host cells and may lead to development of drugs that will spare the host from disease induced anemia.

Methods

Trypanosome cell culture

Bloodstream form *T. b. brucei* Lister 427 (MiTat1.2) and *T. b. rhodesiense* KETRI2482 were grown in HMI-9 medium containing 10% fetal bovine serum (FBS) (Sigma) and Serum Plus supplement (SAFC Biosciences) in 5 % CO_2 at 37°C.

Nanotube and extracellular vesicle induction

Production of nanotubes and EVs was stimulated by stressing BF *T. brucei* with RNAi against the essential BF protein α-KDE1 or by the addition of complement active FBS (Sykes et al., 2015). In all other experiments, EVs were acquired from trypanosomes grown in heat inactivated serum or serum free conditions (for mass spectrometry).

Extracellular vesicle purification

T. brucei was grown in HMI-9 to a density of 1×10^6 cells/ml and EVs were purified as previously described with slight modification to the protocol (Bayer-Santos et al., 2013).

Human erythrocytes

Erythrocytes were removed by centrifugation, washed and stored in sterile PBS with 5 % dextrose, 0.5 mM EDTA.

Microscopy

All DIC and immunofluorescence images were acquired with a Zeiss Axio Observer Z1 as previously described Sykes et al., 2015.

Scanning and transmission electron microscopy

BF *T. brucei* stimulated for the formation of membrane nanotubes were fixed and images were acquired with a JEOL-JEM 1210 transmission electron microscope as previously described (Sykes et al., 2015). For SEM, 2.5% glutaraldehyde-fixed cells were dehydrated on a 0.22 mm membrane, critical point dried, sputter coated with gold and visualized with a Zeiss 1450EP scanning electron microscope. Three-dimensional reconstruction of serial TEM sections was carried out using tools available in the IMOD 4.7 software package (Kremer et al., 1996).

Nanoparticle tracking analysis

The concentration and diameter of freshly prepared EVs from 2×10^8 trypanosomes was determined by analysis with a NanoSight NS300 (Malvern). Fifteen hundred frames were acquired at 25 frames per second at 25°C.

SDS-PAGE and Western blotting

Total cell and purified EV proteins were fractionated by reducing SDS-PAGE and western blotted as previously described using 5×10^5 BF trypanosomes or EVs purified from 2×10^6 cells (Sykes et al., 2015).

SRA transfer assay

For flow cytometry, *T. brucei* was incubated with EVs for 1 hr at 37°C. *T. brucei*, *T. brucei*$^{SRA\text{-}Ty}$ and EV treated *T. brucei* cells were chilled washed with 1 x PBS, fixed with 0.05%

paraformaldehyde and an aliquot was permeabilized with ice cold 0.1% Triton X-100. For microscopy *T. brucei* was incubated with EVs for 1 hr at 3°C or 30 min at 37°C. ConA was added and cells were prepared for fluorescence microscopy.

Overnight survival assay

Co-cultured or transwell co-cultured trypanosomes were treated with TLF for 24 hours at 37°C. Trypanosomes were incubated with purified EVs for 1 hr and then treated with TLF for 24 hr at 37°C. After treatment surviving cells were counted by phase-contrast microscopy and compared against non-TLF treated cultures.

EV protein transfer

Purified EVs were labeled with an Alexa-594 labeling kit (Life Technologies) and $1x10^7$ cell equivalents were added to $1x10^8$ *T. brucei* at 3°C. After washing cells were warmed to 37°C and prepared for microscopy (Sykes et al., 2015).

Membrane fusion assay

Vesicle fusion was measured essentially as described by Vidal and Hoekstra (1995).

Transwell co-culture

T. brucei was co-cultured with *T. brucei* $^{SRA\text{-}Ty}$ or *T. b. rhodesiense* in 0.2 μm transwell culture plates. Cells were co-cultured for 24 hours then split 1/10 and treated with TLF for an overnight survival assay. For erythrocyte co-culture, *T. brucei* was inoculated with mouse or human erythrocytes in transwell plates.

Flow cytometry analysis of lipid and VSG transfer

After co-culture with trypanosomes, erythrocytes were washed prior to analysis. Samples analyzed for lipid transfer by R18 staining were directly analyzed while erythrocytes analyzed

for VSG transfer were first treated using the protocol for fluorescence microscopy staining. All samples were then analyzed using a CyAn ADP Analyzer.

Osmotic lysis assay

Freshly collected human erythrocytes were resuspended in PBS and incubated with EVs. Erythrocytes were incubated in NaCl solutions, pelleted and the absorbance of the supernatant was read. Complete lysis was achieved by incubation in deionized H_2O.

Laurdan spectral analysis

Freshly collected human or mouse erythrocytes were resuspended in and incubated with EVs for 30 min. Erythrocytes were washed, labeled with Laurdan for 30 min, washed three times with PBS and spectra recorded with the Perkin Elmer Life Sciences LS-55 luminescent spectrofluorometer.

Trypanosome infections and EV treatments

Trypanosome infections were initiated by intraperitoneal injection of *T. b. brucei* Lister 427–221 parasites in retired breeder female BALB/c mice (Jackson Laboratory). Parasitemias were determined by the matching method (Herbert and Lumsden, 1976).

For *ex vivo* EV-treatment, erythrocytes from 10 week old mice expressing GFP from a ubiquitin promoter (C57BL/6-Tg(UBC-GFP)30Scha/J) (Jackson Laboratory) were collected and incubated with or without EVs. Erythrocytes were injected into the tail vein of naive C57BL/6J mice. Whole blood collected from the tail vein was analyzed by flow cytometry and GFP-positive erythrocytes were quantified from the ratio of labeled to unlabeled erythrocytes.

For direct EV injections, wild-type BALB/c and C57BL/6J mice were injected intravenously (tail vein) with EVs freshly prepared in PBS. Control mice were injected with an equal volume of PBS. Erythrocyte counts were determined via Coulter counting.

Author contributions

Conceptualization, A. J. S., S. E. S., S. L. H. and J. M. H.; Investigation, A. J. S., S. E. S., R. K., L. W. D., A. C. B., A. G., W. J. M., and J. M. H.; Resources, I. C. A.; Formal Analysis, E. S. N and I. C. A.; Writing – Original Draft, A. J. S., S. L. H. and J. M. H.; Writing – Review & Editing, All authors.

Acknowledgments

This work was supported by NIH grant AI039033 (S. L. H.) and 2G12MD007592 (BBRC/UTEP, I. C. A.). A.J.S. is supported in part by NIH training grant AI060546. We thank Amy Styer for reagents, Julie Nelson (University of Georgia) and Aaron Rae (Emory University) for assistance with flow cytometry, John Shields and Mary Ard (University of Georgia) for assistance with electron microscopy, the Biomolecule Analysis Core Facility at BBRC/UTEP (2G12MD007592) for the proteomic analysis and Ragy Ragheb for use and assistance with the NanoSight NS300.

Raw LC-MS/MS runs and MaxQuant searching results were uploaded to PRIDE database (http://www.ebi.ac.uk/pride/) under accession number PXD002030.

References

Babudieri, B., and Tomasini, N. (1962). Fine struttura dei trypanosomi. Parassitologia *4*, 89-95.

Bayer-Santos, E., Aguilar-Bonavides, C., Rodrigues, S.P., Cordero, E.M., Marques, A.F., Varela-Ramirez, A., Choi, H., Yoshida, N., da Silveira, J.F., and Almeida, I.C. (2013). Proteomic analysis of Trypanosoma cruzi secretome: characterization of two populations of extracellular vesicles and soluble proteins. J Proteome Res *12*, 883-897.

Broadhead, R., Dawe, H.R., Farr, H., Griffiths, S., Hart, S.R., Portman, N., Shaw, M.K., Ginger, M.L., Gaskell, S.J., McKean, P.G.*, et al.* (2006). Flagellar motility is required for the viability of the bloodstream trypanosome. Nature *440*, 224-227.

De Greef, C., and Hamers, R. (1994). The serum resistance-associated (SRA) gene of Trypanosoma brucei rhodesiense encodes a variant surface glycoprotein-like protein. Mol Biochem Parasitol *68*, 277-284.

Dubey, G.P., and Ben-Yehuda, S. (2011). Intercellular nanotubes mediate bacterial communication. Cell *144*, 590-600.

Ellis, D.S., Ormerod, W.E., and Lumsden, W.H. (1976). Filaments of Trypanosoma brucei: some notes on differences in origin and structure in two strains of Trypanosoma (Trypanozoon) brucei rhodesiense. Acta Trop *33*, 151-168.

Emmer, B.T., Daniels, M.D., Taylor, J.M., Epting, C.L., and Engman, D.M. (2010). Calflagin inhibition prolongs host survival and suppresses parasitemia in Trypanosoma brucei infection. Eukaryot Cell *9*, 934-942.

Evans, A.G., Davey, H.M., Cookson, A., Currinn, H., Cooke-Fox, G., Stanczyk, P.J., and Whitworth, D.E. (2012). Predatory activity of Myxococcus xanthus outer-membrane vesicles and properties of their hydrolase cargo. Microbiology *158*, 2742-2752.

Fevrier, B., Vilette, D., Archer, F., Loew, D., Faigle, W., Vidal, M., Laude, H., and Raposo, G. (2004). Cells release prions in association with exosomes. Proc Natl Acad Sci U S A *101*, 9683-9688.

Frevert, U., and Reinwald, E. (1988). Formation of filopodia in Trypanosoma congolense by crosslinking the variant surface antigen. J Ultrastruct Mol Struct Res *99*, 124-136.

Gibson, W., Peacock, L., Ferris, V., Fischer, K., Livingstone, J., Thomas, J., and Bailey, M. (2015). Genetic recombination between human and animal parasites creates novel strains of human pathogen. PLoS Negl Trop Dis *9*, e0003665.

Guther, M.L., Urbaniak, M.D., Tavendale, A., Prescott, A., and Ferguson, M.A. (2014). High-confidence glycosome proteome for procyclic form Trypanosoma brucei by epitope-tag organelle enrichment and SILAC proteomics. J Proteome Res *13*, 2796-2806.

Herbert, W.J., and Lumsden, W.H. (1976). Trypanosoma brucei: a rapid "matching" method for estimating the host's parasitemia. Exp Parasitol *40*, 427-431.

Jensen, B.C., Ramasamy, G., Vasconcelos, E.J., Ingolia, N.T., Myler, P.J., and Parsons, M. (2014). Extensive stage-regulation of translation revealed by ribosome profiling of Trypanosoma brucei. BMC Genomics *15*, 911.

Kremer, J.R., Mastronarde, D.N., and McIntosh, J.R. (1996). Computer visualization of three-dimensional image data using IMOD. J Struct Biol *116*, 71-76.

Magez, S., Schwegmann, A., Atkinson, R., Claes, F., Drennan, M., De Baetselier, P., and Brombacher, F. (2008). The role of B-cells and IgM antibodies in parasitemia, anemia, and VSG switching in Trypanosoma brucei-infected mice. PLoS Pathog *4*, e1000122.

Mantel, P.Y., Hoang, A.N., Goldowitz, I., Potashnikova, D., Hamza, B., Vorobjev, I., Ghiran, I., Toner, M., Irimia, D., Ivanov, A.R.*, et al.* (2013). Malaria-infected erythrocyte-derived microvesicles mediate cellular communication within the parasite population and with the host immune system. Cell Host Microbe *13*, 521-534.

Marcilla, A., Martin-Jaular, L., Trelis, M., de Menezes-Neto, A., Osuna, A., Bernal, D., Fernandez-Becerra, C., Almeida, I.C., and Del Portillo, H.A. (2014). Extracellular vesicles in parasitic diseases. J Extracell Vesicles *3*, 25040.

Mony, B.M., MacGregor, P., Ivens, A., Rojas, F., Cowton, A., Young, J., Horn, D., and Matthews, K. (2014). Genome-wide dissection of the quorum sensing signalling pathway in Trypanosoma brucei. Nature *505*, 681-685.

Naessens, J. (2006). Bovine trypanotolerance: A natural ability to prevent severe anaemia and haemophagocytic syndrome? Int J Parasitol *36*, 521-528.

Oberholzer, M., Langousis, G., Nguyen, H.T., Saada, E.A., Shimogawa, M.M., Jonsson, Z.O., Nguyen, S.M., Wohlschlegel, J.A., and Hill, K.L. (2011). Independent analysis of the flagellum surface and matrix proteomes provides insight into flagellum signaling in mammalian-infectious Trypanosoma brucei. Mol Cell Proteomics *10*, M111 010538.

Oberholzer, M., Lopez, M.A., McLelland, B.T., and Hill, K.L. (2010). Social Motility in African Trypanosomes. PLoS pathogens *6*.

Oli, M.W., Cotlin, L.F., Shiflett, A.M., and Hajduk, S.L. (2006). Serum resistance-associated protein blocks lysosomal targeting of trypanosome lytic factor in Trypanosoma brucei. Eukaryot Cell *5*, 132-139.

Panigrahi, A.K., Ogata, Y., Zikova, A., Anupama, A., Dalley, R.A., Acestor, N., Myler, P.J., and Stuart, K.D. (2009). A comprehensive analysis of Trypanosoma brucei mitochondrial proteome. Proteomics *9*, 434-450.

Proto, W.R., Castanys-Munoz, E., Black, A., Tetley, L., Moss, C.X., Juliano, L., Coombs, G.H., and Mottram, J.C. (2011). Trypanosoma brucei metacaspase 4 is a pseudopeptidase and a virulence factor. J Biol Chem *286*, 39914-39925.

Regev-Rudzki, N., Wilson, D.W., Carvalho, T.G., Sisquella, X., Coleman, B.M., Rug, M., Bursac, D., Angrisano, F., Gee, M., Hill, A.F.*, et al.* (2013). Cell-cell communication between malaria-infected red blood cells via exosome-like vesicles. Cell *153*, 1120-1133.

Remis, J.P., Wei, D., Gorur, A., Zemla, M., Haraga, J., Allen, S., Witkowska, H.E., Costerton, J.W., Berleman, J.E., and Auer, M. (2014). Bacterial social networks: structure and composition of Myxococcus xanthus outer membrane vesicle chains. Environ Microbiol *16*, 598-610.

Rifkin, M.R., and Landsberger, F.R. (1990). Trypanosome variant surface glycoprotein transfer to target membranes: a model for the pathogenesis of trypanosomiasis. Proc Natl Acad Sci U S A *87*, 801-805.

Salmon, D., Vanwalleghem, G., Morias, Y., Denoeud, J., Krumbholz, C., Lhomme, F., Bachmaier, S., Kador, M., Gossmann, J., Dias, F.B.*, et al.* (2012). Adenylate cyclases of Trypanosoma brucei inhibit the innate immune response of the host. Science *337*, 463-466.

Schepilewsky, E. (1912). Fadenförmige Anhängsel bei den Trypanosomen. Zentralblatt fur Bakteriologie, Parasitenkunde, Infektionskrankheiten und Hygiene *65*, 79-83.

Schorey, J.S., Cheng, Y., Singh, P.P., and Smith, V.L. (2015). Exosomes and other extracellular vesicles in host-pathogen interactions. EMBO Rep *16*, 24-43.

Silverman, J.M., Clos, J., de'Oliveira, C.C., Shirvani, O., Fang, Y., Wang, C., Foster, L.J., and Reiner, N.E. (2010). An exosome-based secretion pathway is responsible for protein export from Leishmania and communication with macrophages. J Cell Sci *123*, 842-852.

Stephens, N.A., and Hajduk, S.L. (2011). Endosomal localization of the serum resistance-associated protein in African trypanosomes confers human infectivity. Eukaryot Cell *10*, 1023-1033.

Stijlemans, B., Cnops, J., Naniima, P., Vaast, A., Bockstal, V., De Baetselier, P., and Magez, S. (2015). Development of a pHrodo-based assay for the assessment of in vitro and in vivo erythrophagocytosis during experimental trypanosomosis. PLoS Negl Trop Dis *9*, e0003561.

Sykes, S., Szempruch, A., and Hajduk, S. (2015). The krebs cycle enzyme alpha-ketoglutarate decarboxylase is an essential glycosomal protein in bloodstream African trypanosomes. Eukaryot Cell *14*, 206-215.

Truc, P., Buscher, P., Cuny, G., Gonzatti, M.I., Jannin, J., Joshi, P., Juyal, P., Lun, Z.R., Mattioli, R., Pays, E.*, et al.* (2013). Atypical human infections by animal trypanosomes. PLoS Negl Trop Dis *7*, e2256.

Twu, O., de Miguel, N., Lustig, G., Stevens, G.C., Vashisht, A.A., Wohlschlegel, J.A., and Johnson, P.J. (2013). Trichomonas vaginalis exosomes deliver cargo to host cells and mediate hostratioparasite interactions. PLoS Pathog *9*, e1003482.

Vanhamme, L., Paturiaux-Hanocq, F., Poelvoorde, P., Nolan, D.P., Lins, L., Van Den Abbeele, J., Pays, A., Tebabi, P., Van Xong, H., Jacquet, A.*, et al.* (2003). Apolipoprotein L-I is the trypanosome lytic factor of human serum. Nature *422*, 83-87.

Vickerman, K., and Luckins, A.G. (1969). Localization of variable antigens in the surface coat of Trypanosoma brucei using ferritin conjugated antibody. Nature *224*, 1125-1126.

Vidal, M., and Hoekstra, D. (1995). In vitro fusion of reticulocyte endocytic vesicles with liposomes. J Biol Chem *270*, 17823-17829.

Webb, H., Carnall, N., Vanhamme, L., Rolin, S., Van Den Abbeele, J., Welburn, S., Pays, E., and Carrington, M. (1997). The GPI-phospholipase C of Trypanosoma brucei is nonessential but influences parasitemia in mice. J Cell Biol *139*, 103-114.

Wood, C.R., and Rosenbaum, J.L. (2015). Ciliary ectosomes: transmissions from the cell's antenna. Trends Cell Biol *25*, 276-285.

Wright, K.A., Lumsden, W.H., and Hales, H. (1970). The formation of filopodium-like processes by Trypanosoma (Trypanozoon) brucei. J Cell Sci *6*, 285-297.

Xong, H.V., Vanhamme, L., Chamekh, M., Chimfwembe, C.E., Van Den Abbeele, J., Pays, A., Van Meirvenne, N., Hamers, R., De Baetselier, P., and Pays, E. (1998). A VSG expression site-associated gene confers resistance to human serum in Trypanosoma rhodesiense. Cell *95*, 839-846.

Yanez-Mo, M., Siljander, P.R., Andreu, Z., Zavec, A.B., Borras, F.E., Buzas, E.I., Buzas, K., Casal, E., Cappello, F., Carvalho, J.*, et al.* (2015). Biological properties of extracellular vesicles and their physiological functions. J Extracell Vesicles *4*, 27066.

Zomer, A., Maynard, C., Verweij, F.J., Kamermans, A., Schafer, R., Beerling, E., Schiffelers, R.M., de Wit, E., Berenguer, J., Ellenbroek, S.I.*, et al.* (2015). In Vivo imaging reveals extracellular vesicle-mediated phenocopying of metastatic behavior. Cell *161*, 1046-1057.

Figures

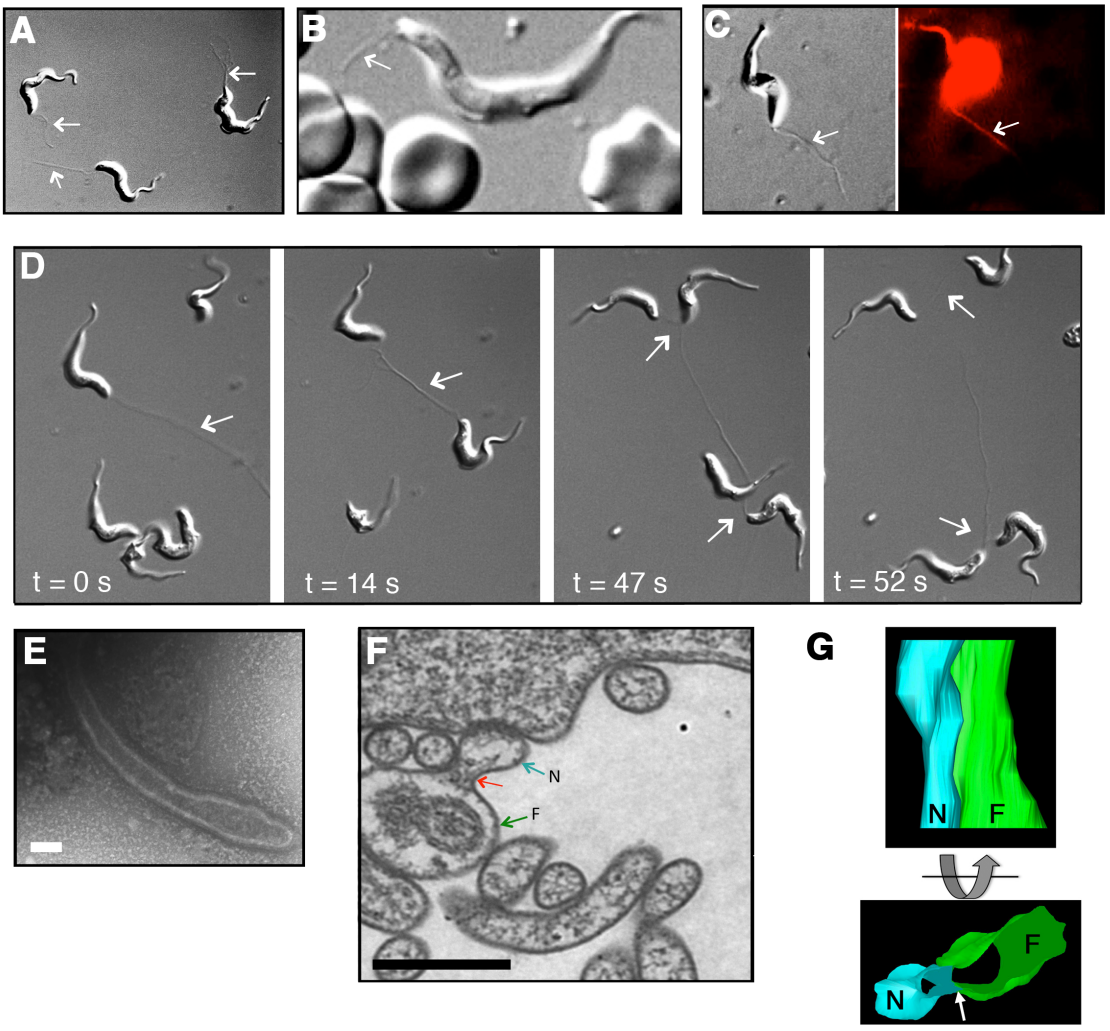

Figure 4.1. Dynamics and flagellar formation of membrane nanotubes. (**A**) Nanotube formation was visualized by DIC microscopy. Arrows indicate nanotubes. (**B**) Nanotubes on *T. brucei* in infected mouse blood. Arrow indicates nanotube. (**C**) Nanotubes were labeled by R18. Left and right panels are consecutive frames from DIC and fluorescence video microscopy, respectively (see Movie S4.1 and S4.2). (**D**) Live cell imaging revealed membrane nanotube dynamics, interactions with multiple cells in sequential DIC frames (see Movie S4.3). (**E**) Nascent nanotube visualized by negative stain TEM (bar = 100 nm). (**F**) TEM thin section

showed flagellar membrane (green arrow, F) budding (red arrow) into nanotube (blue arrow, N) (bar = 500 nm). (**G**) Reconstruction of serial TEM thin sections into a 3D model showed tubulation (blue) of flagellar membrane (green). Arrow indicates nanotube budding point (see Movie S4.4). See also Figures S4.1A-D, Movie S4.1, S4.2, S4.3, and S4.4.

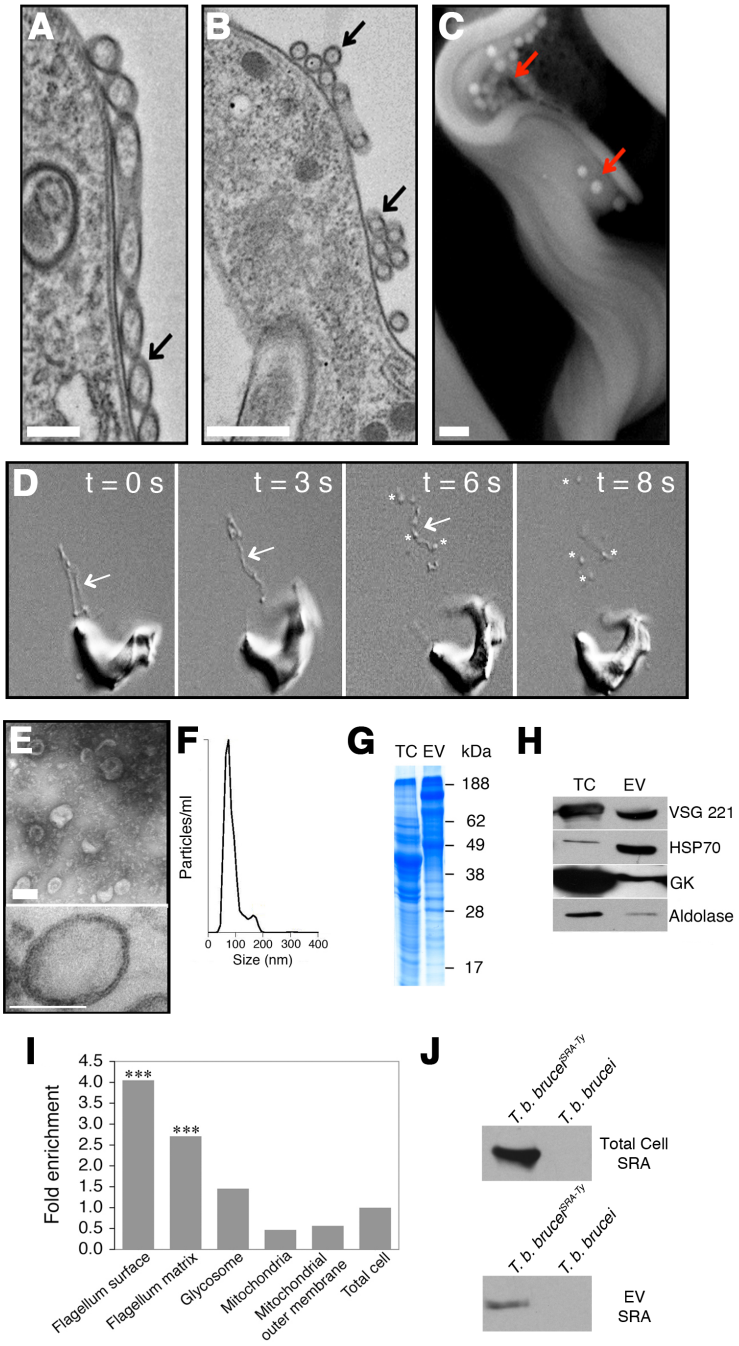

Figure 4.2. Nanotubes vesicularize into EVs. (**A**) TEM of a nanotube (black arrow) (bar = 400 nm) and (**B**) spherical units (black arrow) (bar = 500 nm). (**C**) Free EVs (red arrows) at the trypanosome surface visualized by SEM (bar = 400 nm). (**D**) Successive DIC video frames of nanotubes (arrows) dissociating into free EVs (asterisks) (see Movie S4.5). (**E, upper panel**)

Negative stain TEM of purified EVs (bar = 100 nm). (**E, lower panel**) TEM thin section of purified EVs (bar = 100 nm). (**F**) Nanoparticle tracking analysis of EVs. (**G**) EV proteins visualized by SDS-PAGE (total cell, TC). (**H**) Western blotting of EVs with anti-VSG, HSP70, glycerol kinase and aldolase. (**I**) Analysis of the EV proteome for relative enrichment with flagellar surface, flagellar matrix, glycosome, mitochondria and mitochondrial outer membrane proteins in relation to the total cell proteome (***, $p < 0.001$). (**J**) Western blot of total cell and EVs from *T. b. brucei*$^{SRA\text{-}Ty}$. See also Figures S1E-F, Movie S4.5, Table S4.1 and S4.2.

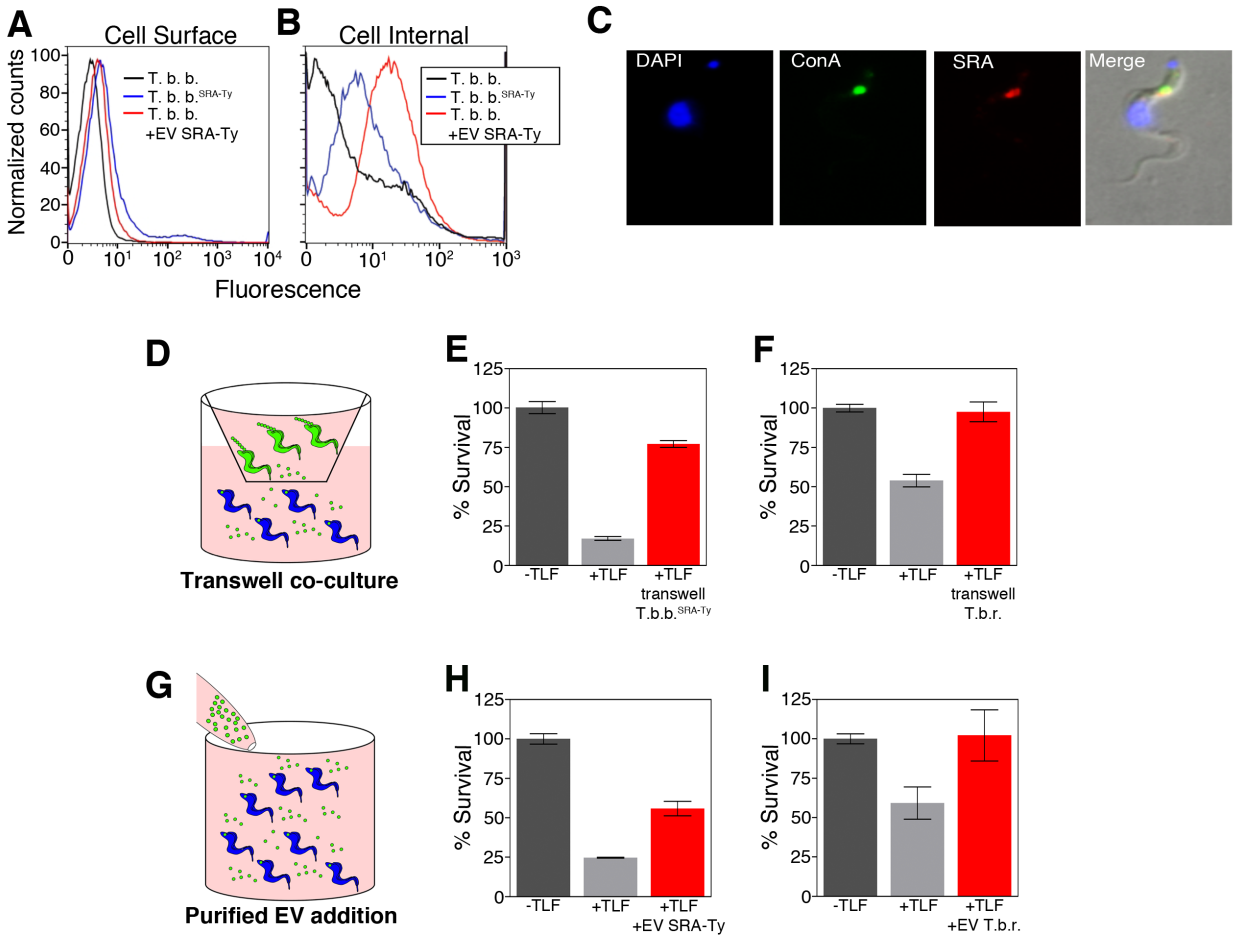

Figure 4.3. EVs transfer TLF resistance. (**A**) Flow cytometry of fixed *T. brucei* (black), *T. b. brucei*$^{SRA\text{-}Ty}$ (blue) and *T. brucei* treated with SRA containing EVs (red). (**B**) Flow cytometry of fixed and permeabilized *T. brucei* (black), *T. b. brucei*$^{SRA\text{-}Ty}$ (blue) and *T. brucei* treated with

SRA containing EVs (red). (**C**) Fluorescence microscopy of *T. brucei* treated with EVs containing SRA. ConA showed internalization and co-localization in the endocytic pathway. (**D**) Diagram of transwell co-culture of *T. brucei* with *T. b. brucei*$^{SRA\text{-}Ty}$ or *T. b. rhodesiense*. (**E & F**) TLF overnight survival assays. *T. b. brucei* not treated with TLF (negative control) (dark grey) *T. b. brucei* treated with TLF (positive control) (light grey). **(E)** Co-culture of *T. b. brucei* with *T. b. brucei*$^{SRA\text{-}Ty}$ (red) and **(F)** co-culture of *T. b. brucei* with *T. b. rhodesiense* (red). (**G**) Diagram depicting addition of EVs from *T. b. brucei*$^{\text{SRA-Ty}}$ or *T. b. rhodesiense* to *T. b. brucei*. (**H & I**) TLF overnight survival assays. *T. b. brucei* not treated with TLF (negative control) (dark grey) *T. b. brucei* treated with TLF (positive control) (light grey). **(H)** Addition of EVs purified from *T. b. brucei*$^{SRA\text{-}Ty}$ (red) and (**I**) addition of EVs purified from *T. b. rhodesiense* (red). Bars represent the mean ± SEM for three experiments. See also Figures S4.2A-E, S4.4 and S4.5.

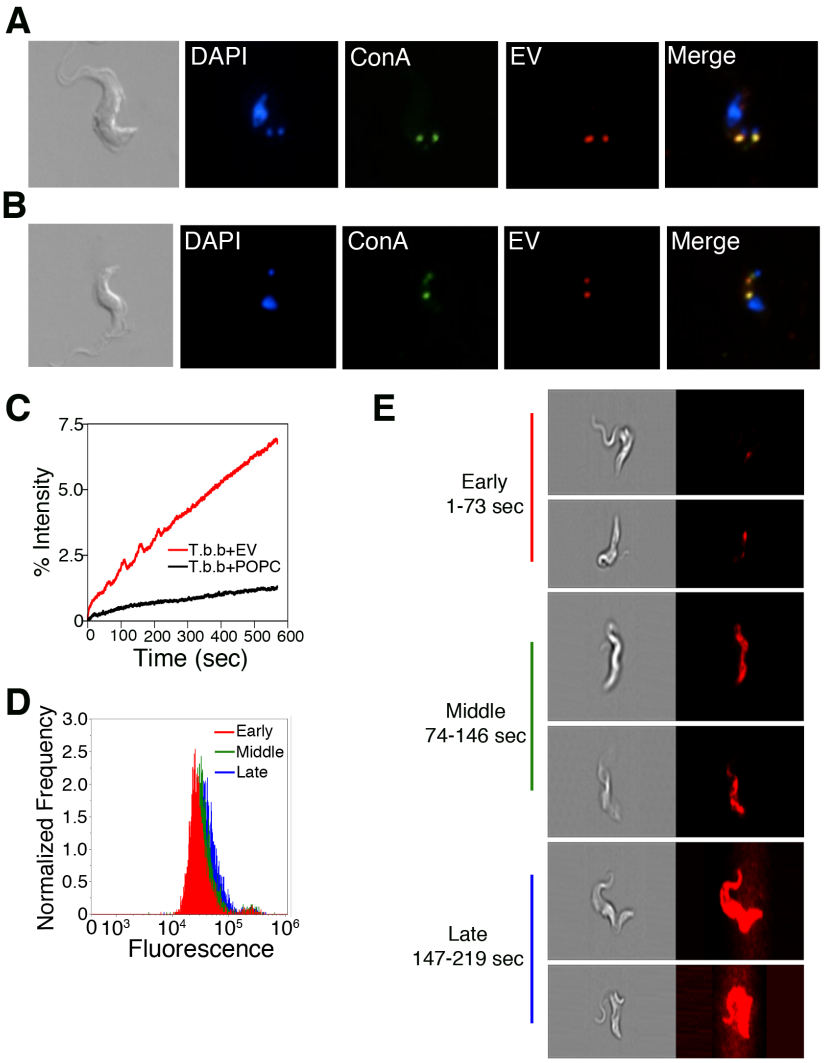

Figure 4.4. EVs interact with *T. brucei* at the flagellar pocket and are endocytosed. (**A & B**) Fluorescence microscopy of *T. brucei* treated with Alexa-594 labeled EVs. **(A)** EVs localized with ConA to the flagellar pocket at 3°C. (**B)** EVs localized with ConA in the endocytic pathway at 37°C. (**C**) Membrane fusion was measured by fluorescence dequenching of R18-labeled EVs (red) with *T. brucei*. Fusion did not occur when *T. brucei* was treated with R18-labeled POPC (black). (**D**) ImageStream flow cytometry showed fluorescence dequenching occurred across the entire cell population with increasing intensity in a time dependent manner (1-73 sec "early", red; 74-146 sec "middle", green; 147-219 sec "late", blue). (**E**) Imaging of individual cells

during the ImageStream analysis showed that during early time cells showed a discreet fluorescent puncta at the posterior end of the cell with fluorescent rapidly distributing across the cell resulting in fully fluorescent cells in later times. See also Figures S4.3A-K and S4.4A-C.

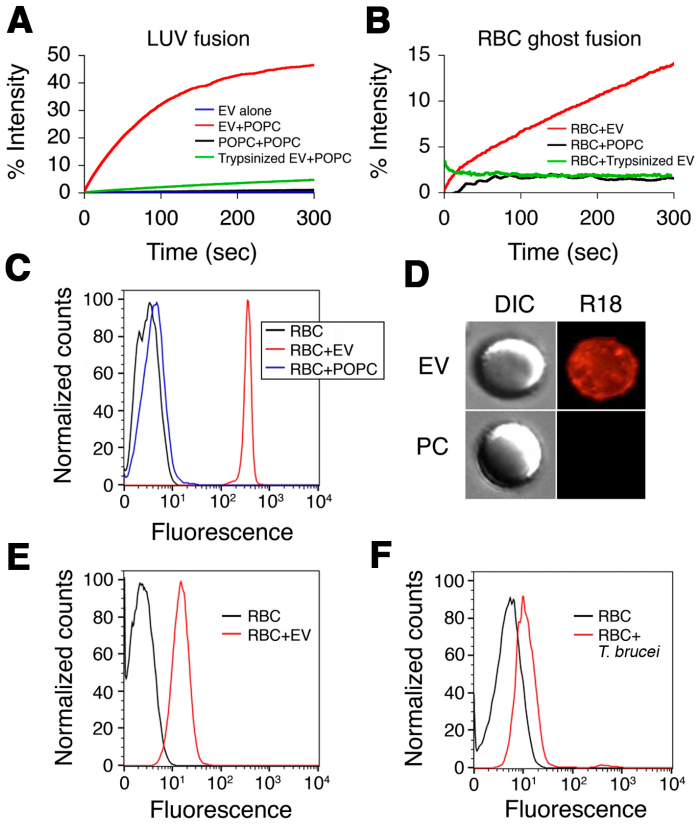

Figure 4.5. Trypanosome EVs fuse with erythrocytes. (**A**) Membrane fusion was measured by fluorescence dequenching of R18-labeled EVs (EV + POPC, red; EVs alone, blue; R18-labeled POPC + POPC, black). Trypsinization of EV ablates fusion with POPC LUV (green). (**B**) EVs (red), but not POPC LUV (black) or trypsinized EVs (green), fuse with human erythrocyte ghosts. (**C**) Intact human erythrocytes (black) were incubated with R18-labeled EVs (red) or R18-labeled POPC LUV (blue) and analyzed by flow cytometry. (**D**) Intact human erythrocytes were incubated with R18-labeled EVs or R18-labeled POPC LUV (PC) and visualized by fluorescence microscopy. (**E**) Alexa-Fluor 488-labeled EVs were incubated with intact human erythrocytes and analyzed by flow cytometry (black, untreated erythrocytes; red, erythrocytes +

EVs). (**F**) Human erythrocytes were incubated overnight in transwells with or without R18-labeled BF *T. brucei* and analyzed by flow cytometry (black, erythrocytes alone; red, erythrocytes + R18-labeled trypanosomes). See also Figure S4.5A-D.

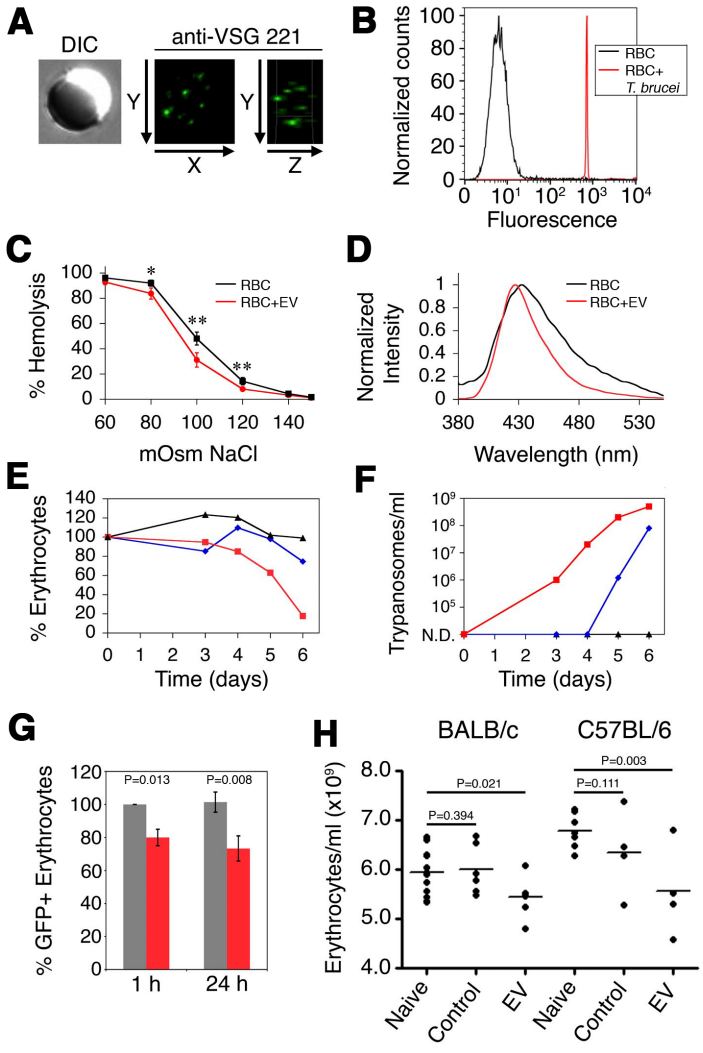

Figure 4.6. EVs alter erythrocyte physicochemical properties and stimulate clearance. (**A**) Erythrocytes were incubated with EVs, probed with anti-VSG 221 and visualized by fluorescence microscopy. (**B**) Erythrocytes were incubated in transwells in the presence (red) or absence (black) of *T. brucei*, probed with anti-VSG 221 and analyzed by flow cytometry. (**C**) Erythrocyte lysis was measured by quantifying hemoglobin concentration in supernatant (black, untreated erythrocytes; red, erythrocytes + EVs) (*, $p < 0.05$; **, $p \leq 0.005$). Scale bars represent

the mean ± SEM for four experiments. (**D**) Laurdan emission spectra of erythrocytes alone (black) or treated with EVs (red). (**E**) Anemia in *T. brucei*-infected mice was followed by hemocytometer counts, normalized to pre-infection, in a heavily infected mouse (red), moderately infected mouse (blue) and a mouse with undetectable parasitemia (black). (**F**) Parasitemia of the mice shown in panel E. (**G**) Mouse erythrocytes containing GFP were incubated with (red) or without (grey) purified EVs and injected into the tail vein of naive mice. GFP-erythrocytes were quantified by flow cytometry. Scale bars represent the mean ± SEM for four experiments. (**H**) Purified EVs were intravenously injected into naive mice and erythrocytes were quantified 1 h post injection. P-values were calculated by one-tailed student T-test. See also Figures S4.5.

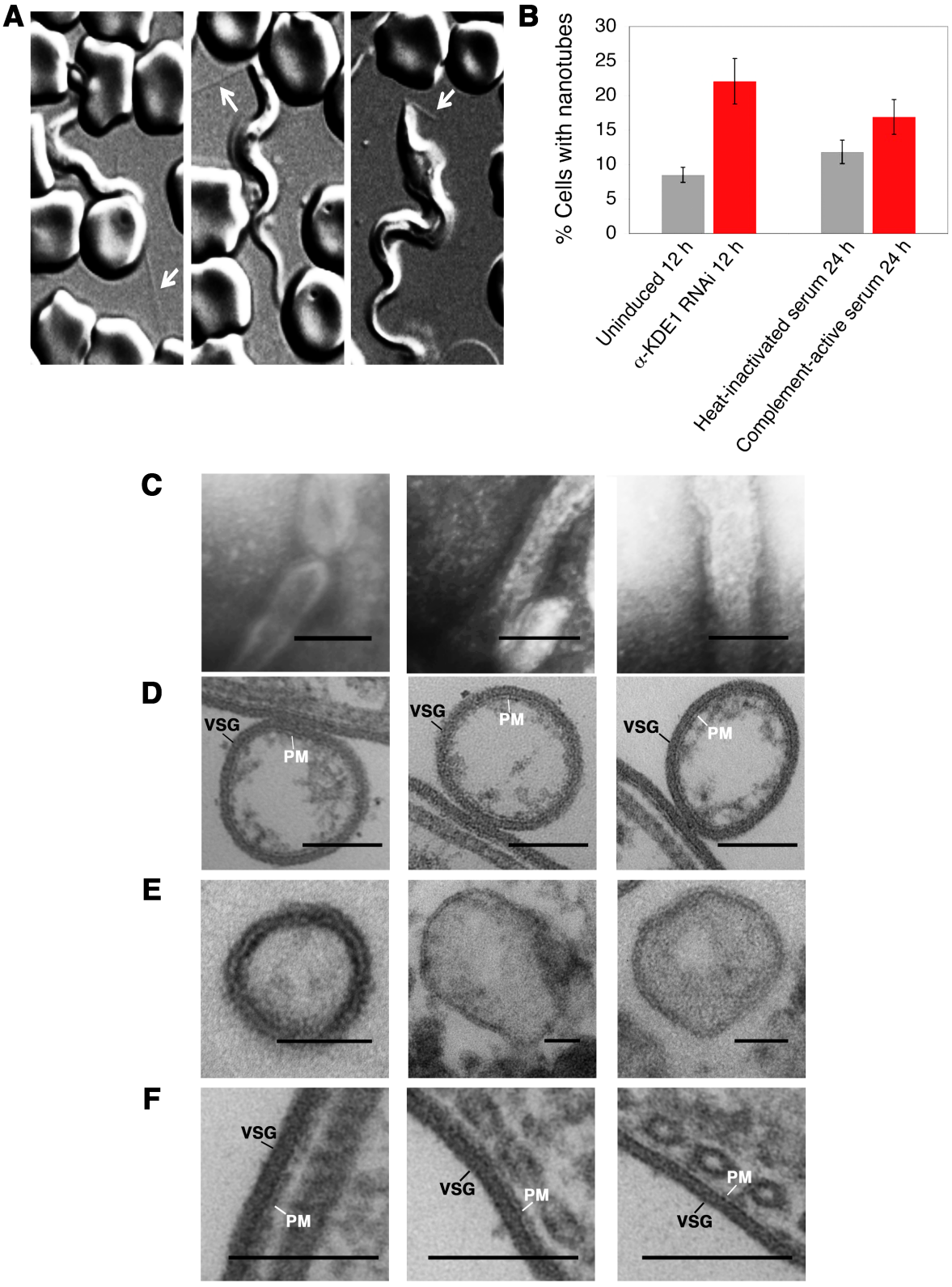

Figure S4.1. Nanotubes were present on trypanosomes from infected mice. Stress and complement active serum induced formation of nanotubes. Electron microscopy shows

morphological similarities between nanotube membrane, cell membrane and EV membrane. Related to Figure 4.1 and Figure 4.2. (**A**) Blood from a BALB/c mouse infected with *T. brucei* was visualized with DIC microscopy (63 x). Arrows indicate nanotubes extending from the posterior end of trypanosomes. (**B**) BF *T. brucei* were stressed by RNAi induction against the essential Krebs cycle enzyme α-KDE1 for 12 h or growth in complement active FBS for 24 h. At least 200 cells were scored for the presence of nanotubes when viewed by DIC microscopy at 40 x magnification. Values are the mean of triplicate counts from independent cultures with standard deviations. Scale bars represent the mean ± SEM for three experiments. (**C**) Negative stain TEM analysis of membrane nanotubes shows membrane like structure of ~10-15 nm thickness (black bar = 100 nm). (**D**) Thin section TEM analysis of membrane nanotubes shows membrane/surface coat structure morphology similarities to cell membrane structure. (black bar = 100 nm). (**E**) Thin section TEM analysis of purified EVs show membrane like morphology (~10 nm) similar to cell membrane morphology (black bar = 50 nm). (**F**) Thin section TEM analysis of cell membranes shows similar morphology to nanotubes and EV thin sections (black bar = 100 nm).

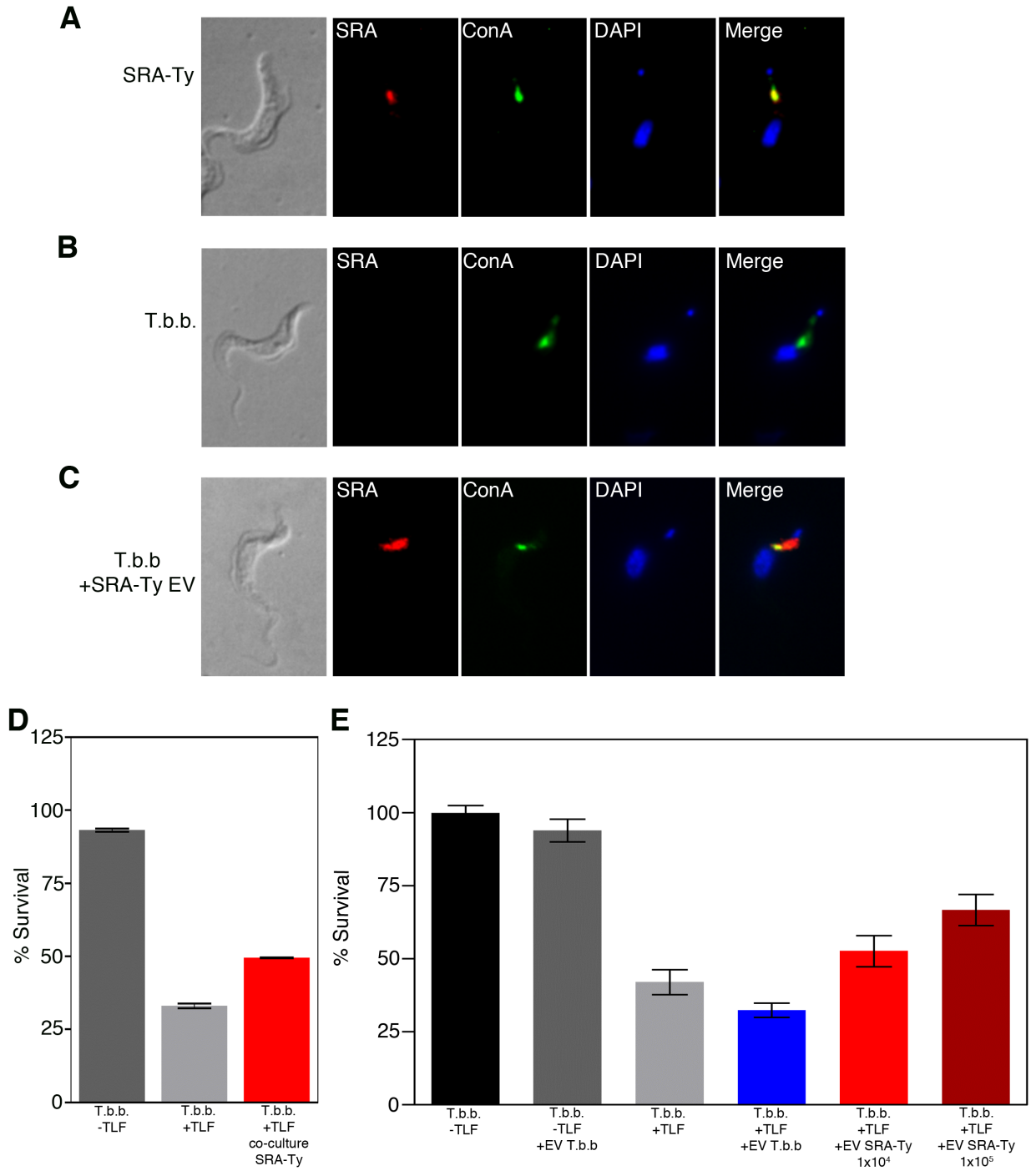

Figure S4.2. EVs purified from *T. b. brucei*$^{SRA\text{-}Ty}$ transferred SRA that co-localized with ConA in the endocytic pathway. Co-culture of *T. b. brucei* and *T. b. brucei*$^{SRA\text{-}Ty}$ results in increased overnight survival during TLF treatment. *T. b. brucei*$^{SRA\text{-}Ty}$ EVs showed titratable protection against TLF in overnight survival assays. Related to Figure 4.3. (**A**) *T.*

b. brucei$^{SRA\text{-}Ty}$ showed co-localization of endogenous SRA with endocytosed ConA. (**B**) *T. b. brucei* take-up ConA but showed no SRA fluorescence. (**C**) *T. b. brucei* treated with EVs from *T. b. brucei*$^{SRA\text{-}Ty}$ showed SRA transfer and co-localization with ConA. (**D**) *T. b. brucei* with a drug selectable marker for hygromycin was grown with *T. b. brucei*$^{SRA\text{-}Ty}$ for 24 hours. Cells were then selected with Geneticin for 48 hours, resulting in death of *T. b. brucei*$^{SRA\text{-}Ty}$ but not *T. b. brucei*. *T. b. brucei* was then treated overnight with TLF and showed ~25% increased survival relative to *T. b. brucei* not co-cultivated with *T. b. brucei*$^{SRA\text{-}Ty}$. Scale bars represent the mean ± SEM for three experiments. (**E**) The addition of EVs purified from *T. b. brucei*$^{SRA\text{-}Ty}$, but not treated with TLF (dark grey) showed increase in growth. Treatment of *T. b. brucei* with EVs purified from TLF sensitive *T .b. brucei* cells showed no protection against TLF (blue bar). Addition of EVs purified from *T. b. brucei*$^{SRA\text{-}Ty}$ at $1x10^4$ and $1x10^5$ cell equivalents showed a dose dependent increase in overnight survival of *T.b. brucei* cells treated with TLF. Scale bars represent the mean ± SEM for three experiments.

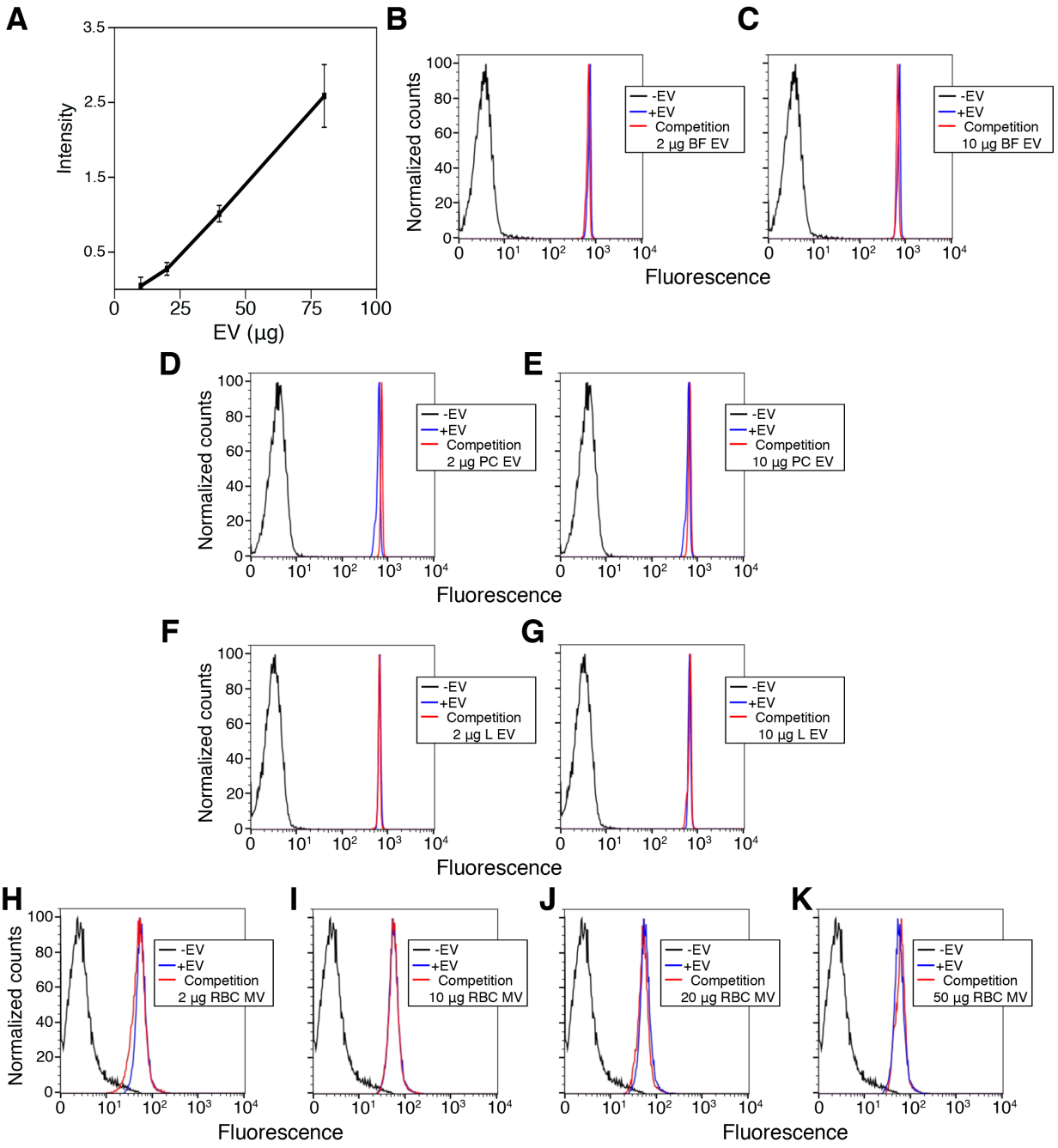

Figure S4.3. EV binding to *T. brucei* showed non-saturatable, receptor independent interaction. Labeled EV interaction could not be competed with EVs from other cell types. Related to Figure 4.4. (**A**) Cells blocked for endocytosis (3°C) and treated with increasing concentrations of EVs showed non-saturatable binding (receptor independent) by flow cytometry. Scale bars represent the mean ± SEM for three experiments. (**B**) Unlabeled

bloodstream form (BF EV) *T. brucei* EVs at 2 µg or (**C**) 10 µg showed no competition with 2 µg of labeled bloodstream form EVs during 3°C binding. (**D**) Unlabeled procyclic form (PF EV) T. brucei EVs at 2 µg or (**E**) 10 µg showed no competition with 2 µg of labeled bloodstream form EVs during 3°C binding. (**F**) Unlabeled promastigote *Leishmania tarentolae* (L EV) EVs at 2 µg or (**G**) 10 µg show no competition with 2 µg of labeled bloodstream form EVs during 3°C binding. (**H**) Unlabeled human erythrocyte (RBC MV) microvesicles show no competition at 2 µg (**I**) 10 µg (**J**) 20 µg or (**K**) 50 µg with labeled bloodstream form EVs during 3°C binding. All flow experiments carried out in triplicate and a representative experimental trace (red) was plotted against untreated control (black) and labeled EV alone control (blue).

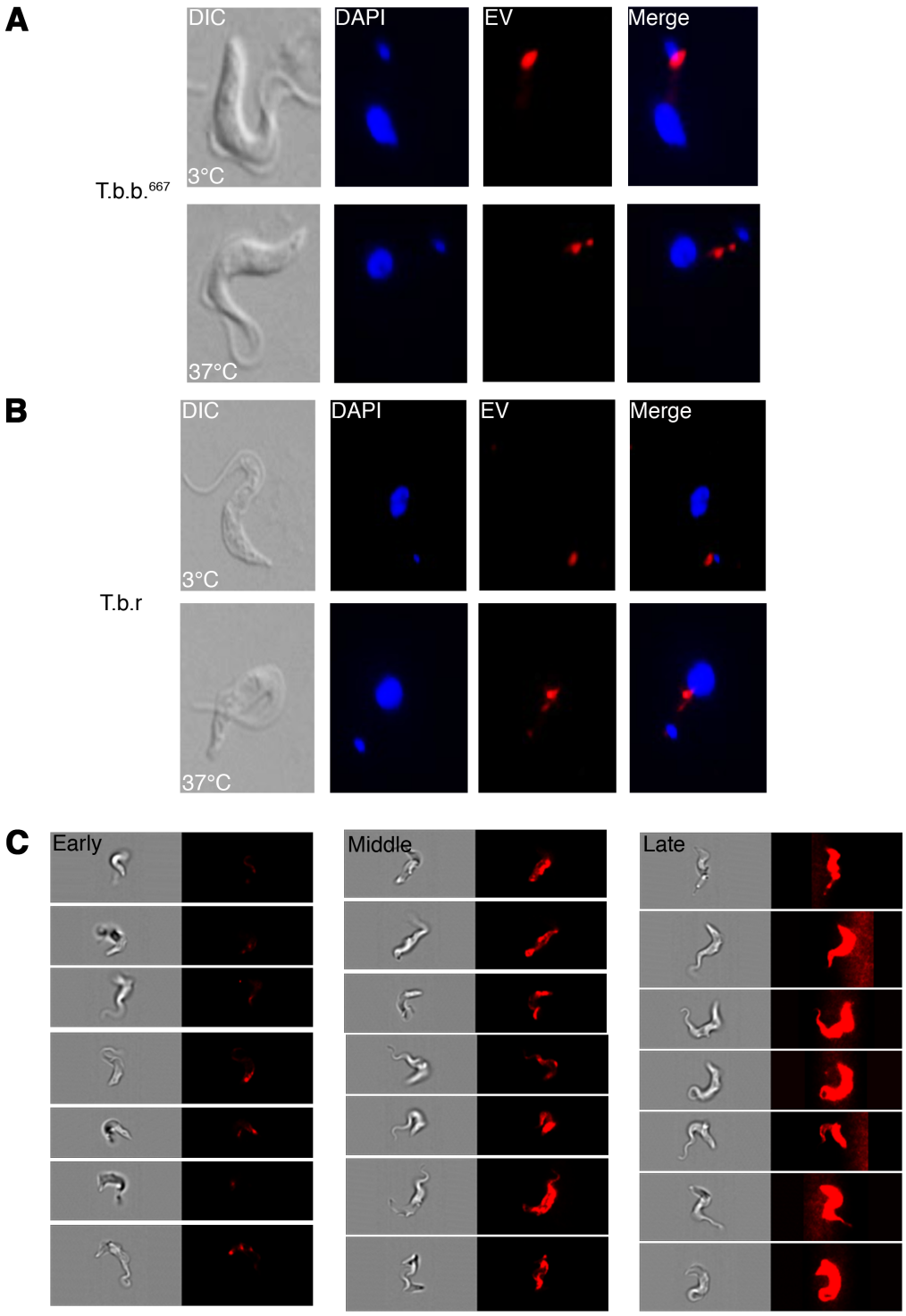

Figure S4.4. EV protein transfer was independent of expressed VSG and subspecies. ImageStream analysis showed rapid, polar, fusion of EVs with *T. brucei*. Related to Figure 4.4. (**A**) Treatment of *T. b. brucei* TREU667 with Alexa-594 labeled EV from *T. b. brucei* 427

expressing a different VSG coat (VSG221) showed binding (3°C) and subsequent endocytosis (37°C) of EVs. (**B**) Treatment of *T. b. rhodesiense* KETRI 2482 with Alexa-594 labeled EVs from a different sub-species, *T. b. brucei* 427, showed binding (3°C) and subsequent endocytosis (37°C) of EVs. (**C**) Additional images from early time (1-73 sec), middle time (74-146 sec) and late time (147-219 sec) showed highly polar posterior end interaction of EVs resulting in distribution of R18 extending along the cell body resulting in brightly labeled cells.

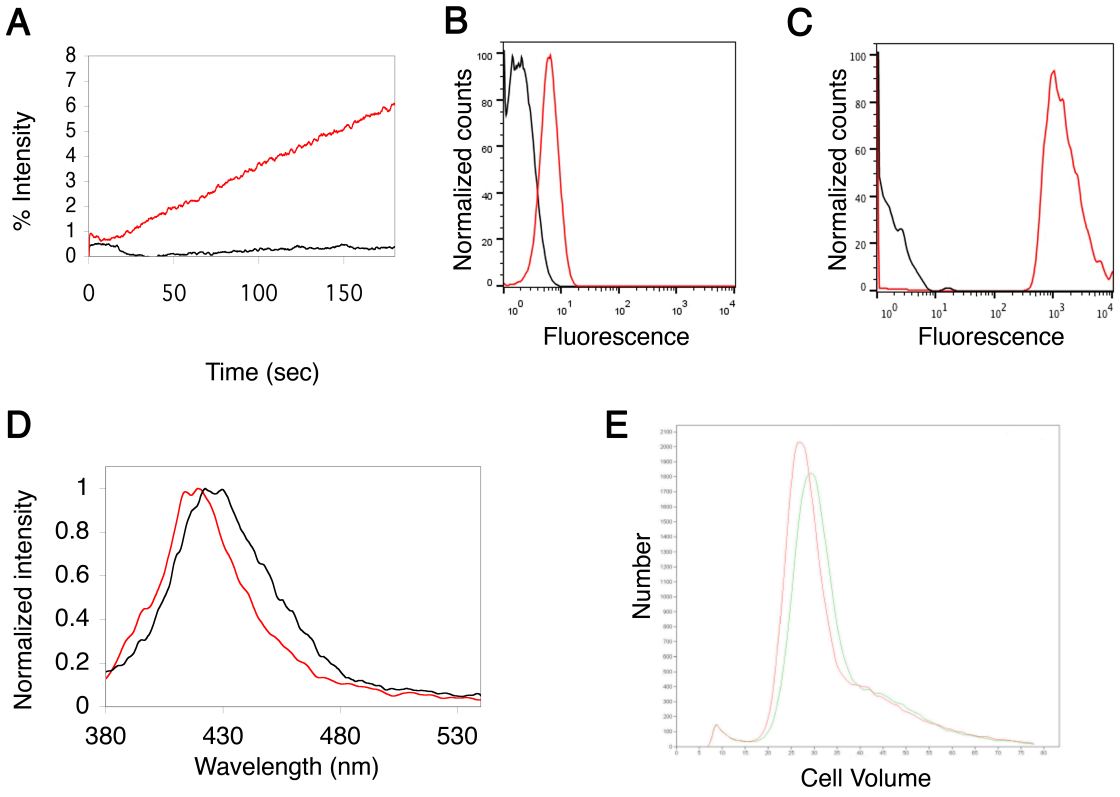

Figure S4.5. *T. brucei* EVs fused with mouse erythrocytes (BALB/c) depositing lipid, VSG and increasing lipid packing of the plasma membrane. Coulter counting of mouse blood pre- and post injection with EVs. Related to Figure 4.5 and Figure 4.6. (**A**) Mouse erythrocyte ghosts were mixed with R18-labeled EV (red) or R18-labeled POPC LUV (black). (**B**) Freshly collected, intact mouse erythrocytes were co-cultured in 0.2 μm transwells with R18-

labeled, exponentially growing BF *T. brucei* (red) or alone (black) for 18 h and analyzed by flow cytometry. (**C**) Freshly collected, intact mouse erythrocytes were co-cultured in 0.2 μm transwells with exponentially growing BF *T. brucei* for (red) or alone (black) for 18 h, probed with anti-VSG 221 and analyzed by flow cytometry. (**D**) Freshly collected, intact mouse erythrocytes were co-cultured in 0.2 μm transwells with exponentially growing BF *T. brucei* (red) or alone (black) for 18 h, labeled with Laurdan and analyzed via fluorescence spectrophotometry. The emission spectra were background subtracted with unlabeled mouse erythrocytes. (**E**) Whole blood from BALB/c mice was collected from tail vein and analyzed by Coulter counting. Red trace shows blood collected from mice pre-injection of EVs. Green trace shows blood collected 1 h post-intravenous EV injection. Traces are the average of counts from 6 mice. The increase in volume may be due to acquisition of lipid from EV fusion.

Table S4.1. Extracellular vesicle proteins identified by mass spectrometry and functional class enrichment. Related to Figure 2. Available online at http://www.cell.com/cms/attachment/2058104976/2061907361/mmc2.xls

Table S4.2. Comparison of extracellular vesicle proteome with *T. brucei* organellar proteomes. EV proteome was also analyzed for published microscopy localization and ribosome profiling expression data. Related to Figure 2. Available online at http://www.cell.com/cms/attachment/2058104976/2061907362/mmc3.xls

Movie S4.1. Nanotubes are dynamic posterior end extensions. Related to Figure 1. Live DIC microscopy (63 x) of R18 labeled *T. brucei* showed posterior end membrane nanotube extensions as dynamic filamentous extensions. A representative frame was shown in Figure 1C. Available online at http://www.cell.com/cms/attachment/2058104976/2061907356/mmc4.flv%20/cms/attachment/2

058104976/2061907365/mmc4.mp4

Movie S4.2. Nanotubes are lipid membrane structures. Related to Figure 1. Fluorescence microscopy (63 x) of R18 labeled *T. brucei* from Movie S1 cells showed that membrane nanotubes were bounded by a lipid bilayer. A representative frame was shown in Figure 1C. Available online at http://www.cell.com/cms/attachment/2058104976/2061907357/mmc5.flv%20/cms/attachment/2058104976/2061907366/mmc5.mp4

Movie S4.3. Nanotubes rapidly interact with multiple trypanosomes. Related to Figure 1. Live DIC microscopy (63 x) of *T. brucei* showed highly dynamic nanotube interactions between adjacent trypanosomes. Nanotube connections were broken and reformed, forming long range connections. Representative frames were shown in Figure 1D. Available online at http://www.cell.com/cms/attachment/2058104976/2061907358/mmc6.flv%20/cms/attachment/2058104976/2061907367/mmc6.mp4

Movie S4.4. Nanotubes bud from the flagellar membrane. Related to Figure 1. Three-dimensional reconstruction of serial TEM sections showed flagellar membrane (green) budding to form a defined nanotube membrane (blue). After the initial budding event both membranes become independent units running parallel to each other. Representative frames was shown in Figure 1G. Available online at http://www.cell.com/cms/attachment/2058104976/2061907359/mmc7.flv%20/cms/attachment/2058104976/2061907368/mmc7.mp4

Movie S4.5. Nanotubes vesicularize to form EV. Related to Figure 2. Live DIC microscopy (63 x) of *T. brucei* stimulated for nanotube formation showed rapid nanotube synthesis and disassociation. After nanotube disassociation the structure break down into free EV.

Representative frames were shown in Figure 2D. Avaialable online at http://www.cell.com/cms/attachment/2058104976/2061907360/mmc8.flv%20/cms/attachment/2058104976/2061907369/mmc8.mp4

CHAPTER 5

SENDING A MESSAGE: EXTRACELLULAR VESICLES OF PATHOGENIC PROTOZOAN PARASITES

Szempruch, A.J., Dennison, L., Kieft, R., Harrington, J.M., and S.L. Hajduk. In press at Nature Reviews Microbiology. Reprinted with permission from the publisher.

Abstract

Parasitic unicellular eukaryotes exploit extracellular vesicles (EVs) as vehicles for intercellular communication and host manipulation. By using varied mechanisms to generate EVs and by transferring a wide range of molecules through EVs, pathogenic protozoans are able to establish infective niches, modulate the immune system of the host and cause disease. In addition to effects on the host, EVs are also able to transfer virulence factors, drug resistance genes and differentiation factors between parasites. Here we explore recent insights into the biology of EVs from human infectious protozoan parasites, including *Trichomonas vaginalis*, *Plasmodium* spp. and kinetoplastids, such as *Trypanosoma* spp and *Leishmania* spp.

Introduction

Pathogenic protozoans are responsible for a wide range of human and animal diseases globally, and they cause a substantial socioeconomic burden in many developing nations. These parasites use diverse mechanisms for survival and persistence within their hosts. Recent research has shown that many of these parasites use extracellular vesicles (EVs) to deliver biologically active effector molecules. EVs fall into two major classes of secreted vesicles: exosomes, which are generated within multivesicular bodies (MVBs) and ectosomes, which are produced by budding of the plasma membrane. Both exosomes and ectosomes can be described as EVs, which serves as a general term for all secreted vesicles[1]. Secretion of EVs has profound biological effects that result from the transfer of proteins, lipids and nucleic acids to both adjacent and distant cells[2,3]. EVs interact with target membranes through receptor-dependent and receptor-independent processes[4]. A single organism may use several different mechanisms to produce and to interact with EVs and generates a population of EVs with varied cargos and functions[5].

Although our understanding of the biology of EVs in mammals and other eukaryotes has rapidly expanded, parasitology has largely lagged behind. The mechanisms of production, interaction and function of eukaryotic EVs have been reviewed thoroughly[3,6]. Recent research has identified EVs produced by many human pathogenic protozoan parasites, including members of the Metamonada, Apicomplexa and Kinetoplastida. Other pathogens including parasitic worms, viruses and fungi also use EVs during infection [5,7-13]. The production of EVs by parasites has been observed *in vitro* and *in vivo* in animal models, human hosts and insect vectors[5,11,12,14].

The urogenital parasite *T. vaginalis* is a member of the phylum Metamonada and is the most prevalent non-viral sexually transmitted human pathogen[15]. These extracellular parasites adhere to the epithelium of the urogenital tract of both males and females and EVs are important for adherence and pathogenesis (see below).

The phylum Apicomplexa includes the genus *Plasmodium,* members of which are responsible for human malaria. *Plasmodium* spp. are transferred by the bite of an infected mosquito, which results in the injection of sporozoites, the liver infectious form. After invasion of hepatocytes, the parasites divide, differentiate, egress and subsequently infect circulating erythrocytes[16]. The most common forms of human malaria are caused by *P. falciparum, P. vivax* and *P. malariae,* but the mouse-specific *P. berghei* and *P. yoelii* are often used experimentally because they are more amenable to studying the complete life cycle of the parasite[16]. EVs have been detected in all of the above-mentioned *Plasmodium* spp.and *in vitro* studies have focused on inter-erythrocytic stages of the parasite. To date the, the capacity of extracellular parasite forms to produce EVS has not been analyzed.

The class Kinetoplastida contains a diverse group of parasites that cause a wide range of important diseases in humans and animals[17]. This group includes *Trypanosoma brucei,* the

causative agent of African sleeping sickness and Nagana in cattle; *Trypanosoma cruzi,* which causes Chagas disease; and *Leishmania* spp., which cause human leishmaniasis[17,18]. All of these kinetoplastids are transmitted by insect vectors to their mammalian host and undergo a series of differentiation steps during their life cycle[17]. Kinetoplastid EVs are some of the best-studied parasite EVs.

Many recent studies on pathogenic protozoans have focused on how EVs modulate the immune system of the host and how they elicit a pro-inflammatory response (**Box 5.1**). For example, treatment with EVs from *T. vaginalis* induces changes in interleukin levels that resemble changes observed during infection with the parasite[19]. Similarly, both purified EVs from *L. donovani* and infection with the parasite induce a Th1 response in $CD4^+$ T cells*i*[20]. Proteins purified from EVs have also been shown to mirror the effects of infection with *L. donovani* on liver function, that is, both reduce the levels of circulating cholesterol[21]. In addition, purified EVs mediate pathological changes that resemble the effects of *T. brucei in vivo*[22]. Besides causing pathology or provoking an immune response in the host, EVs can also substantially change parasite population; for example, EVs have been shown to cause cellular differentiation of *P. falciparum*[23,24], which is crucial for continuation of the parasite's life cycle. EVs might also have a role in the life cyle progression of *Trypanosoma cruzi*[25]. Additionally, EVs can transfer virulence factors between parasites, a process that enables *T. brucei* to spread resistance to innate immune factors of the host to the whole parasite population [22].

In this Progress, we present the most compelling evidence for the role of EVs from pathogenic protozoans in sending a message within the parasite population and to the host. Although the message has not been fully deciphered, what we do know is that it has profound implications for parasite development, disease progression and pathology in the host.

Assembling the message: mechanisms to generate EVs

Exosomes

Exosomes were first described in eukaryotes in the early 1980s and the mechanism of their formation and secretion has been the subject of a number of reviews[3,26-28]. Exosomes are membrane-bound structures of homogeneous size that are derived from MVBs. MVBs are specialized late endosomes that contain exosomes and can traffic to the plasma membrane, with which they fuse to release their exosome cargo[3,27]. Exosomes are formed by the invagination of endosomal membranes, which creates vesicles that display cell surface lipids and proteins on their exterior face[3] (**Figure 5.1a**). Released exosomes interact with target cells through three major mechanisms: receptor-mediated binding, membrane fusion and bulk-phase nonspecific entry through the endocytic pathway, and fusion with endosomal membranes[3] (**Figure 5.1b**). Although exosomes contain cell-surface proteins and lipids, they are often enriched in unique molecules and show a differential distribution of proteins and lipids compared to the cell surface membrane[27]. Exosomes are also enriched in luminal cargo molecules including specific proteins and nucleic acids[2,27]. During endosomal recycling, MVBs fuse with the cell surface membrane, which results in the release of exosomes[26-28]. Initial electron microscopy studies showed that erythrocytes produce MVBs and release EVs as a mechanism of membrane maturation and homeostasis[26]. Light and fluorescence microscopy showed that *T. vaginalis* produces large MVB-like structures [19]. Additionally, electron microscopy studies have shown that the kinetoplastids *T. cruzi* and *Leishmania* spp. produce MVBs to secrete vesicles[29,30]. However, the mechanisms that govern MVB formation and subsequent exosome release in parasites are unknown.

Ectosomes

Ectosomes are important products of secretion, which are formed through budding of the plasma membrane and encompass a wide range of vesicle types (reviewed extensively in [3,6]). Ectosomes have a membrane-bound structure and are often of heterogeneous size[3,6]. Ectosomes are derived from the entire cell membrane or from specialized regions of the membrane, such as the cilium and flagellum or from membrane nanotubes [3,6] (**Figure 5.1a**). Ecotosomes interact with target cells through similar mechanisms as exosomes[3] (**Figure 5.1b**). For example, plasmodium-infected erythrocytes generate EVs that contain parasite proteins through budding of the plasma membrane[23,24]. Kinetoplastids use several mechanisms to generate and release EVs. Both *T. cruzi* and *Leishmania* spp. release EVs through budding along the cell body and at flagellar membranes[29,30]. The *T. brucei* flagellum gives rise to a membrane nanotube that can break down and release EVs[22]. Thus, a single parasite can use multiple mechanisms to generate EVs. The methods to dissect the functions of individual subpopulations of EVs have not been well established, therefore, it is critical to note that most experiments with EVs involve a mixture of subpopulations[31].

Discussion

Sending the message: interactions of EVs within parasite populations

Adherence of *T. vaginalis*

T. vaginalis produces large MVB structures, which are visible by fluorescence microscopy, when exposed to ectocervical cells, but not in the absence of host cells[19]. *T. vaginalis*-derived EVs share physical characteristics with mammalian exosomes, including size, density and protein composition. Short-term incubation of the *T. vaginalis* strain G3, which has low levels of adherence, with purified EVs from other *T. vaginalis* isolates showed that EVs can increase the adherence of this strain to ectocervical cells (**Figure 5.2**). Addition of purified EVs

from parasites with preferential adherence to male prostate epithelium cells or female ectocervical cells could transfer this phenotype of tissue-tropic adherence to G3 parasites. This observation has profound implications for *T. vaginalis* infection, as it might allow mixed populations to survive in both male and female hosts and impact the severity of disease.

Drug resistance and sexual differentiation of *Plasmodium* spp.

While inside host erythrocytes, *Plasmodium* spp. alter the quantity and composition of erythrocyte-derived EVs[32-34]. These changes include the incorporation of parasite proteins, lipids and nucleic acids, including drug resistance genes[23,24]. Recently, EVs from resistant *P. falciparum* were shown to transfer drug resistance to sensitive parasites through episomal DNA, and the authors of this study speculated that this mechanism facilitates the transfer of drug resistance during human infection[23] (**Figure 5.2**). This effect was observed both during co-cultivation of parasites separated by semi-permeable transwells and when purified EVs were directly added to cultures of sensitive parasites with a titratable response. The *P. falciparum* erythrocyte membrane protein 1 trafficking protein 2 (PfPTP2) was localized to structures that budded from the surface of infected erythrocytes. Deletion of PfPTP2 substantially decreased the amount of released vesicles and abolished the ability to transfer drug resistance. In addition, EVs have a role during the differentiaton of *P. falciparum*[23,24]. Before egress from erythrocytes, which is an important point in the parasite life cycle for sexual commitment and differentiation, the levels of released EVs substantially increase[23,24,33]. *In* vitro, the addition of purified EVs stimulates the differentiation of asexual *P. falciparum* into the gametes, which is the parasite that infects mosquitoes and thus is essential for continuation of the life cycle[23,24]. This suggests that alterations of the levels of secreted EVs *in vivo* could directly impact the frequency at which *P. falciparum* infects mosquito by increasing the number of gametes.

Virulence and development of *T. brucei*, *T. cruzi* and *Leishmania* spp.

Bloodstream forms of *T. brucei* produce membrane nanotubes through budding and extension of the flagellar membrane[22]. These nanotubes vesicularize, which produces free EVs that are ~80 nm in size and enriched in flagellar proteins. This process resembles the ciliary release of EVs in the unicellular alga *Chlamytomonas reinhardtii*[6,35]. The animal pathogen *Trypanosoma brucei brucei* does not infect humans and is readily killed in human serum by the primate-specific innate immune molecules, which are known as trypanosome lytic factors (TLFs). The closely related subspecies *Trypanosoma brucei rhodesiense* has evolved a mechanism of resistance to TLF through expression of the serum resistance-associated protein (SRA), which can bind TLF and allows the parasite to persist in a primate host[36,37]. Co-cultivation or direct addition of EVs from SRA-expressing parasites results in the transfer of SRA to *T. b. brucei* and subsequent TLF resistance (**Figure 5.2**). These data may explain the report of mixed trypanosome infections in humans[38]. *T. brucei* undergoes density-dependent differentiation in the bloodstream, in which EVs have been proposed to participate[39]. It has been shown that *T. brucei* can achieve significantly higher culture densities when grown in transwells by exchanging media that diffuses across a four-hundred nanometere membrane[40]. This may suggest that diffusion of EVs through the membrane might reduce the concentration of EVs and thus also any stimulatory effect they have on differentiation.

T. cruzi produces EVs through the secretion of MVB-derived exosomes and shedding of ecotosomes at the cell surface membrane. Early work on the *T. cruzi* secretome showed that mucin proteins were released as components of EVs[41,42]. Protemoic analysis of *T. cruzi* EVs showed a enrichment in immunogenic proteins and further fractionation detected the presence of tRNA-derived small RNAs (tsRNAs), which have been proposed to have functions similar to

siRNAs in other organisms[43,44]. These tsRNAs co-localize with the *T. cruzi*-specific argonaute protein TcPIWI-tryp and were transferred between cells in transwell co-cultivation experiments[43]. The addition of purified EVs resulted in *T. cruzi* differentiation[25] (**Figure 5.2**). Similarly, EVs purified from the related kinetoplastids *L. donovani* and *L. braziliensis* also show enrichment of tsRNAs, although their role in *Leishmania* spp. interactions has yet to be investigated[45] (**Figure 5.2**). Transfer of small regulatory RNAs by EVs may change the transcriptional landscape of a parasite population during infection and in response to stress.

Sending the message: interactions of EVs with the host

***T. vaginalis* and pro-inflammatory cytokines**

T. vaginalis EVs interact with host ectocervical cells through fusion at the plasma membrane, which results in the transfer of lipids and luminal cargo proteins to host cells[19]. Incubation of EVs with ectocervical cells also results in the secretion of the pro-inflammatory cytokines IL-6 and IL-8[19] (**Figure 5.3**). However, pretreatment of ectocervical cells with EVs followed by infection with *T. vaginalis* showed overall dampening of the IL-8 response, which may allow increased parasite growth and pathology without provoking a strong early immune response[19]. These results suggest that EVs have a role in immunomodulation of the host, which may dampen the immune response and allows increased parasite attachment.

***Plasmodium* spp. and immune activation**

Human and murine infections with *Plasmodium* spp. have been shown to increase the overall number of circulating EVs, derived from erythrocytes and other host cell types[32-34]. Increased production of EVs during infection has also been correlated with disease severity in human and animal malaria[32,34]. Using rodent malaria models it was shown that EVs have broad immunomodulatory effects, which often result in a pro-inflammatory response[5,11,12] (**Figure 5.3**).

EVs isolated from mice with cerebral malaria caused by infection with *P. berghei* activate cultured macrophages and increase the expression of tumor necrosis factor (TNF) and the TNF-receptor superfamily protein CD40[46]. EVs generated during infection with *P. berghei* adhere to blood vessels in the brain and may have a role in disease development[32]. Knockout of host ATP-binding cassette transporter 1, which is responsible for distribution of phosphatidylserine in the plasma membrane, substantially decreased the levels of EVs, prolonged survival and reduced cerebral pathology during *P. berghei* infection[47]. EVs may also be important for the cell-type tropism of *Plasmodium* spp.[48]. It has been shown that transfer of EVs from a *P. yoelii* strain that preferentially infects reticulocytes, which are immature erythrocytes, can change the tropism of other *P. yoelii* strains from mature erythrocytes to reticulocytes[48]. EVs derived from erythrocytes that were infected *in vitro* with *P. falciparum* activated monocytes isolated from naïve human peripheral blood mononuclear cells. Activated cells showed an up-regulation of the inflammatory response markers CD40, CD54 and CD86 and a down-regulation of CD163[24]. These EVs also activated human macrophages and stimulated the production of IL-10 and the pro-inflammatory cytokines IL-6, IL-12 and IL-1β[24]. These studies show that EVs generated during malaria infection activate an inflammatory response in the host and broadly modulate immune cells.

***T. brucei*, *T. cruzi* and *Leishmania* spp. pathology, immunomodulation and host metabolism**

It has been suggested that differences in the secretome of *T. brucei* may directly impact disease progression and immune response[49]. Experiments with bloodstream forms of *T. brucei* show that nanotube-derived EVs fuse with host erythrocyte membranes, and that fusion is mediated by an unidentified surface-exposed protein on the EVs[22]. Fusion results in the transfer of lipids and parasite-specific antigens, including the immunogenic variant surface glycoprotein (VSG), to the erythrocyte surface. This interaction also alters the physical properties of the

erythrocyte membrane and may cause clearance of infected erythrocytes by macrophages in the liver and spleen[22]. Infection with *T. brucei* of non-primate mammals causes anemia and often results in death of the host[50,51]. When erythrocytes that were treated *ex vivo* with purified EVs, were injected into naïve mice, they were rapidly cleared and injection of EVs resulted in anemia in two different mouse strains[22] (**Figure 5.3**). These observations suggest that the severe anemia observed during *T. brucei* infection might be caused by biochemical and biophysical remodeling of erythrocytes by EVs.

Proteomic analysis of EVs secreted by *T. cruzi* showed enrichment of proteins that have been implicated in host-parasite interactions, immunomodulation and cell signaling[30]. Injection of purified EVs into naïve mice increased parasitemia and reduced survival of the mice when they were challenged with *T. cruzi*[52]. Mice treated with EVs before infection had more parasites in the cardiac tissue and increased mortality than controls and injection of EVs increased IL-4 and IL-10 mRNA levels in cardiac tissue [52] (**Figure 5.3**). Increased mortality was linked to secreted IL-4 and IL-10 as monoclonal antibody treatment against both cytokines restored survival to the levels of controls [52]. EVs from *T. cruzi* also caused splenocytes to produce IL-10 and the pro-inflammatory cytokines TNF, IFN-γ and IL-6 with some parasite strain-specific variation[53] (**Figure 5.3**). *T. cruzi* EVs that were produced *in vitro* contain a class of antigens known as *T. cruzi* surface membrane proteins (TcSMPs)[54]. Purified TcSMP alters calcium signaling in host cells, which inhibits invasion of host cells by the parasite [54]. EVs may locally disperse TcSMP to limit parasite invasion of cells immediately adjacent to sites of high parasite burden[54] and thereby also tissue destruction and recruitment of immune cells. These findings suggest that *T. cruzi* EVs regulate organ tropism and provide some site-specific protection.

The first evidence for the secretion of EVs from *L. donovani, L. mexicana* and *L. major* came from the analysis of secreted proteins. Proteomic analysis showed a substantial enrichment of proteins that had been identified previously in EVs from other eukaryotes including, GAPDH, cyclophilin A and the surface metalloprotease gp63, which is a known parasite virulence factor[29,55,56]. *L. donovani* EVs contain a number of immunomodulatory proteins known to be T cell antigens, as well as virulence factors that are required for survival during host cell invasion[57]. Addition of purified *L. donovani* EVs to macrophages *in vitro* initially increases the production of IL-8; however, long-term treatment of monocytes with purified EVs inhibits the production of TNF and IL-8[57] (**Figure 5.3**). Consistent with these *in vitro* results, mice that were infected 3 weeks after the injection of EVs from *L. donovani* and *L. major* had higher parasite loads than control mice[20]. Analysis of *L. infantum* and *L. major* within the sand fly vector showed that EVs are produced and transfered, together with the parasite inoculum, to the mammalian host, where they stimulate an inflammatory response[14]. In mice, *L. donovani* can invade liver cells, which changes the lipid metabolism in the liver and reduces serum cholesterol levels[21]. Reduction of serum cholesterol levels was shown to be due to inhibition in miR-122 mediated gene repression[21]. Treatment of hepatoma cells with purified EVs recapitulated these changes to host miR-122 and was shown to depend on the EV metalloprotease gp63[21]. Purified gp63 degraded Dicer1 *in vitro* and overexpression of Dicer1 or expression of a miR-122 variant that does not require processing by Dicer1 rescued EV-mediated changes to miR-122 regulation. Treatment of mice with gp63 decreased Dicer1 levels *in vivo* and a subsequently also the levels of miR-122 processing[21]. These studies show that EVs from *Leishmania* spp. have a wide range of targets within mammalian hosts and have broad immune dampening roles (**Figure 5.3**).

Intercepting the message: using EVs for detection and treatment

By identifying the message delivered by EVs within a host it may be possible to detect even low levels of the parasite that broadcasts that message. Many parasites have developed sophisticated mechanisms to evade the innate and adaptive immune response through alterations of their surface proteins[58-60]. However, parasite-derived EVs are enriched in invariant immunogenic proteins and nucleic acids, many of which can be found in the circulation of infected hosts[22,24,29,30]. It may be possible to screen individuals for the presence of cargo molecules as a first line of detection. EVs produced by mammalian cells as biomarkers for diseases such as cancer and cardiovascular diseases also are subjects of active research[31,61].

As discussed above, parasite EVs have two broad effects immunomodulation, often eliciting a pro-inflammatory response, and modulation of disease development through direct interactions with tissues and specific cell types. Blocking the interaction of EVs with target host cells could alleviate immune activation and pathogenesis, for example by decreased immune dampening and reduced parasite burden and disease severity during *Plasmodium* spp. and *Leishmania* spp. infection. In the case of the cattle disease Nagana, which is caused by *T. brucei*, it has been proposed that the ability to resist anemia is more important for survival than the control of parasitemia[50,51]. *T. brucei*-derived EVs interact with target membranes by proteins that are exposed on the surface of EVs[22]. Future efforts to identify these fusogens may provide a powerful tool for preventing disease, including anemia, and possibly migration of *T. brucei* to specific host tissues.

In addition to therapeutic and diagnostic application during an active infection EVs may provide a powerful new tool for vaccination. Immunization with EVs from *Plasmodium* spp. showed promising results in an animal model[48]. In mouse studies of *L. major and* the protozoan parasite *Toxoplasma gondii,* use of host cell-derived EVs pretreated with parasite antigens or

parasite cells elicited a protective immune response to parasite challenge[62,63]. Using parasite-derived and host-derived EVs are promising new therapeutic options.

Conclusions

The biology of EVs from protozoan parasites has only recently started to be unraveled. This delay compared to research in other organisms may be due to the difficulty associated with identifying and characterizing the production of EVs by parasites in a multi-cellular host[64-67]. Another challenge has been to determine if there is tissue-specific and cell-specific targeting of EVs that are produced *in vivo*. In a cancer animal model, it has been shown that cancer-derived EVs are important for tissue-specific metastatic niche formation[68]. A recent mouse study used Cre mRNA secreted into EVs to identify target cells of EVs, organ-specific interactions and cell reprogramming mediated by metastatic tumor cells[69]. Similar approaches could be used to identify the targets of parasite-derived EVs *in vivo*. Research on EVs in other organisms have resulted in the generation of powerful community databases that contain extensive data sets (for example, Vesiclepedia (http://www.microvesicles.org/) and ExoCarta (http://www.exocarta.org/)). Recently data of parasite-specific EVs have also begun to be incorporated into EuPathDB (http://eupathdb.org/eupathdb/). Ample evidence suggests that parasites, like other eukaryotes, use EVs to send a message. With powerful new techniques being developed to understand the interactions and effects of EVs *in vivo* it is only a matter of time before the field of parasitology catches up to cancer biology and other fields. Deciphering, intercepting and blocking the message carried by EVs may change the way we think about and how we treat parasitic diseases in the future.

Acknowledgments

This work was supported by NIH grant AI039033 (S.L.H.). A.J.S. is an ARCS Foundation Fellows and is supported in part by NIH training grant AI060546.

Conflicts of interest

The authors declare no conflicts of interest.

References

1. Gould, S.J. & Raposo, G. As we wait: coping with an imperfect nomenclature for extracellular vesicles. *J Extracell Vesicles* **2**(2013).
2. Valadi, H. et al. Exosome-mediated transfer of mRNAs and microRNAs is a novel mechanism of genetic exchange between cells. *Nat Cell Biol* **9**, 654-9 (2007).
3. Cocucci, E. & Meldolesi, J. Ectosomes and exosomes: shedding the confusion between extracellular vesicles. *Trends Cell Biol* **25**, 364-72 (2015).
4. EL Andaloussi, S., Mager, I., Breakefield, X.O. & Wood, M.J. Extracellular vesicles: biology and emerging therapeutic opportunities. *Nat Rev Drug Discov* **12**, 347-57 (2013).
5. Marcilla, A. et al. Extracellular vesicles in parasitic diseases. *J Extracell Vesicles* **3**, 25040 (2014).
6. Wood, C.R. & Rosenbaum, J.L. Ciliary ectosomes: transmissions from the cell's antenna. *Trends Cell Biol* **25**, 276-85 (2015).
7. Schorey, J.S. & Harding, C.V. Extracellular vesicles and infectious diseases: new complexity to an old story. *J Clin Invest* **126**, 1181-9 (2016).
8. Siles-Lucas, M., Morchon, R., Simon, F. & Manzano-Roman, R. Exosome-transported microRNAs of helminth origin: new tools for allergic and autoimmune diseases therapy? *Parasite Immunol* **37**, 208-14 (2015).

9. Barteneva, N.S., Maltsev, N. & Vorobjev, I.A. Microvesicles and intercellular communication in the context of parasitism. *Front Cell Infect Microbiol* **3**, 49 (2013).

10. Coakley, G., Maizels, R.M. & Buck, A.H. Exosomes and Other Extracellular Vesicles: The New Communicators in Parasite Infections. *Trends Parasitol* **31**, 477-89 (2015).

11. Mantel, P.Y. & Marti, M. The role of extracellular vesicles in Plasmodium and other protozoan parasites. *Cell Microbiol* **16**, 344-54 (2014).

12. Marti, M. & Johnson, P.J. Emerging roles for extracellular vesicles in parasitic infections. *Curr Opin Microbiol* **32**, 66-70 (2016).

13. Schorey, J.S., Cheng, Y., Singh, P.P. & Smith, V.L. Exosomes and other extracellular vesicles in host-pathogen interactions. *EMBO Rep* **16**, 24-43 (2015).

14. Atayde, V.D. et al. Exosome Secretion by the Parasitic Protozoan Leishmania within the Sand Fly Midgut. *Cell Rep* **13**, 957-67 (2015).

This publication presents evidence that parasites activley produce EVs within there insect vector and that these EVs are egested into the mamalian host resulting in an increased inflamatory response.

15. Kissinger, P. Trichomonas vaginalis: a review of epidemiologic, clinical and treatment issues. *BMC Infect Dis* **15**, 307 (2015).

16. Cowman, A.F., Berry, D. & Baum, J. The cellular and molecular basis for malaria parasite invasion of the human red blood cell. *J Cell Biol* **198**, 961-71 (2012).

17. Rodrigues, J.C., Godinho, J.L. & de Souza, W. Biology of human pathogenic trypanosomatids: epidemiology, lifecycle and ultrastructure. *Subcell Biochem* **74**, 1-42 (2014).

18. Maudlin, I. African trypanosomiasis. *Ann Trop Med Parasitol* **100**, 679-701 (2006).

19. Twu, O. et al. Trichomonas vaginalis exosomes deliver cargo to host cells and mediate host:parasite interactions. *PLoS Pathog* **9**, e1003482 (2013).

An exceptional study on EV function in parasite tissue attachment tropism and *in vitro* host immune modulation, which demonstrates transfer of luminal EV cargo proteins to host cell cytoplasm.

20. Silverman, J.M. et al. Leishmania exosomes modulate innate and adaptive immune responses through effects on monocytes and dendritic cells. *J Immunol* **185**, 5011-22 (2010).

This study provides evidence that parasite derived EVs alter host cell cytokine production and are released into host cells during invasion.

21. Ghosh, J., Bose, M., Roy, S. & Bhattacharyya, S.N. Leishmania donovani targets Dicer1 to downregulate miR-122, lower serum cholesterol, and facilitate murine liver infection. *Cell Host Microbe* **13**, 277-88 (2013).

This study provides strong data showing that EVs are produced by the parasite with in the insect vector and that these exosomes stimulate a proinflammatory response.

22. Szempruch, A.J. et al. Extracellular Vesicles from Trypanosoma brucei Mediate Virulence Factor Transfer and Cause Host Anemia. *Cell* **164**, 246-257 (2016).

This publication presencts data that EVs mediate the transfer of functional parasite specific virulence factors and remodel host cells resulting in disease pathology.

23. Regev-Rudzki, N. et al. Cell-cell communication between malaria-infected red blood cells via exosome-like vesicles. *Cell* **153**, 1120-33 (2013).

This publication provides data that supports that EVs mediate transfer of drug resistnace, through episomal DNA transfer, and stimulate parasite gamete formation *in vitro*.

24. Mantel, P.Y. et al. Malaria-infected erythrocyte-derived microvesicles mediate cellular communication within the parasite population and with the host immune system. *Cell Host Microbe* **13**, 521-34 (2013).

This study on the role of EV stimulation of parasite gamete formation and *in vitro* host immune modulation also shows EV uptake by parasitized host erythrocytes.

25. Garcia-Silva, M.R. et al. Extracellular vesicles shed by Trypanosoma cruzi are linked to small RNA pathways, life cycle regulation, and susceptibility to infection of mammalian cells. *Parasitol Res* **113**, 285-304 (2014).

26. Harding, C., Heuser, J. & Stahl, P. Receptor-mediated endocytosis of transferrin and recycling of the transferrin receptor in rat reticulocytes. *J Cell Biol* **97**, 329-39 (1983).

27. Harding, C.V., Heuser, J.E. & Stahl, P.D. Exosomes: looking back three decades and into the future. *J Cell Biol* **200**, 367-71 (2013).

28. Pan, B.T. & Johnstone, R.M. Fate of the transferrin receptor during maturation of sheep reticulocytes in vitro: selective externalization of the receptor. *Cell* **33**, 967-78 (1983).

29. Silverman, J.M. et al. Proteomic analysis of the secretome of Leishmania donovani. *Genome Biol* **9**, R35 (2008).

30. Bayer-Santos, E. et al. Proteomic analysis of Trypanosoma cruzi secretome: characterization of two populations of extracellular vesicles and soluble proteins. *J Proteome Res* **12**, 883-97 (2013).

31. Thery, C. Cancer: Diagnosis by extracellular vesicles. *Nature* **523**, 161-2 (2015).

32. El-Assaad, F., Wheway, J., Hunt, N.H., Grau, G.E. & Combes, V. Production, fate and pathogenicity of plasma microparticles in murine cerebral malaria. *PLoS Pathog* **10**, e1003839 (2014).

33. Nantakomol, D. et al. Circulating red cell-derived microparticles in human malaria. *J Infect Dis* **203**, 700-6 (2011).

34. Campos, F.M. et al. Augmented plasma microparticles during acute Plasmodium vivax infection. *Malar J* **9**, 327 (2010).

35. Cao, M. et al. Uni-directional ciliary membrane protein trafficking by a cytoplasmic retrograde IFT motor and ciliary ectosome shedding. *Elife* **4**(2015).

36. Stephens, N.A. & Hajduk, S.L. Endosomal localization of the serum resistance-associated protein in African trypanosomes confers human infectivity. *Eukaryot Cell* **10**, 1023-33 (2011).

37. De Greef, C. & Hamers, R. The serum resistance-associated (SRA) gene of Trypanosoma brucei rhodesiense encodes a variant surface glycoprotein-like protein. *Mol Biochem Parasitol* **68**, 277-84 (1994).

38. Truc, P. et al. Atypical human infections by animal trypanosomes. *PLoS Negl Trop Dis* **7**, e2256 (2013).

39. Mugnier, M.R., Papavasiliou, F.N. & Schulz, D. Vesicles as Vehicles for Virulence. *Trends Parasitol* (2016).

40. Ajoko, C. & Steverding, D. A cultivation method for growing bloodstream forms of Trypanosoma brucei to higher cell density and for longer time. *Parasitol Res* **114**, 1611-2 (2015).

41. da Silveira, J.F., Abrahamsohn, P.A. & Colli, W. Plasma membrane vesicles isolated from epimastigote forms of Trypanosoma cruzi. *Biochim Biophys Acta* **550**, 222-32 (1979).

42. Goncalves, M.F. et al. Trypanosoma cruzi: shedding of surface antigens as membrane vesicles. *Exp Parasitol* **72**, 43-53 (1991).

43. Garcia-Silva, M.R. et al. Gene expression changes induced by Trypanosoma cruzi shed microvesicles in mammalian host cells: relevance of tRNA-derived halves. *Biomed Res Int* **2014**, 305239 (2014).

44. Bayer-Santos, E., Lima, F.M., Ruiz, J.C., Almeida, I.C. & da Silveira, J.F. Characterization of the small RNA content of Trypanosoma cruzi extracellular vesicles. *Mol Biochem Parasitol* **193**, 71-4 (2014).

45. Lambertz, U. et al. Small RNAs derived from tRNAs and rRNAs are highly enriched in exosomes from both old and new world Leishmania providing evidence for conserved exosomal RNA Packaging. *BMC Genomics* **16**, 151 (2015).

46. Couper, K.N. et al. Parasite-derived plasma microparticles contribute significantly to malaria infection-induced inflammation through potent macrophage stimulation. *PLoS Pathog* **6**, e1000744 (2010).

47. Combes, V. et al. ABCA1 gene deletion protects against cerebral malaria: potential pathogenic role of microparticles in neuropathology. *Am J Pathol* **166**, 295-302 (2005).

48. Martin-Jaular, L., Nakayasu, E.S., Ferrer, M., Almeida, I.C. & Del Portillo, H.A. Exosomes from Plasmodium yoelii-infected reticulocytes protect mice from lethal infections. *PLoS One* **6**, e26588 (2011).

49. Geiger, A. et al. Exocytosis and protein secretion in Trypanosoma. *BMC Microbiol* **10**, 20 (2010).

50. Berardi, R. et al. Anemia may influence the outcome of patients undergoing neo-adjuvant treatment of rectal cancer. *Ann Oncol* **17**, 1661-4 (2006).

51. Berthier, D. et al. Tolerance to Trypanosomatids: A Threat, or a Key for Disease Elimination? *Trends Parasitol* **32**, 157-68 (2016).

52. Trocoli Torrecilhas, A.C. et al. Trypanosoma cruzi: parasite shed vesicles increase heart parasitism and generate an intense inflammatory response. *Microbes Infect* **11**, 29-39 (2009).

This study provides evidence that EVs play an important role in parasite mediate immune modulation, organ tropism and invasion *in vivo*.

53. Nogueira, P.M. et al. Vesicles from different Trypanosoma cruzi strains trigger differential innate and chronic immune responses. *J Extracell Vesicles* **4**, 28734 (2015).

54. Martins, N.O. et al. Molecular Characterization of a Novel Family of Trypanosoma cruzi Surface Membrane Proteins (TcSMP) Involved in Mammalian Host Cell Invasion. *PLoS Negl Trop Dis* **9**, e0004216 (2015).

55. Hassani, K. & Olivier, M. Immunomodulatory impact of leishmania-induced macrophage exosomes: a comparative proteomic and functional analysis. *PLoS Negl Trop Dis* **7**, e2185 (2013).

56. Hassani, K., Shio, M.T., Martel, C., Faubert, D. & Olivier, M. Absence of metalloprotease GP63 alters the protein content of Leishmania exosomes. *PLoS One* **9**, e95007 (2014).

57. Silverman, J.M. et al. An exosome-based secretion pathway is responsible for protein export from Leishmania and communication with macrophages. *J Cell Sci* **123**, 842-52 (2010).

58. De Pablos, L.M. & Osuna, A. Multigene families in Trypanosoma cruzi and their role in infectivity. *Infect Immun* **80**, 2258-64 (2012).

59. Mugnier, M.R., Cross, G.A. & Papavasiliou, F.N. The in vivo dynamics of antigenic variation in Trypanosoma brucei. *Science* **347**, 1470-3 (2015).

60. Scherf, A., Lopez-Rubio, J.J. & Riviere, L. Antigenic variation in Plasmodium falciparum. *Annu Rev Microbiol* **62**, 445-70 (2008).

61. Barteneva, N.S. et al. Circulating microparticles: square the circle. *BMC Cell Biol* **14**, 23 (2013).

62. Schnitzer, J.K., Berzel, S., Fajardo-Moser, M., Remer, K.A. & Moll, H. Fragments of antigen-loaded dendritic cells (DC) and DC-derived exosomes induce protective immunity against Leishmania major. *Vaccine* **28**, 5785-93 (2010).

63. Aline, F., Bout, D., Amigorena, S., Roingeard, P. & Dimier-Poisson, I. Toxoplasma gondii antigen-pulsed-dendritic cell-derived exosomes induce a protective immune response against T. gondii infection. *Infect Immun* **72**, 4127-37 (2004).

64. Robbins, P.D. & Morelli, A.E. Regulation of immune responses by extracellular vesicles. *Nat Rev Immunol* **14**, 195-208 (2014).

65. Thery, C., Ostrowski, M. & Segura, E. Membrane vesicles as conveyors of immune responses. *Nat Rev Immunol* **9**, 581-93 (2009).

66. Brown, L., Wolf, J.M., Prados-Rosales, R. & Casadevall, A. Through the wall: extracellular vesicles in Gram-positive bacteria, mycobacteria and fungi. *Nat Rev Microbiol* **13**, 620-30 (2015).

67. Schwechheimer, C. & Kuehn, M.J. Outer-membrane vesicles from Gram-negative bacteria: biogenesis and functions. *Nat Rev Microbiol* **13**, 605-19 (2015).

68. Hoshino, A. et al. Tumour exosome integrins determine organotropic metastasis. *Nature* **527**, 329-35 (2015).

69. Zomer, A. et al. In Vivo imaging reveals extracellular vesicle-mediated phenocopying of metastatic behavior. *Cell* **161**, 1046-57 (2015).

70. Silverman, J.M. & Reiner, N.E. Exosomes and other microvesicles in infection biology: organelles with unanticipated phenotypes. *Cell Microbiol* **13**, 1-9 (2011).

71. Kapsenberg, M.L. Dendritic-cell control of pathogen-driven T-cell polarization. *Nat Rev Immunol* **3**, 984-93 (2003).

72. Risbud, M.V. & Shapiro, I.M. Role of cytokines in intervertebral disc degeneration: pain and disc content. *Nat Rev Rheumatol* **10**, 44-56 (2014).

73. Kasper, L.H. & Buzoni-Gatel, D. Ups and downs of mucosal cellular immunity against protozoan parasites. *Infect Immun* **69**, 1-8 (2001).

74. Engel, P. et al. CD Nomenclature 2015: Human Leukocyte Differentiation Antigen Workshops as a Driving Force in Immunology. *J Immunol* **195**, 4555-63 (2015).

75. Wynn, T.A. Fibrotic disease and the T(H)1/T(H)2 paradigm. *Nat Rev Immunol* **4**, 583-94 (2004).

Figures

Box 5.1. Inflammatory response of the host

The inflammatory response is part of the host innate immunity against invading microorganisms but can also contribute to and cause disease. In general, the inflammatory response is caused by the recruitment and activation of leukocytes[71,72]. Inflammation is often associated with increased secretion of cytokines, including interleukins (IL) IL-1β, IL-4, IL-6, IL-8, IL-10, IL-12, tumor necrosis factor (TNF) and interferon-γ (IFN-γ)[71-73]. Activation of immune cells also requires interactions with cluster of differentiation (CD) proteins and stimulation of CD proteins can serve as a marker for pro-inflammatory responses[74]. Stimulation of CD40, CD54 and CD86 are

all associated with this process and down-regulation of the anti-inflammatory CD163 molecule is pro-inflammatory[72,73]. These factors are part of a type 1 proliferating helper T cell (Th1) response that results in activation and recruitment of macrophages, monocytes and other leukocytes to the site of infection[71,75].

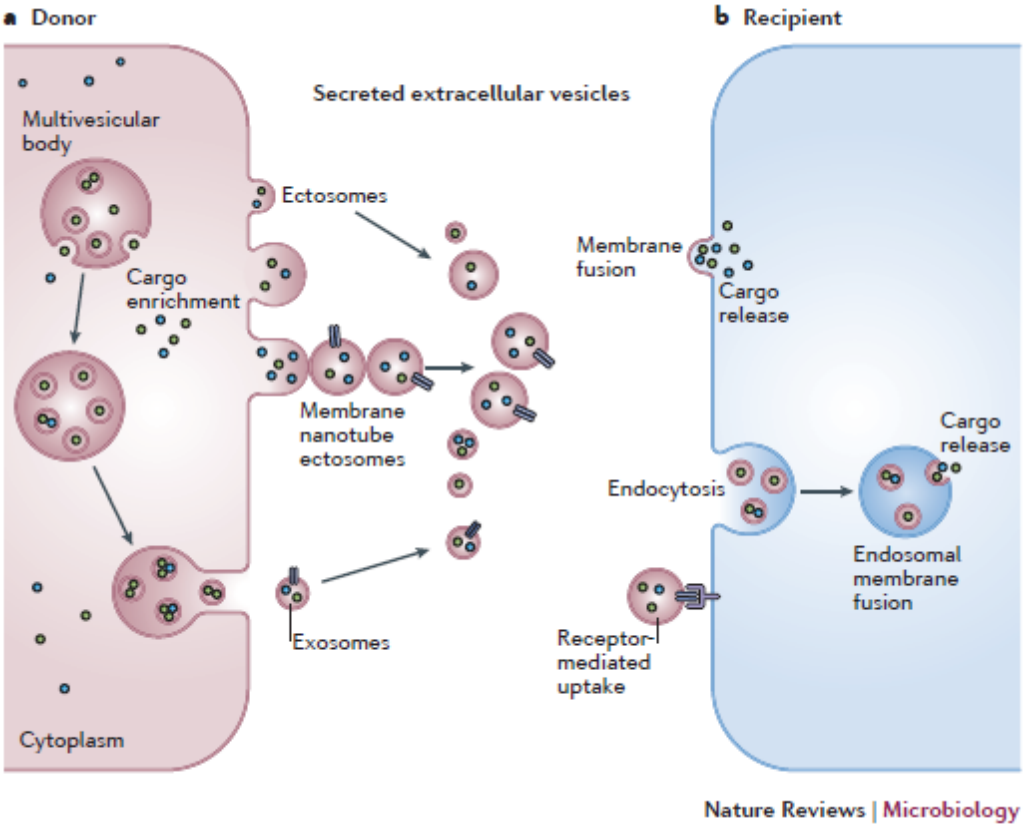

Figure 5.1. **Formation and mechanisms of interaction of parasite EVs. A)** Donor cells generate EVs with enrichment of specific cargo molecules, including lipids, proteins and nucleic acids[2,3,27]. The composition of EVs is not just due the packaging of abundant molecules, but rather supports functional sorting of cargo molecules. The formation of multivesicular bodies, through invagination of the endosomal membrane, results in exosomes of homogeneous size with components of cell surface membrane on the exterior[3]. Ectosome formation occurs from budding at the plasma membrane or along specialized portions of the membrane, such as

membrane nanotubes. Many cells use several mechanisms to generate EVs, which results in a mixed population of secreted EVs[3,5,6]. **B)** Interactions of EVs with recipient cells occur through three major mechanisms: membrane fusion, receptor-mediated binding, membrane fusion and bulk-phase nonspecific entry trhough the endocytic pathway and fusion with endosomal membranes[64,65]. These interactions can result in cargo delivery and incorporation of lipids and proteins from the EVs into the recipient membranes[70].

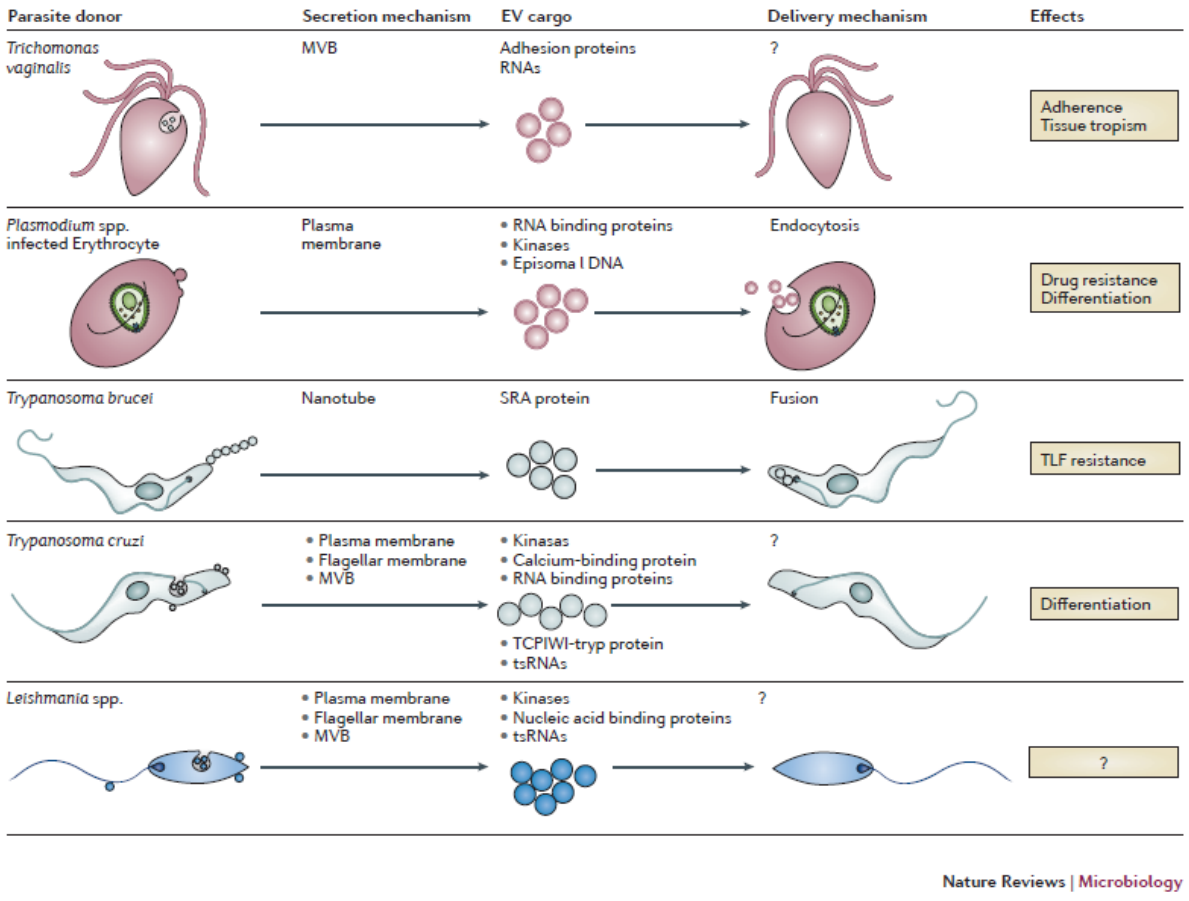

Figure 5.2. Interactions of EVs in the parasite population. EVs can transport cargo proteins, lipids and nucleic acids that mediate interactions within the parasite population. In many cases it remains unclear which mechanism protozoan parasite-derived EVs use to interact with target cells. However, it has been shown that EVs from *P. falciparum* are endocytosed by infected erythrocytes and that EVs from *T. brucei* interact within the parasite population through

membrane fusion. EVs mediate a wide range of effects on parasites including alterations of tissue tropism, differentiation, drug resistance and resistance to host immune factors.

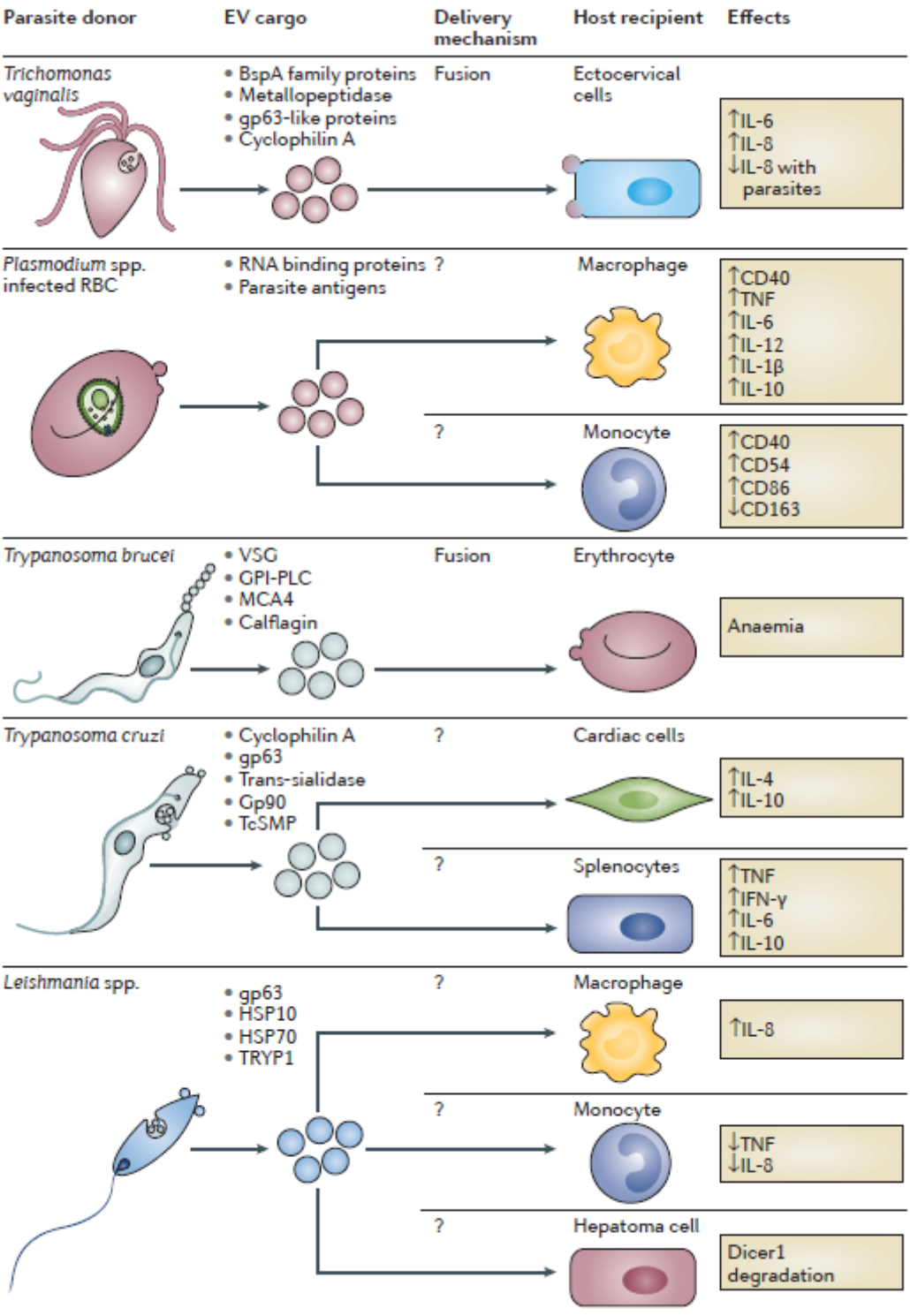
Parasite donor
EV cargo
Delivery mechanism
Host recipient
Effects
Trichomonas vaginalis
• BspA family proteins
• Metallopeptidase
• gp63-like proteins
• Cyclophilin A
Fusion
Ectocervical cells
↑IL-6
↑IL-8
↓IL-8 with parasites
Plasmodium spp. infected RBC
• RNA binding proteins
• Parasite antigens
?
Macrophage
↑CD40
↑TNF
↑IL-6
↑IL-12
↑IL-1β
↑IL-10
?
Monocyte
↑CD40
↑CD54
↑CD86
↓CD163
Trypanosoma brucei
• VSG
• GPI-PLC
• MCA4
• Calflagin
Fusion
Erythrocyte
Anaemia
Trypanosoma cruzi
• Cyclophilin A
• gp63
• Trans-sialidase
• Gp90
• TcSMP
?
Cardiac cells
↑IL-4
↑IL-10
?
Splenocytes
↑TNF
↑IFN-γ
↑IL-6
↑IL-10
Leishmania spp.
• gp63
• HSP10
• HSP70
• TRYP1
?
Macrophage
↑IL-8
?
Monocyte
↓TNF
↓IL-8
?
Hepatoma cell
Dicer1 degradation
Nature Reviews | Microbiology

Figure 5.3. Interactions of EVs with host cells. Parasite EVs contain cargo proteins and nucleic acids that have been implicated in immunomodulation and virulence within a host. The EVs from *T. vaginalis* and *T. brucei* have been shown to fuse with host cells, which results in the transfer of cargo proteins and lipids. A broad range of target host cells, types of interactions and resulting effects have been identified . Often EVs elicit a pro-inflammatory response, which increases the parasite burden in the host and/or disease. (↑) denotes increase in expression or secretion and (↓) denotes a decrease in expression or secretion.

CHAPTER 6

CONCLUSIONS

Using ASREs to Understand Mitochodnrial RNA Function in *T. brucei*

In Chapter 2 ASREs are used to specifically target and cleave a mitochondrial mRNA in PF *T. brucei* that results in a loss of function phenotype consistent with the known function of the encoded protein. The results presented here provide the proof of concept to allow application of ASRE targeted knockdowns to investigate the function of other mitochondrial RNAs in trypanosomes.

Until the research in Chapter 2, methods were not available for functional analysis of kDNA encoded RNAs in kinetoplastids. Due to a lack of suitable tools previous studies on *T. brucei* mitochondrial function was forced to rely on indirect methods including mutagenized cells and dominant negative protein effects. Dyskinetoplastic trypanosomes, akin to petite mutants in yeast, have been studied and have provided limited specific information about the function of individual mitochondrial RNAs since dyskinetoplastic trypanosomes completely lack both maxicircles and minicircles resulting in pleotropic phenotypes [1,2]. Similarly, naturally occurring trypanosome lacking all or part of the maxicircle (*Trypanosoma equiperdum, Tryanosoma evansi* and *Trypanosoma equinum*) are available but cell lines carrying a single maxicircle gene mutation have not been reported.

Another approach used to study the function of mitochondrial encoded proteins relied on the transfection and nuclear expression of a recoded mitochondrial gene [3]. In this study a unique, short 60 amino acid hydrophilic portion of the AEP-1, protein encoded by an alternatively edited version of COIII mRNA, fused to a sequence coding a mitochondrial

localization sequence, was transfected into the ribosomal RNA locus within the nucleus of *T. brucei*. Nuclear expression and mitochondrial localization of this truncated version of AEP-1 resulted in a dominant negative phenotype leading to loss of kDNA organization [3]. While these experiments successfully defined a function for AEP-1 the application of this approach is limited since most mitochondria encoded proteins are extremely hydrophobic and cannot be synthesized in the cytosol and imported into the mitochondrion. Other direct approaches, including mitochondrial gene knockouts and mitochondrial RNAi have been unsuccessful in trypanosomes.

The recent development of ASRE mediated RNA cleavage has allowed the disruption of specific mitochondrial transcripts to analyze function [4]. Target sequence selection is critical since the sequence must be single-stranded and found exclusively on the RNA being targeted. In the studies reported in Chapter 2, we found that the A6-ASRE was specific for the mitochondrial A6 mRNA and did not cleave the cytosolic mRNAs for eIF containing the same 8-nucleotide targeting sequence [5]. The lack of activity of ASREs outside the mitochondrion may be a consequence of the relatively high mitochondrial Mn^{2+} concentration and the metal ion selectivity of the PIN endoribonuclease [4]. This effect was also observed in mammalian cells. Use of an ASRE directed against the mammalian mitochondria encoded NADH dehydrogenase subunit 5 (ND5) was specific and did not cleave cytosolic mRNAs containing the ND5 targeting sequence [4]. The expression an ND5-ASRE lacking a mitochondrial localization sequence resulted in accumulation in the cytoplasm but had no effect on cell growth suggesting that nuclear encoded mRNAs were not targeted for cleavage by the ND5-ASRE in HEK293 cells [4].

The development of ASREs as a tool for *T. brucei* will allow for new functional studies investigating alternatively edited mitochondrial mRNAs, allowing for specific knockdown and

phenotype analysis. This method would also provide a method to analyze the three mitochondrial unidentified reading frame (MURF) RNAs, which are canonically edited but produce RNAs of unknown function.

Differential Localization of Moonlighting Proteins

In Chapter 3 α-ketoglutarate decarboxylase E1, α-KDE1, is shown to be essential in BF *T. brucei*. This is surprising since the only known function of α-KDE1 is associated with the mitochondrial Krebs cycle which is absence in BF *T. brucei*. However, in our studies I found that RNAi knockdown resulted in growth arrest and caused death within 24 hours. Knockdown also resulted in rapid morphological changes to the α-KDE1 RNAi *T. brucei* that included extensive and rapid swelling of the flagellar pocket, which was mediated by sequestering of both flagella and plasma membrane into the pocket. The function of α-KDE1 in BF *T. brucei* was addressed by examining the intracellular localization of the protein by immunofluorescence microscopy. Unexpectedly we found that α-KDE1exclusively localized to glycosomes in BF *T. brucei* and we showed that the N-terminal 18 amino acids of α-KDE1 contained overlapping mitochondrial and glycosomal targeting sequences. Together these results showed that α-KDE1was preferentially targeted to glycosomes in BF *T. brucei* and while the function of α-KDE1 in glycosome is unknown it is essential. Induction of RNAi in these cells also leads to secretion of copious amounts of free extracellular vesicles (EVs), possibly as a stress response to the lethal RNAi phenotype.

Organisms use a wide array of mechanisms to compensate for a seeming limitless need for biological diversity in the face of rather limited genetic potential. Generation of functionally distinct proteins from a single gene by genetic recombination, alternative mRNA processing and post translational modifications contributes to changes in most organisms in response to

environmental and developmental cues [6,7,8]. In addition, a small number of moonlighting proteins can carry out multiple functions without sequence or post-translation change. The moonlighting functions of several canonical metabolic enzymes have been described in mammals, fungi, plants and protozoa [9,10,11]. Identifying moonlighting activities for essential proteins is difficult since conventional loss of function analyses generally cannot distinguish a single versus multiple activities for a protein. The developmental regulation of mitochondrial carbohydrate metabolism in *T. brucei* allowed us to initially investigate the function of the enzyme components of the inoperative Krebs cycle in BF *T. brucei*. An earlier study reported that the dihydrolipoyl succinyltransferase, α-KDE2, was expressed in BF *T. brucei* and was associated with the kDNA network and mitochondrial membrane. This protein was essential for the maintenance of the kDNA during cell division [9]. This study also showed that α-KDE1 was also expressed in BF *T. brucei.* The developmental regulation of *T. brucei* mitochondria makes these organisms a powerful model to understand moonlighting function. New candidate proteins could be identified through a comparison of BF and PF gene expression data. Genes that are expressed in a life cycle where the corresponding metabolic process is nonfunctional could be new candidates for investigate this mechanism for generating functional protein diversity.

Parasitic Protozoans EVs in Progression of Disease

In Chapter 4 BF *T. brucei* are shown to secrete EVs through the vesiclularization of membrane nanotubes. These EVs transfer functional proteins to other BF *T. brucei* and are able to fuse with host erythrocytes causing disease pathology. However, *T. brucei* is not unique in its use of EVs for cellular communication as bacteria and other eukaryotes exploit this mechanism for cellular communication [12,13,14,15,16,17]. By understanding the immune modulation functions and cellular communication of other organisms EVs we may better understand other

potential roles of *T. brucei* EVs. Chapter 5 presents the most compelling evidence that pathogenic protozoan's use EVs for a wide range of biological functions. Often EVs are used to drive tissue tropism, cell differentiation, persistence within the host and a pro-inflammatory response.

EVs from the parasite *Trichomonas vaginalis* interact with host ectocervical cells results in the production of the pro-inflammatory cytokines IL-6 and IL-8 [18]. While pretreatment of ectocervical cells with EVs followed by infection with *T. vaginalis* showed dampening of the IL-8 response which may allow for increased parasite growth and pathology without a significant initial immune response [18].

Plasmodium infections have been shown to increase the overall number of circulating EVs, derived from erythrocytes and other host cell types, in human and murine malaria [19,20,21]. Increased production of EVs during infection has also been correlated with disease severity in human and animal malaria cases [19,21]. Using rodent malaria models it was shown that EVs have broad immunomodulatory effects, often resulting in a pro-inflammatory response [22,23,24]. It has been shown that EV transfer from a *P. yoelii* strain that preferentially infect reticulocytes, which are immature erythrocytes, can make other *P. yoelii* strains shift cell tropism from mature erythrocytes to reticulocytes [25]. The use of *in vitro* derived EVs from *P. falciparum* infected erythrocytes showed activation of monocytes derived from naïve human peripheral blood mononuclear cells. Activated cells showed an up-regulation of the inflammatory response markers CD40, CD54 and CD86 and a down-regulation of CD163 [25]. These EVs also interacted with human macrophages and stimulated the production of the pro-inflammatory cytokines IL-6, IL-12 and IL-1β as well as IL-10 [26]. These studies show the broadly immune

modulating nature of parasite derived EVs and the common feature of generation of stimulating a pro-inflammatory response.

Though BF *T. brucei* derived EVs have only recently been described, there have been several important pathological features associated with unknown secretion products produced in *T. brucei* culture medium [27,28,29,30,31]. Infection of a mammalian host elicits immune dampening through changes to TNF-α levels [29]. This effect has been attributed to secretion of a flagellar associated adenylate cyclase (GRESAG4), but the mechanism of delivery to host cells was unknown [29]. In Chapter 4 we show that GRESAG4 is a component of EVs, along with other virulence factors required for survival [32]. It is not unreasonable to hypothesize that *T. brucei*, like other protozoan parasites, use EVs for immune modulation of the host.

Exploiting EVs for Detection and Treatment

The results in Chapter 4 and those presented in Chapter 5 suggest EVs may be important molecules to target for both parasite detection and possibly treatment. By identifying EVs secreted within a host it may be possible to detect low levels of the infecting parasites. Many parasites have developed complicated mechanisms to evade the innate and adaptive immune response through alterations to surface proteins, thus making it difficult to detect through conventional serological analysis [33,34,35]. However, parasite derived EVs are enriched in invariant proteins and nucleic acids, many of which have been found in the circulation of infected hosts [26,32,36,37]. Current diagnostics require free parasites within the circulation; however during chronic infection parasitimia is often undetectable. The use of serological tests is not effective for detection of new patient infections in endemic regions. Since these tests rely on circulating antibody to parasite antigens it is impossible to determine if a positive test result is due to a previous infection or an ongoing one. It may be possible to screen individuals for the

presence of EV cargo molecules as a first line of detection. EVs are currently being used as biomarkers for detection of other human diseases including early cancer detection [38,39]. There have been promising results showing that EVs can be accurately used for detection, when previous analysis would require whole body imaging of the patient and invasive biopsy procedures [40].

EVs may also be important therapeutic targets. By blocking EV interactions with host cells, it may be possible to disrupt immune activation and disease pathology. In the case of *T. brucei*, it has been proposed that the ability to resist anemia is more important for survival than the control of parasitemia in infected cattle [41,42]. In Chapter 4 *T. brucei* derived EVs are shown to fuse with target membranes by EV surface proteins [32]. Future efforts to identify the fusogens may provide a powerful tool for preventing disease pathology. Disrupting *T. brucei* EVs may alleviate severe anemia in animals, thus allowing for increased survival. Though, the generation of a parasite tolerant host may bring about a new series of complications. It is important to point out that indigenous cattle varieties in sub-Saharan Africa are refractory to parasite-induced anemia [41]. Targeting EVs in other parasitic diseases would block the pro-inflamatory response often required for enhanced infection and tissue invasion. Blocking EV interactions may have profound implications in parasitic disease progression within the host.

References

1. Dean S, Gould MK, Dewar CE, Schnaufer AC (2013) Single point mutations in ATP synthase compensate for mitochondrial genome loss in trypanosomes. Proc Natl Acad Sci U S A 110: 14741-14746.

2. Schnaufer A, Domingo GJ, Stuart K (2002) Natural and induced dyskinetoplastic trypanosomatids: how to live without mitochondrial DNA. Int J Parasitol 32: 1071-1084.

3. Ochsenreiter T, Anderson S, Wood ZA, Hajduk SL (2008) Alternative RNA editing produces a novel protein involved in mitochondrial DNA maintenance in trypanosomes. Mol Cell Biol 28: 5595-5604.

4. Choudhury R, Tsai YS, Dominguez D, Wang Y, Wang Z (2012) Engineering RNA endonucleases with customized sequence specificities. Nat Commun 3: 1147.

5. Szempruch AJ, Choudhury R, Wang Z, Hajduk SL (2015) In vivo analysis of trypanosome mitochondrial RNA function by artificial site-specific RNA endonuclease-mediated knockdown. RNA 21: 1781-1789.

6. Cooper MD, Alder MN (2006) The evolution of adaptive immune systems. Cell 124: 815-822.

7. Graveley BR (2001) Alternative splicing: increasing diversity in the proteomic world. Trends Genet 17: 100-107.

8. Moore MJ, Proudfoot NJ (2009) Pre-mRNA processing reaches back to transcription and ahead to translation. Cell 136: 688-700.

9. Sykes SE, Hajduk SL (2013) Dual functions of alpha-ketoglutarate dehydrogenase E2 in the Krebs cycle and mitochondrial DNA inheritance in Trypanosoma brucei. Eukaryot Cell 12: 78-90.

10. Jeffery CJ (1999) Moonlighting proteins. Trends Biochem Sci 24: 8-11.

11. Huberts DH, van der Klei IJ (2010) Moonlighting proteins: an intriguing mode of multitasking. Biochim Biophys Acta 1803: 520-525.

12. Wood CR, Rosenbaum JL (2015) Ciliary ectosomes: transmissions from the cell's antenna. Trends Cell Biol 25: 276-285.

13. Schwechheimer C, Kuehn MJ (2015) Outer-membrane vesicles from Gram-negative bacteria: biogenesis and functions. Nat Rev Microbiol 13: 605-619.

14. Campos JH, Soares RP, Ribeiro K, Andrade AC, Batista WL, et al. (2015) Extracellular Vesicles: Role in Inflammatory Responses and Potential Uses in Vaccination in Cancer and Infectious Diseases. J Immunol Res 2015: 832057.

15. Brown L, Wolf JM, Prados-Rosales R, Casadevall A (2015) Through the wall: extracellular vesicles in Gram-positive bacteria, mycobacteria and fungi. Nat Rev Microbiol 13: 620-630.

16. Twu O, Johnson PJ (2014) Parasite extracellular vesicles: mediators of intercellular communication. PLoS Pathog 10: e1004289.

17. Mantel PY, Marti M (2014) The role of extracellular vesicles in Plasmodium and other protozoan parasites. Cell Microbiol 16: 344-354.

18. Twu O, de Miguel N, Lustig G, Stevens GC, Vashisht AA, et al. (2013) Trichomonas vaginalis exosomes deliver cargo to host cells and mediate hostratioparasite interactions. PLoS Pathog 9: e1003482.

19. Campos FM, Franklin BS, Teixeira-Carvalho A, Filho AL, de Paula SC, et al. (2010) Augmented plasma microparticles during acute Plasmodium vivax infection. Malar J 9: 327.

20. Cao M, Ning J, Hernandez-Lara CI, Belzile O, Wang Q, et al. (2015) Uni-directional ciliary membrane protein trafficking by a cytoplasmic retrograde IFT motor and ciliary ectosome shedding. Elife 4.

21. El-Assaad F, Wheway J, Hunt NH, Grau GE, Combes V (2014) Production, fate and pathogenicity of plasma microparticles in murine cerebral malaria. PLoS Pathog 10: e1003839.

22. Barteneva NS, Maltsev N, Vorobjev IA (2013) Microvesicles and intercellular communication in the context of parasitism. Front Cell Infect Microbiol 3: 49.

23. Coakley G, Maizels RM, Buck AH (2015) Exosomes and Other Extracellular Vesicles: The New Communicators in Parasite Infections. Trends Parasitol 31: 477-489.

24. Marti M, Johnson PJ (2016) Emerging roles for extracellular vesicles in parasitic infections. Curr Opin Microbiol 32: 66-70.

25. Martin-Jaular L, Nakayasu ES, Ferrer M, Almeida IC, Del Portillo HA (2011) Exosomes from Plasmodium yoelii-infected reticulocytes protect mice from lethal infections. PLoS One 6: e26588.

26. Mantel PY, Hoang AN, Goldowitz I, Potashnikova D, Hamza B, et al. (2013) Malaria-infected erythrocyte-derived microvesicles mediate cellular communication within the parasite population and with the host immune system. Cell Host Microbe 13: 521-534.

27. Emmer BT, Daniels MD, Taylor JM, Epting CL, Engman DM (2010) Calflagin inhibition prolongs host survival and suppresses parasitemia in Trypanosoma brucei infection. Eukaryot Cell 9: 934-942.

28. Proto WR, Castanys-Munoz E, Black A, Tetley L, Moss CX, et al. (2011) Trypanosoma brucei metacaspase 4 is a pseudopeptidase and a virulence factor. J Biol Chem 286: 39914-39925.

29. Salmon D, Vanwalleghem G, Morias Y, Denoeud J, Krumbholz C, et al. (2012) Adenylate cyclases of Trypanosoma brucei inhibit the innate immune response of the host. Science 337: 463-466.

30. Webb H, Carnall N, Vanhamme L, Rolin S, Van Den Abbeele J, et al. (1997) The GPI-phospholipase C of Trypanosoma brucei is nonessential but influences parasitemia in mice. J Cell Biol 139: 103-114.

31. Geiger A, Hirtz C, Becue T, Bellard E, Centeno D, et al. (2010) Exocytosis and protein secretion in Trypanosoma. BMC Microbiol 10: 20.

32. Szempruch AJ, Sykes SE, Kieft R, Dennison L, Becker AC, et al. (2016) Extracellular Vesicles from Trypanosoma brucei Mediate Virulence Factor Transfer and Cause Host Anemia. Cell 164: 246-257.

33. De Pablos LM, Osuna A (2012) Multigene families in Trypanosoma cruzi and their role in infectivity. Infect Immun 80: 2258-2264.

34. Mugnier MR, Cross GA, Papavasiliou FN (2015) The in vivo dynamics of antigenic variation in Trypanosoma brucei. Science 347: 1470-1473.

35. Scherf A, Lopez-Rubio JJ, Riviere L (2008) Antigenic variation in Plasmodium falciparum. Annu Rev Microbiol 62: 445-470.

36. Silverman JM, Chan SK, Robinson DP, Dwyer DM, Nandan D, et al. (2008) Proteomic analysis of the secretome of Leishmania donovani. Genome Biol 9: R35.

37. Bayer-Santos E, Aguilar-Bonavides C, Rodrigues SP, Cordero EM, Marques AF, et al. (2013) Proteomic analysis of Trypanosoma cruzi secretome: characterization of two populations of extracellular vesicles and soluble proteins. J Proteome Res 12: 883-897.

38. Thery C (2015) Cancer: Diagnosis by extracellular vesicles. Nature 523: 161-162.

39. Barteneva NS, Fasler-Kan E, Bernimoulin M, Stern JN, Ponomarev ED, et al. (2013) Circulating microparticles: square the circle. BMC Cell Biol 14: 23.

40. Melo SA, Luecke LB, Kahlert C, Fernandez AF, Gammon ST, et al. (2015) Glypican-1 identifies cancer exosomes and detects early pancreatic cancer. Nature 523: 177-182.

41. Naessens J (2006) Bovine trypanotolerance: A natural ability to prevent severe anaemia and haemophagocytic syndrome? Int J Parasitol 36: 521-528.

42. Berthier D, Breniere SF, Bras-Goncalves R, Lemesre JL, Jamonneau V, et al. (2016) Tolerance to Trypanosomatids: A Threat, or a Key for Disease Elimination? Trends Parasitol 32: 157-168.